

# *Geological Field Trips and Maps*

2022

Vol. 14 (2.3)



ISSN: 2038-4947



**Stratigraphy and facies of the Apennine Carbonate Platform  
(southern Italy): the record of Mesozoic OAEs and Miocene transgression**

**FT3 Preconference Field Trip of the 3rd International Congress on Stratigraphy STRATI 2019,  
Milan (Italy), 29<sup>th</sup> -30<sup>th</sup> June 2019.**

<https://doi.org/10.3301/GFT.2022.06>



**SOCIETÀ GEOLOGICA ITALIANA**

FONDATA NEL 1881 - ENTE MORALE R. D. 17 OTTOBRE 1885



## GFT&M - Geological Field Trips and Maps

Periodico semestrale del Servizio Geologico d'Italia - ISPRA e della Società Geologica Italiana  
Geol. F. Trips Maps, Vol.14 No.2.3 (2022), 75 pp., 35 figs., 1 tab. (<https://doi.org/10.3301/GFT.2022.06>)

### Stratigraphy and facies of the Apennine Carbonate Platform (southern Italy): the record of Mesozoic OAEs and Miocene transgression

FT3 Preconference Field Trip of the 3rd International Congress on Stratigraphy STRATI 2019,  
Milan (Italy), 29<sup>th</sup> -30<sup>th</sup> June 2019.

**Mariano Parente<sup>1</sup>, Sabrina Amodio<sup>2\*</sup>, Alessandro Iannace<sup>1</sup>, Monia Sabbatino<sup>1,3</sup>**

<sup>1</sup> Dipartimento di Scienze della Terra, dell'Ambiente e delle Risorse, Università degli Studi di Napoli "Federico II", Complesso Universitario di Monte Sant'Angelo, via Cintia 21, 80126 Naples, Italy

<sup>2</sup> Dipartimento di Scienze e Tecnologie, Università degli Studi di Napoli "Parthenope", Centro Direzionale, Isola C4, 80143 Naples, Italy

<sup>3</sup> present address: Eni SpA, Upstream and Technical Services, SPES Department, Via Emilia 1, 20097 San Donato Milanese (Mi), Italy

\* Corresponding author e-mail: [sabrina.amodio@uniparthenope.it](mailto:sabrina.amodio@uniparthenope.it)

Responsible Director  
*Maria Siclari* (ISPRA-Roma)

Editor in Chief  
*Andrea Zanchi* (Università Milano-Bicocca)

Editorial Manager  
*Angelo Cipriani* (ISPRA-Roma) - *Silvana Falchetti* (ISPRA-Roma)  
*Fabio Massimo Petti* (Società Geologica Italiana - Roma) - *Diego Pieruccioni*  
(ISPRA - Roma) - *Alessandro Zuccari* (Società Geologica Italiana - Roma)

Associate Editors  
*M. Berti* (Università di Bologna), *M. Della Seta* (Sapienza Università di Roma),  
*P. Gianolla* (Università di Ferrara), *G. Giordano* (Università Roma Tre),  
*M. Massironi* (Università di Padova), *M.L. Pampaloni* (ISPRA-Roma),  
*M. Pantaloni* (ISPRA-Roma), *M. Scambelluri* (Università di Genova),  
*S. Tavani* (Università di Napoli Federico II)

Editorial Advisory Board  
*D. Bernoulli*, *F. Calamita*, *W. Cavazza*, *F.L. Chiocci*, *R. Compagnoni*,  
*D. Cosentino*, *S. Critelli*, *G.V. Dal Piaz*, *P. Di Stefano*, *C. Doglioni*, *E. Erba*,  
*R. Fantoni*, *M. Marino*, *M. Mellini*, *S. Milli*, *E. Chiarini*, *V. Pascucci*, *L. Passeri*,  
*A. Peccerillo*, *L. Pomar*, *P. Ronchi*, *L. Simone*, *I. Spalla*, *L.H. Tanner*,  
*C. Venturini*, *G. Zuffa*

Technical Advisory Board for Geological Maps  
*F. Capotorti* (ISPRA-Roma), *F. Papasodaro* (ISPRA-Roma),  
*D. Tacchia* (ISPRA-Roma), *S. Grossi* (ISPRA-Roma),  
*M. Zucali* (University of Milano), *S. Zanchetta* (University of Milano-Bicocca),  
*M. Tropeano* (University of Bari), *R. Bonomo* (ISPRA-Roma)

**Cover page Figure:** The Maiellaro quarry, near Mercato San Severino (Salerno). The quarry face exposes the passage between the "Lithotis member" of the *Palaeodasycladus* Limestones and the overlying "oolitic and oncolitic limestones".

ISSN: 2038-4947 [online]

<http://gftm.socgeol.it/>

**The Geological Survey of Italy, the Società Geologica Italiana and the Editorial group are not responsible for the ideas, opinions and contents of the guides published; the Authors of each paper are responsible for the ideas, opinions and contents published.**

**Il Servizio Geologico d'Italia, la Società Geologica Italiana e il Gruppo editoriale non sono responsabili delle opinioni espresse e delle affermazioni pubblicate nella guida; l'Autore/i è/sono il/i solo/i responsabile/i.**

## Index

### Information

Abstract .....	4
Program summary .....	5
Safety .....	5
Hospitals .....	5
Accommodations .....	7

### Excursion notes

The southern Apennines fold-and-thrust belt .....	8
Stratigraphy of the Apennine Carbonate Platform .....	9

### Itinerary

<b>DAY 1</b> .....	15
<b>Stop 1.1:</b> San Lorenzello section. An example of Milankovitch cyclicity in shallow-water platform carbonates of the Valanginian/Hauterivian (41°16'49.16"N – 14°32'23.24"E).....	15

<b>Stop 1.2:</b> The Early Miocene transgression at Pietraroja (41°20'59"N - 14°33'09"E) .....	24
--	----

<b>Stop 1.3:</b> The mid-Cretaceous bauxites at Regia Piana (41°21'50"N - 14°31'46"E) .....	28
---	----

<b>Stop 1.4:</b> The Early Miocene transgression and the Middle Miocene drowning of the carbonate platform at Regia Piana (41°21'36"N - 14°32'09"E) .....	31
---	----

<b>DAY 2</b> .....	35
--------------------	----

<b>Stop 2.1:</b> The <i>Lithiotis</i> limestones and the carbonate platform record of the early Toarcian OAE in the Maiellaro quarry of Mercato San Severino (40°46'43"N - 14°43'37"E) .....	35
--	----

<b>Stop 2.2:</b> The Orbitolina level at Mt Tobenna and its relations with the Aptian OAE1 (40°41'56"N - 14°51'49"E) .....	45
--	----

<b>Stop 2.3:</b> The <i>Thalassinoides</i> beds and the carbonate platform record of the Cenomanian-Turonian boundary OAE2 at Monteforte Cilento (40°22'10"N - 15°11'27"E) ....	52
---	----

<b>References</b> .....	63
-------------------------	----

## Abstract

The Apennine Carbonate Platform of southern Italy witnesses nearly 150 Myr (Late Triassic to Late Cretaceous) of shallow-water carbonate sedimentation in the subtropical central Tethys. During this field trip, you will have a look at the stratigraphy and facies across some key intervals of global palaeoenvironmental perturbation and at some important stratigraphic discontinuities in the history of the platform.

During the first day, you will visit three localities of the Matese Mts. At San Lorenzello you will look at Milankovitch cyclicity expressed in Lower Cretaceous (Valanginian-Hauterivian) peritidal carbonates. At Pietraroja you will have a look at the foramol facies of the Cusano formation, marking the Early Miocene transgression on top of the eroded Cretaceous substrate. Moving north, at the Regiapiana you will see the abandoned mines that exploited the mid-Cretaceous karst bauxites, which mark a prolonged subaerial exposure. Moreover, you will walk through the Middle Miocene synorogenic history of the platform, from its exposure and erosion in the forebulge to its incipient flexural subsidence, highlighted by the Lower Miocene carbonates of the Cusano formation, to its drowning below the photic zone, marked by a phosphatic hardground overlain by the "Orbulina marls" of the Longano formation.

During the second day, you will head south toward Salerno. In a quarry at Mercato San Severino, you will look at the record of the early Toarcian oceanic anoxic event, marked by the abrupt demise of lithiotid bivalves and dasycladalean algae, the major carbonate producers of the Lower Jurassic carbonate platforms. At the base of Mt Tobenna, you will look at the Aptian *Orbitolina* level: a marker bed whose palaeoenvironmental meaning has been long debated. From Mt Tobenna you will move south toward Monteforte Cilento where you will look at the record of the Cenomanian-Turonian OAE2 in the Apennine Carbonate Platform.

## Keywords

*shallow-water carbonates, facies, cyclostratigraphy, isotope stratigraphy, oceanic anoxic events, biotic crises, southern Apennines, Italy*

## Program summary

### First day

From Napoli to San Lorenzello (BN) – stop 1: Milankovitch cyclicity in Lower Cretaceous peritidal carbonates. From San Lorenzello to Pietraroja (BN) – stop 2: Lower Miocene foramol carbonates of the Cusano formation unconformably overlying the Lower Cretaceous limestones. From Pietraroja to the Regiapiana – stop 3: mid-Cretaceous karst bauxites; stop 4 – Early Miocene transgression (Cusano formation) and Middle Miocene platform drowning (phosphatic hardground and “*Orbulina* marls”) (Fig. 1).

### Second day

From Napoli to Mercato San Severino (SA) – stop 1: Lower Jurassic lithiotid limestones and oolitic limestones. From Mercato San Severino to the southern slope of Mt Tobenna – stop 2: the Aptian *Orbitolina* level. From Mt Tobenna to Monteforte Cilento (SA) – stop 3: Cenomanian-Turonian carbonates and the record of OAE2 in the Apennine Carbonate Platform (Fig. 1).

### Safety

The stops are generally easily accessible and located very close to the parking areas. Hiking boots and comfortable clothing are necessary; in addition, high-visibility jackets must be worn for the road stops, and protective helmets only for the 2.1 stop. Outcrops are close to localities where there are small shops and pharmacies. The Campania region is usually sunny, but rains or rain showers can occasionally occur. Sunscreen protection and rain jackets are thus needed.

General Emergency contact number: 112 (Carabinieri, Police, Ambulance, Firefighters)

### Hospitals

Day 1 - The nearest hospital is the Presidio Ospedaliero S. Alfonso Maria de' Liguori, Contrada San Pietro, 1, 82019 S. Agata de' Goti, BN; Phone: (+39) 082 3313710, which is at about 30 km from stop 1.1 and at about 60 km from stop 1.2.

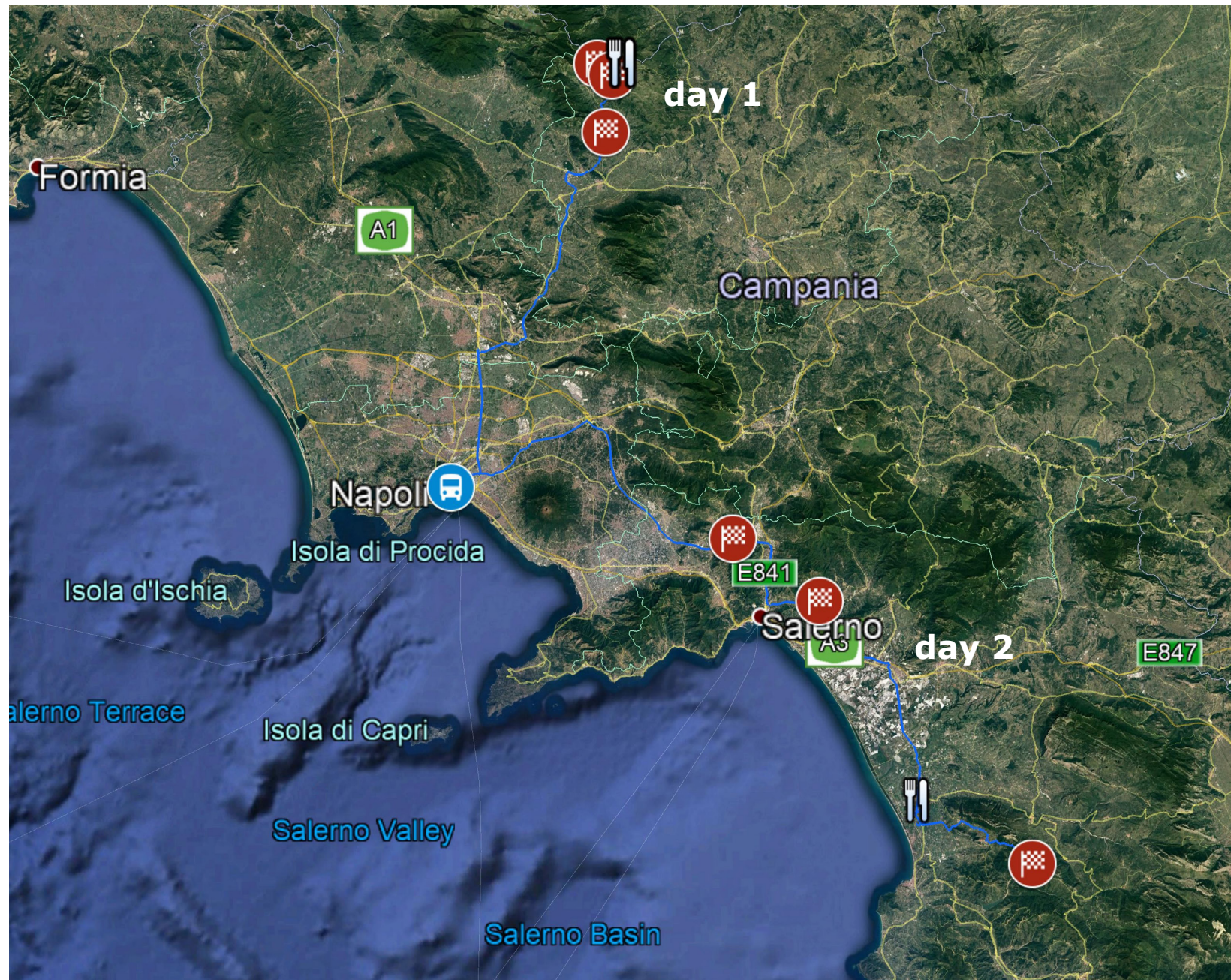


Fig. 1 - Field trip itinerary. The stops are marked by the flags.

Day 2 – The nearest hospital for stop 2.1 (at about 1 km) is the Ospedale Gaetano Fucito, Corso Umberto I, 84085 Mercato San Severino, SA; Phone: (+39) 089 9925283; for stop 2.2 the Ospedale San Giovanni di Dio e Ruggi d’Aragona is at about 10 km, Via San Leonardo, 84131 Salerno; Phone: (+39) 089 671111; for stop 2.3 the Presidio Ospedaliero San Luca is at about 26 km, Via Francesco Cammarota, 84078 Vallo della Lucania, SA; Phone: (+39) 089 671111.

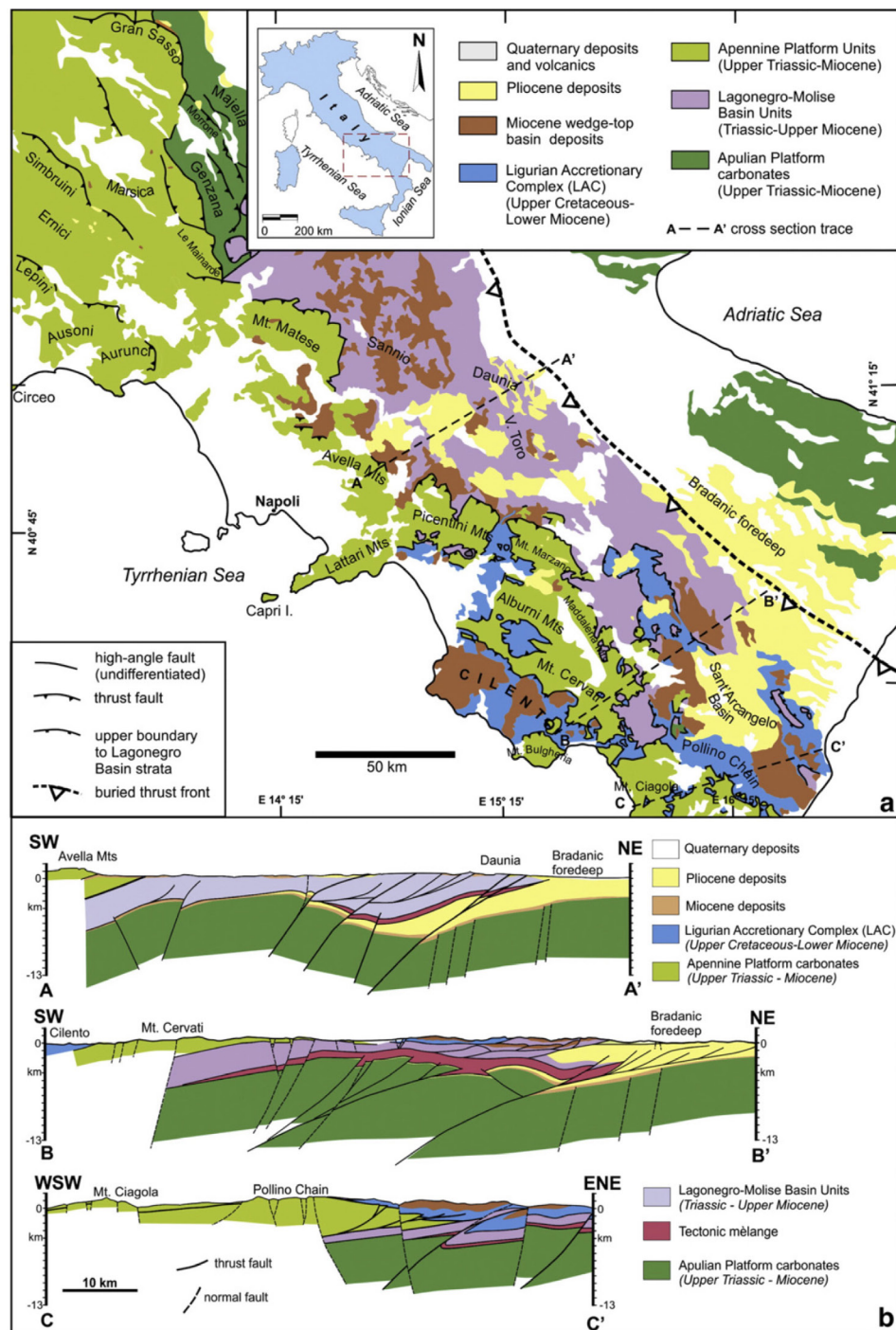
## **Accommodations**

The suggested itineraries allow people to leave from and return to Naples during the two-day excursion. Naples offers many options for hotel accommodations; it is possible to browse and book from websites dedicated to hotel reservations. Main tourist information about the city as maps, accommodations, transports, places of interest and monuments can be found at: <https://www.comune.napoli.it/flex/cm/pages/ServeBLOB.php/L/EN/IDPagina/5802>



## The southern Apennines fold-and-thrust belt

The southern Apennines is a fold-and-thrust system that evolved in the framework of the convergence of Africa-Europe major plates during the Late Cretaceous to Quaternary times (Dewey et al., 1989; Schettino and Turco, 2011; Ascione et al., 2012; Vitale and Ciarcia 2013 and references therein) and is mainly separated by the Ortona–Roccamonfina and the Sangineto structural lines, respectively from the central Apennines at the north and the Calabrian arc at the south. The Africa-Europe convergence involved the consumption of most of the Neo-Tethyan oceanic lithosphere originally interposed between the two continental palaeo-margins. The Mesozoic pre-orogenic palaeogeography consisted of two wide carbonate platform areas, the Apennine Carbonate Platform to the west and the Apulian Carbonate Platform to the east, separated by the deep-water Lagonegro Basin (Mostardini and Merlini, 1986). The latter basinal setting was originated during the Late Triassic – Early Jurassic rifting phase that disarticulated a tropical intracratonic carbonate platform at the northern margin of Adria, a promontory of the African Plate (Oldow et al., 2002; Patacca and Scandone, 2007). The southern Apennine segment of the fold-and-thrust belt originated by the progressive deformation of these domains, starting from the Early Miocene. It consists of two main parts (Mazzoli et al., 2008 and references therein): (i) the Apennine Accretionary Wedge (AAW), whose deformation started in the Early Miocene (Langhian) and (ii) the buried Apulian Platform Inversion Belt (APIB), which was deformed starting from the latest Miocene (Messinian). The AAW is made of sedimentary units derived from the Apennine Carbonate Platform and the Lagonegro Basin, with their stratigraphic cover of Neogene foredeep and wedge-top basin sediments (Fig. 2). The structure is dominated by low-angle faults, separating carbonate platform/slope successions of the Apennine Carbonate Platform, in the hanging wall, from pelagic successions of the Lagonegro Basin in the footwall. The AAW presently forms an allochthonous wedge overlying carbonate platform strata of the Apulian Platform, continuous with those exposed in the Apulian promontory to the NE (Mostardini and Merlini, 1986; Shiner et al., 2004), which represents the orogenic foreland. The major detachment presently separating the allochthonous wedge from the buried Apulian Platform carbonates is marked by a *mélange* zone (Mazzoli et al., 2001). Messinian evaporites and, more to the east, progressively younger Pliocene siliciclastics occur on top of the Mesozoic-Cenozoic shallow-water carbonates of the Apulian Platform. The buried portion of the Apulian Platform was involved in the final shortening phases, giving rise to the subsurface APIB (Shiner et al., 2004). Therefore, a switch from thin-skinned thrusting to thick-skinned inversion appears to have occurred in the southern Apennines as the Apulian Platform carbonates, and the underlying thick continental lithosphere, were deformed (Mazzoli et al., 2000;



Butler et al., 2004). Crustal shortening ceased in the early part of the Middle Pleistocene, at about 0.7 Ma (Patacca and Scandone, 2001). A new tectonic regime was established in the chain and adjacent foothills (Cello et al., 1982; Cinque et al., 1993; Hippolyte et al., 1994; Montone et al., 1999) characterised by a NE-SW oriented maximum extension and by dominantly extensional faults that postdate and dissect the thrust belt (Cello et al., 1982; Butler et al., 2004).

### Stratigraphy of the Apennine Carbonate Platform

The Apennine Carbonate Platform (ApCP) of southern Italy comprises Meso-Cenozoic carbonate successions that were deposited in shallow tropical to sub-tropical waters at the southwestern margin of the Neo-Tethys Ocean. This carbonate platform was part of a palaeotectonic domain, variously called Adria or Apulia, which has been alternatively interpreted as a promontory of the African continent (Channell et al., 1979; Schettino and Turco, 2011) or as an independent continental block, separated from Africa by an oceanic corridor (Dercourt et al., 1986; Stampfli and Mosar, 1999, Bosellini, 2002, Zarcone et al., 2010, van Hinsbergen et al., 2020 for a review on the promontory vs. microplate controversy). Carbonate platform sedimentation was established over large areas in the Late Triassic and persisted with minor interruptions

Fig. 2 - Tectonic map (a) and schematic geological cross-sections (b) of the central and southern Apennines. From Vitale and Ciarcia (2003).



until the Late Cretaceous (Fig. 3). After a long phase of subaerial exposure, neritic carbonate sedimentation was locally re-established in the Eocene with the foraminiferal limestones and characean marls of the Trentinara formation (Selli, 1962) and again in the Early Miocene, with the red algae and bryozoan limestones of the Roccadaspide, Cerchiara, and Cusano formations (Selli, 1957). This last phase of shallow-water carbonate sedimentation was eventually terminated in the Middle Miocene by drowning below the photic zone, followed by the deposition of deep-water siliciclastics (Lirer et al., 2005; Patacca and Scandone, 2007).

The oldest outcropping deposits of the ApCP, exposed in the Picentini Mountains (Salerno), consist of massive dolostones, known as the "*dolomia massiva di base*" formation ("basal massive dolostone" fm). A probable Carnian age is accepted for these unfossiliferous unit, based on the Carnian age of the overlying "*calcari e marne ad Avicula e Myophoria*" formation ("limestones and marls with *Avicula* and *Myophoria*"). The overlying Norian-Rhaetian "*dolomia superiore*" formation ("upper dolostone" formation), the southern Apennines equivalent of Dolomia Principale of the southern Alps (Berra et al., 2007; 2010; Caggiati et al., 2018), is mainly represented by peritidal dolostones. This formation is exposed over a very wide area, from the Matese Mts., at the border between Campania-Molise and Lazio, to the Pollino ridge in northern Calabria. Upper Norian-Rhaetian restricted intraplatform basinal facies, bordered by microbial-serpulid buildups, are locally present in the Picentini Mts. (Iannace and Zamparelli, 1996; Zamparelli et al., 1999). Upper Norian-Rhaetian platform margin facies with corals and sponges, with facies similar to the "Dachstein Limestone" of the Calcareous Alps, occur locally in the Mt Marzano area and in Matese Mts. (Iannace and Zamparelli, 2002; Iannace et al., 2005). The total outcropping thickness of Upper Triassic units is about 1800-2000 m.

The Jurassic is mainly represented by inner platform peritidal and lagoonal facies, which are lithostratigraphically subdivided into the Lower Jurassic *Calcari a Palaeodasycladus* formation (*Palaeodasycladus* Limestones), the Middle Jurassic "*calcari oolitici e oncolitici*" formation ("oolitic and oncolitic limestones") and the Middle-Upper Jurassic "*calcari con Cladocoropsis e Clypeina*" formation ("*Cladocoropsis* and *Clypeina* limestones") (Fig. 3). The upper part of the *Calcari a Palaeodasycladus* is made by the well-known "*Lithiotis* member", characterised by the occurrence of biostromes of lithiotid bivalves, a biofacies that is widely distributed in the carbonate platforms of the Tethyan domain (Fraser et al., 2004; Posenato et al., 2018 and references therein). Platform-margin facies with *Ellipsactinia* buildups, well known more to north in the Marsica area (Abruzzo; Rusciadelli et al., 2011) and to the east in the Gargano Promontory (Puglia; Morsilli and Bosellini, 1997; Kiani Harchegani and Morsilli, 2019), are poorly represented in the southern Apennines, where they only occur in the Capri Island (Barattolo and Pugliese, 1987). The total thickness of Jurassic units is about 1300-1400 m.

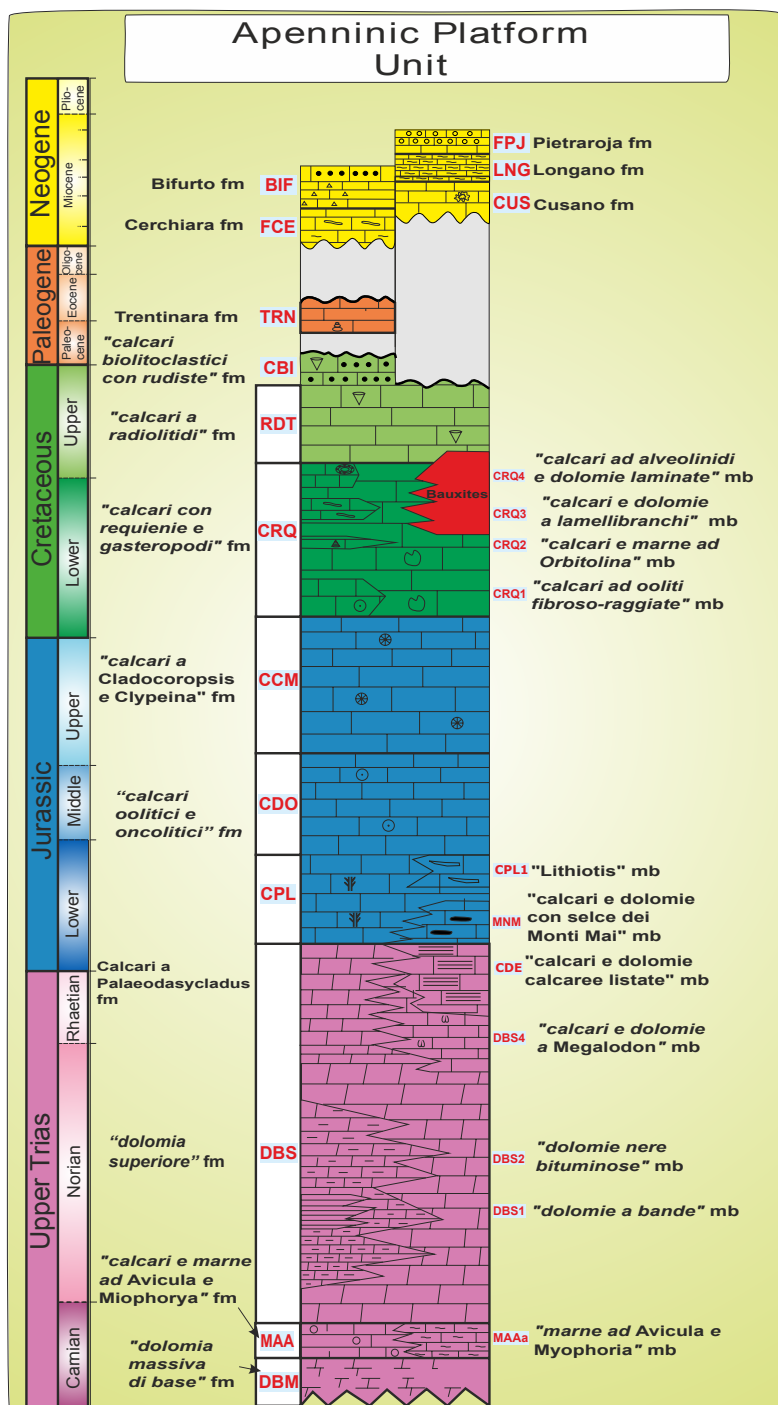


The Cretaceous platform carbonates of the southern Apennines are mainly represented by two lithostratigraphic units: the Berriasian-Cenomanian "*calcarei con requienie e gasteropodi*" formation ("requienid and gastropod limestones") and the Turonian-Campanian "*calcarei a radiolitidi*" formation ("radiolitid limestones"), (Fig. 3). The total thickness of Cretaceous platform carbonates is about 1000-1200 m. The "requienid and gastropod limestones" are represented by inner platform peritidal and lagoonal facies, with fossil associations dominated by calcareous algae (mainly dasycladaleans), benthic foraminifers (including orbitolinids and alveolinids), gastropods and bivalves (mainly requienid rudists). A distinctive facies, consisting of grainstone-rudstone with oversized radial-fibrous calcitic ooids, is found in the lowermost part of this formation, straddling the boundary with the underlying "*Cladocoropsis* and *Clypeina* limestones" (D'Argenio et al., 1975; see also Husinec and Read, 2006, describing the coeval occurrence of this facies in the Adriatic Carbonate Platform). Higher-up there is a m-thick very distinctive level, named the "*Orbitolina* level", consisting of marly limestones crowded with flat orbitolinid shells (*Mesorbitolina parva* and *M. texana*). This level, which is dated as upper Aptian (Gargasian) by biostratigraphy and isotope stratigraphy (Raspini, 1998; D'Argenio et al., 2004; Di Lucia et al., 2012 and references therein), represents a key level for the chronostratigraphic calibration of the biostratigraphic schemes of the ApCP. The uppermost part of the "requienid and gastropod limestones" is represented by the Cenomanian "alveolinid limestones", an interval characterised by high diversity and rich larger foraminiferal assemblages, dominated by alveolinids and soritids. In the Cilento promontory and in the Basilicata-northern Calabria sector the upper Cenomanian, starting with the *Cisalveolina fraasi* level, is represented by an interval of mottled dolostones and dolomitic limestones with selectively dolomitised *Thalassinoides* burrows (Martelli and Nardi, 2005; Bonardi et al., 2016).

In the southern sector of the ApCP, the upper Cenomanian levels of the "requienid and gastropod limestones" are conformably overlain by the Turonian-Campanian "radiolitid limestones". A different stratigraphy occurs more to the north, starting from the Taburno-Camposauro and Matese-Monte Maggiore areas and continuing into the Lazio and Abruzzi sector of central Apennines. There, sedimentation was interrupted, across the Albian-Turonian time interval by one or two subsequent episodes of prolonged subaerial exposure (Fig. 3). Stratigraphic gaps are of variable duration in different areas and are marked by a bauxite level, associated with the main stratigraphic gap, and the occurrence of a complex network of palaeokarstic cavities in the Lower Cretaceous and Cenomanian substrate (see Carannante et al. 1994; D'Argenio and Mindszenty, 1995; Carannante et al., 2009; D'Argenio et al., 2011 and references therein).



Following the abrupt disappearance of the high-diversity larger foraminiferal assemblages of the upper Cenomanian, which has been associated with the Oceanic Anoxic Event 2 (Parente et al., 2007, 2008), the “radiolitid limestones” starts with a 60-80 m thick poorly fossiliferous interval, generally dated as Turonian (Fig. 3). This is overlain by Coniacian-Campanian rudist-rich limestones. The depositional system and fossil associations of the Upper Cretaceous rudist limestones have been described in several papers (see Simone et al., 2003 for a synthesis and an exhaustive reference list). Two end-member depositional settings have been recognised based on sedimentological, taphonomic, and palaeontological characters. In the more external and/or high-energy areas, rudist lithosomes are thicker, grade laterally into clean bioclastic grainstone, and are made of highly diversified rudist assemblages dominated by large hippuritids and thick-shelled radiolitids and plagiptychids. In more internal and/or low-energy areas, rudist-rich beds alternate with fine-grained foraminiferal limestones and are characterised by oligotypic rudist assemblages dominated by small radiolitids. Ammonites, planktic foraminifers and calcareous nannofossils, which are the foundation of Mesozoic biochronology, have never been found in the Mesozoic platform carbonates of the southern Apennines. Biostratigraphic zonations, based mainly on calcareous algae and benthic foraminifers, have been erected and refined since the 60’s of past century (Sartoni and Crescenti, 1962; De Castro, 1991; Chiocchini et al., 2008 and references therein). The main limitation of these biozonations, even in their most recent version (Chiocchini et al., 2008), is the low resolution. The average duration of biozones is about 7 Myr in the Late Triassic and Jurassic, 9 Myr in the Early Cretaceous, 6 Myr in the Late Cretaceous (see Chiocchini et al., 2008). An even worse drawback is the poor chronostratigraphic calibration, which severely hampers correlation with coeval deep-water successions. While the succession of the biozones is firmly established, the chronostratigraphic age of the biostratigraphic events is at most tentative. These problems have been recently tackled by integrating biostratigraphy with carbon and strontium isotope stratigraphy and with cyclostratigraphy. Resolution in the range of 20-100 Kyr has been attained by cyclostratigraphy for the late Valanginian to early Albian interval, using a combination of carbon isotope stratigraphy and biostratigraphy to constrain the cycle duration (see D’Argenio et al., 1999; Amodio et al., 2013a, b, and references therein). Carbon isotope stratigraphy has been used to increase stratigraphic resolution and for chronostratigraphic calibration of biostratigraphic events in the intervals straddling the three major Mesozoic Oceanic Anoxic Events (namely the early Toarcian OAE, Trecalli et al., 2012; the early Aptian OAE1a, Wissler et al., 2004; Di Lucia et al., 2012; the late Cenomanian OAE2, Parente et al., 2007, 2008). Finally, strontium isotope stratigraphy and carbon isotope stratigraphy have been used to increase resolution and chronostratigraphic dating in the late Cenomanian-middle Campanian interval (Frijia et al., 2015).



After a long stratigraphic gap, encompassing the late Campanian to Palaeocene, shallow-water carbonate sedimentation resumed with the Eocene "Trentinara formation" (Selli, 1962; Fig. 3), but only in limited areas, distributed mainly from the Cilento promontory, in southern Campania, to the Pollino massif, at the northern border of Calabria. Even more sparse outcrops are present more to the north in the Aurunci Mts ("Spirolina facies" in Chiocchini and Mancinelli, 1977). The "Trentinara formation" has a very variable thickness, from a few metres to 120-150 m. It consists mainly of inner platform algal-foraminiferal limestones, with lenticular intercalations of marls and clays representing palaeosols and palustrine deposits. The biostratigraphy of the "Trentinara formation" is based on calcareous algae and larger benthic foraminifera, documenting an early to middle Eocene age (Ypresian-Lutetian) (Vecchio et al., 2007; Vecchio and Hottinger, 2007).

After another phase of prolonged subaerial exposure, encompassing at least the late Eocene and the Oligocene, the "Trentinara formation" is overlain by Lower Miocene open shelf limestones with red algae, bryozoans and ostreid bivalves, which are named "Cerchiara formation" (Bonardi et al., 2016) in the Pollino-Basilicata area and "Roccadaspide formation" in the Cilento promontory (Selli, 1957; Carannante et al., 1988). These deposits mark the beginning of a synorogenic transgressive cycle, which is deposited above the forebulge unconformity generated by the flexural bending of the foreland plate. More to the north, i.e., in the Matese area, the Miocene transgressive limestones with red algae and bryozoans of the "Cusano formation" rest directly above the Cretaceous rudist limestones (Fig. 3). More details on the facies

Fig. 3 - Lithostratigraphy of the Apennine Carbonate Platform (ApCP).

<https://doi.org/10.3301/GFT.2022.06>



and palaeoenvironmental interpretation of the “Cusano formation” can be found in [Carannante and Simone \(1996\)](#) and in [Bassi et al. \(2010\)](#). Equivalent facies in the Latium-Abruzzi sector of the Apennines have been referred to the “*calcari a briozi e litotamni*” formation (“bryozoan and lithotamnion limestones”; see [Brandano et al., 2010](#) and references therein). The age of the Lower Miocene transgressive deposits of the southern Apennines (“Cerchiara”, “Roccadaspide”, and “Cusano” formations) is only constrained by the sparse occurrence of miogypsinid larger benthic foraminifera. More precise dating has been recently obtained by strontium isotope stratigraphy ([Sabbatino et al., 2020, 2021](#)).

The Upper Triassic to Lower Cretaceous carbonates of the southern Apennines are generally referred to flat-topped, tropical carbonate platforms, dominated by chloralgal or chlorozoan associations (*sensu* [Lees, 1975](#)), whereas the depositional system of the Upper Cretaceous rudist limestones has been interpreted as a temperate-type open shelf dominated by foramol assemblages (*sensu* [Lees, 1975](#); [Carannante et al., 1995, 1997](#)). The Lower Miocene shallow-water carbonates of the southern Apennines can be referred to a foramol-rhodalgal carbonate factory (*sensu* [Carannante et al., 1988](#)). Modern and fossil examples of foramol/rhodalgal deposits develop in temperate to cool water open shelves (see [Pedley and Carannante, 2006](#) and references therein) and are characterised mainly by heterozoan assemblages ([James, 1997](#)).



## DAY 1

Starting from Naples, you will follow northwards the highway A1 to Caserta Sud. (Fig. 1). Then, you will approach the calcareous mountains of the Apennines, mercilessly incised by large limestone quarries, and underpass the "Ponti della Valle", a roman-fashion aqueduct built in the XVIII century by the dutch architect Luigi Vanvitelli to divert waters for the gardens and waterfalls of the Caserta Royal Palace. Following the "Fondo Valle Isclero" highway, you will reach Telesse, a little town proud of its sulphide-rich (and smelly) waters, and after a few kilometres, you will reach the southern slopes of the Matese massif. A few kilometres before arriving at the San Lorenzello village, you can admire the Mesozoic thick sequence of Mt Monaco di Gioia (Upper Triassic/mid-Cretaceous).

At San Lorenzello village, the road ascends the southeastern flank of the Monaco di Gioia massif, where you will observe the cyclic organisation of the shallow-water platform carbonates. Leaving San Lorenzello, you will pass the Cerreto Sannita village and get in the Titerno River canyon, a deep gorge excavated within the Cretaceous eastern slopes of Mt Monaco di Gioia-Mt Cigno. Crossed a gallery, you enter the Titerno valley, a large depression that has preserved the younger Miocene terrigenous deposits in its downfaulted interior, while all around stand the high cliffs of Jurassic/Cretaceous and Miocene carbonates. To the East a tectonic line runs at the horizon, marking the thrust of the basinal "Sannitic Units" (Cretaceous-Miocene) over the Triassic-Miocene carbonate platform units of the Matese massif.

After Pietraroia, the road climbs up the southern slope of Mt Mutria, where, at the locality Regiapiana, you will stop to look at the bauxite deposits, marking a long gap within the Cretaceous carbonate platform succession, and at the transgressive Lower Miocene shallow-water limestones unconformably overlying the Cretaceous substrate.

### **Stop 1.1: San Lorenzello section. An example of Milankovitch cyclicity in shallow-water platform carbonates of the Valanginian/Hauterivian (41°16'49.16"N – 14°32'23.24"E)**

The San Lorenzello section is well exposed along a roadcut, which starts from the village and arrives to the viewpoint of Colle la Sella-La Pizzuta (Fig. 4). This road traverses the southeastern slope of the Mt Monaco di Gioia (Fig. 5). The section is ~ 240 m thick, late Valanginian – late Barremian in age. Detailed studies of biostratigraphy, sedimentology, cyclostratigraphy, sequence-stratigraphy, and C-isotope stratigraphy



Fig. 4 - Google Earth view of the southeastern slope of Mt Monaco di Gioia, showing the roadcut of stop 1.1.

(D'Argenio et al., 1997; Ferreri et al., 2004; Amodio, 2006; Amodio et al., 2008, 2018, 2020; Martino et al., 2019; Barattolo et al., 2021; Amodio et al., 2023) have been carried out. This stop centres on the first 90 m.

### Sedimentology

By following the standard facies analysis (e.g., Flügel, 2010), textures, grain types (skeletal and non-skeletal), sedimentary and early diagenetic structures have been sequentially tabulated, so that four lithofacies associations, including seven lithofacies, have been identified (Table 1).

It is essential for readers unfamiliar with some sedimentological terms

to give specific definitions that are ascribed to them. *Lithofacies* is defined as a discrete rock volume (i.e., a bed, or part of it), which can be distinguished by its primary characteristics (textures and sedimentary structures, grain types, variety, and abundance of fossil associations), which allow an identification with respect to its adjacent over- and underlying deposits (*sensu* D'Argenio et al., 1997). A lithofacies is considered to have formed in a specific depositional (sub)environment and can present a variable degree of modification due to early diagenesis in a marine and/or meteoric environment. However, a more precise interpretation of the original depositional environment requires the identification of lithofacies associations.

*Lithofacies associations* are representative of relatively more extensive carbonate platform areas (e.g., open lagoon, restricted lagoon, tidal flat) and are expressed by rock volumes whose composition includes a certain number of lithofacies (deposited in related sub-environments). For these groups of lithofacies, the textures and



Fig. 5 - Mt Monaco di Gioia: panoramic view from south.

sedimentary structures, together with the fossil assemblages, indicate similar genetic conditions linked to the chemistry (e.g., salinity, oxygenation) and physics (e.g., turbulence) of the environment. Some deposits, which occur as episodic intercalations within the various lithofacies associations, represent the product of a sudden rise in hydrodynamic energy caused by wave, current and/or storm activity, and can be generically interpreted as tempestites (*sensu*

Aigner, 1985). Tempestites are deposited on large areas of the platform and by their nature are considered as trans-environmental events (not belonging to a specific environment).

The biostratigraphic analysis, mainly carried out on benthic foraminifers and calcareous algae (Martino et al., 2019; Amodio et al., 2020; Barattolo et al., 2021), is based on the Early Cretaceous biozonation schemes for the Tethyan carbonate platforms (De Castro, 1991; Carras et al., 2006; Chiocchini et al., 2008).

The San Lorenzello section consists of well-bedded grey limestones and whitish to grey dolomitic limestones (wackestones, packstones) with benthic foraminifers, green algae, and molluscs (subtidal deposits). Mudstone and loferitic mudstone-wackestone (peritidal deposits) horizons are subordinate (Fig. 6). High-energy deposits of intraclasts, ooids, and bioclasts with erosional bases locally form episodic intercalations (tempestites). The upper surfaces of beds commonly show evidence of subaerial weathering, with karstic cavities infilled by greenish clayey calcisiltites, which can also form thin, discontinuous horizons. Dolomitisation, recorded in some intervals, characterises frequently the upper part of beds, where also calcrete horizons locally occur.



Table 1 - San Lorenzello section (stop 1.1):

Lithofacies description grouped in lithofacies associations and their depositional environments.

LITHOFACIES ASSOCIATIONS	LITHOFACIES	DEPOSITIONAL ENVIRONMENT
MOLLUSCAN LIMESTONES (M)	<p><b>M1:</b> wackestone, bioturbated wackestone-packstone and floatstone with benthic foraminifera, calcareous algae, bivalves (mainly ostreids and requienids), gastropods (nerineids), peloids, intraclasts.</p> <p><b>M2:</b> wackestone and bioturbated wackestone-packstone with benthic foraminifera, small and thin molluscs, cyanophyceans, codiaceans and peloids.</p>	OPEN LAGOON
BIO-PELOIDAL LIMESTONES (BP)	<p><b>BP1:</b> packstone, packstone-grainstone and grainstone with bioclasts (benthic foraminifers ostracods, calcareous algae, molluscs), intraclasts, ooids and peloids.</p> <p><b>BP2:</b> wackestone-packstone, packstone with peloids, benthic foraminifera, <i>Cayeuxia</i> sp., small gastropods, rare calcareous algae.</p>	INNER SHOALS
FOR-OSTRACOD LIMESTONES (FO)	<p><b>FO1:</b> wackestone-packstone and wackestone, with benthic foraminifera, ostracods, small gastropods, rare calcareous algae (small <i>Salpingoporella</i> spp. and <i>Clypeina</i> spp.) and rare peloids.</p> <p><b>FO2:</b> wackestone, wackestone-mudstone and mudstone locally bioturbated with miliolids, ostracods, rare small <i>Salpingoporella</i> sp. and <i>Cayeuxia</i> sp.</p>	RESTRICTED LAGOON
LAMINATED LIMESTONES (L)	<p><b>L1:</b> Loferitic mudstone and bindstone with microbial mat, small intraclasts, peloids and rare ostracods.</p>	TIDAL FLAT

### Cyclostratigraphy

In the studied section, 86 shallowing-upward elementary cycles have been recognised, normally corresponding to single beds. They are revealed by vertical changes in lithofacies and by related early diagenetic features, testifying to a variable water depth and environmental oscillations (i.e., from more open marine to more

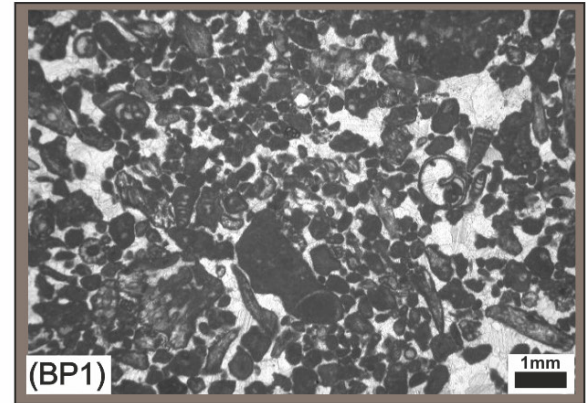
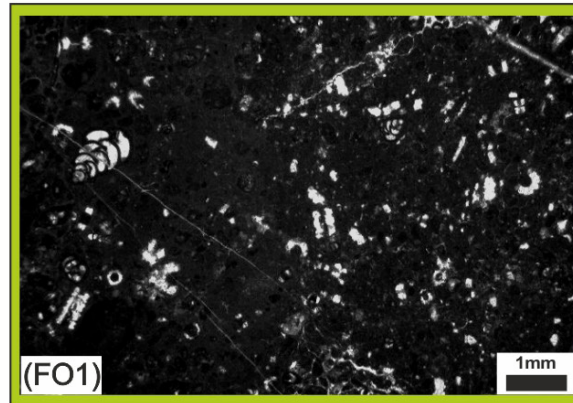
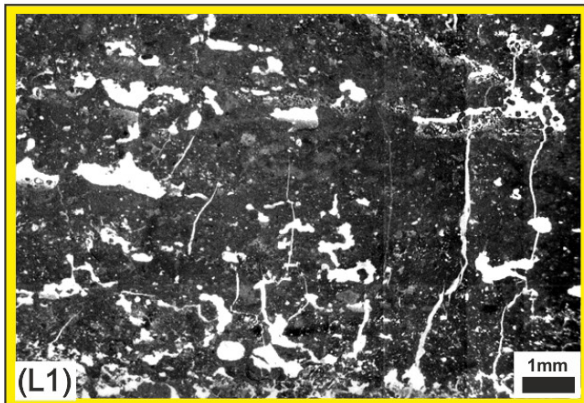
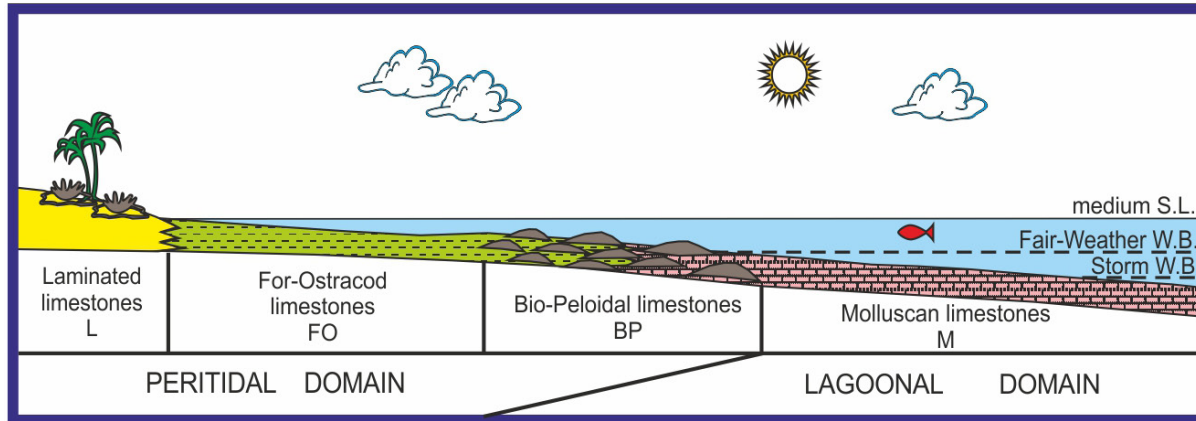
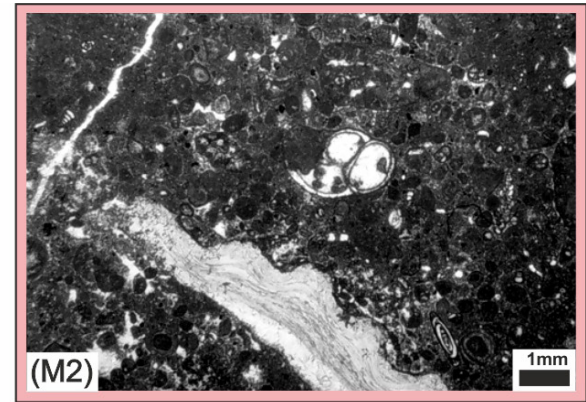
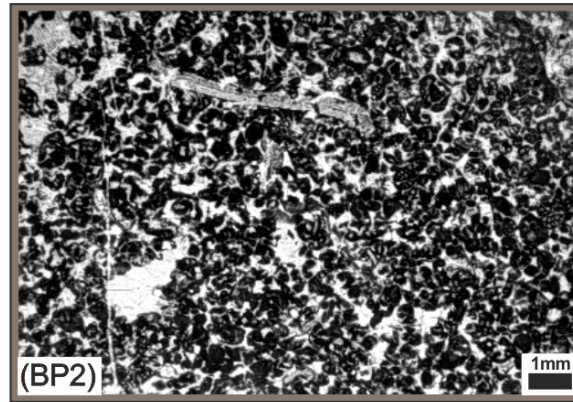
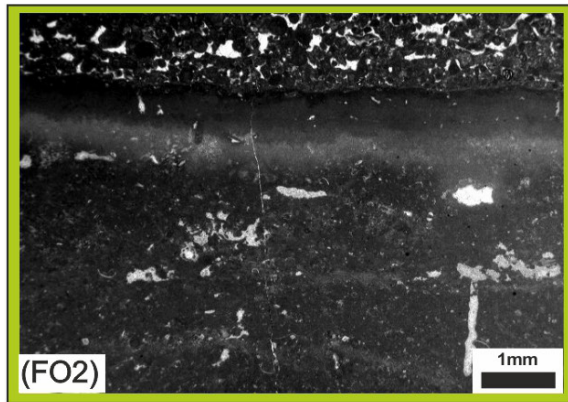


Fig. 6 - Main lithofacies in thin section and related environmental model. See Table 1 for the description of lithofacies.



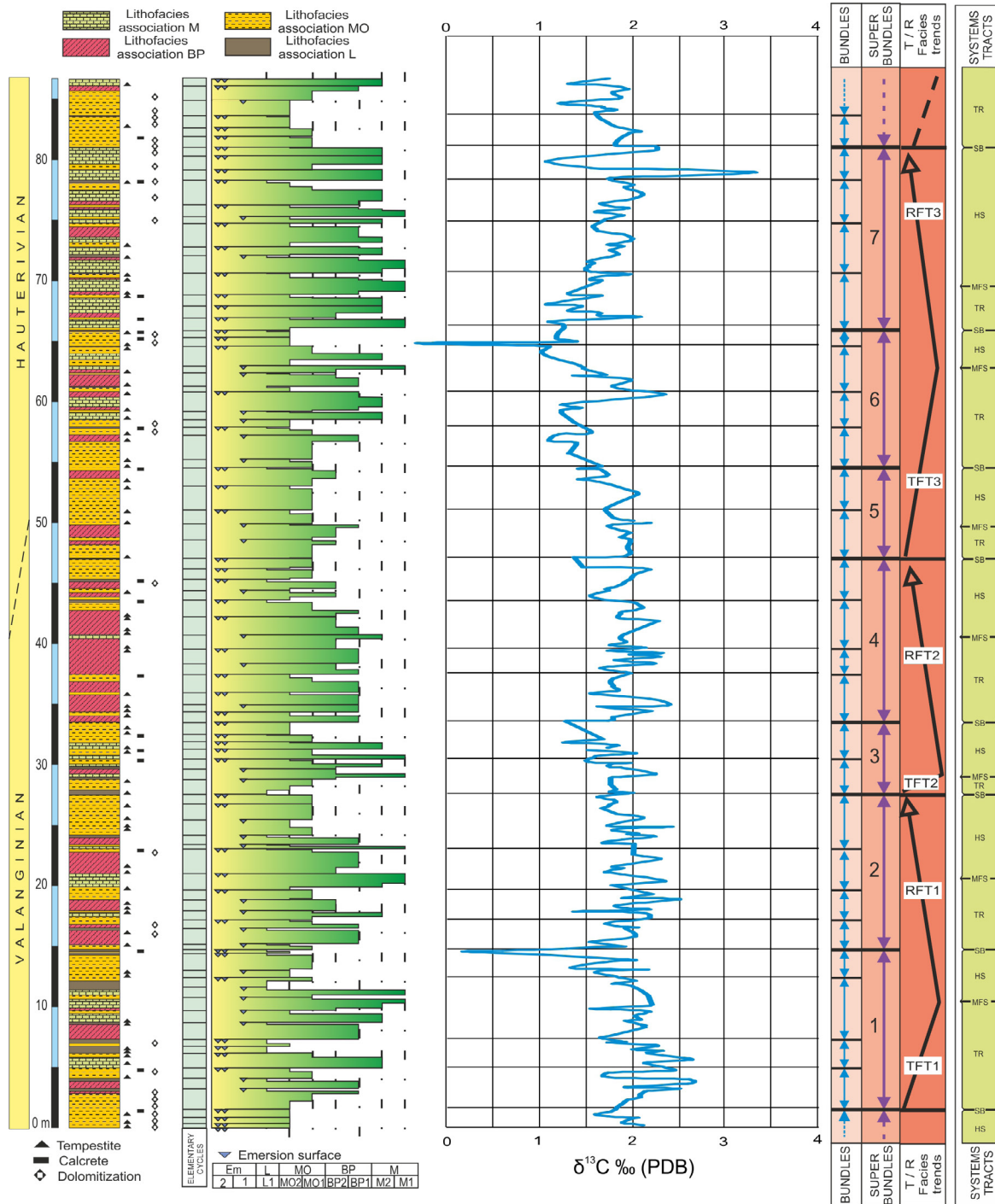
restricted conditions; D'Argenio et al., 1997; Ferreri et al., 2004; Amodio, 2006) (Fig. 7). Fifty-nine elementary cycles show subaerial diagenetic caps directly superimposed on subtidal deposits, while only 27 elementary cycles show subaerial exposure superimposed on tidal flat deposits. The upper surfaces of the elementary cycles are variably overprinted by early meteoric diagenetic modifications, which allow for the definition of two different types of cycle boundaries: Em1-boundaries, characterised by microkarst and weak pedogenesis; Em2-type boundaries, characterised by karst and/or palaeosoils. In the latter case, the meteoric overprint is enhanced and deeply penetrates the cycle, implying more prolonged emersion.

The elementary cycles (alias sedimentary cycles), as here used following the cyclostratigraphic approach, represent one succession of lithofacies that repeats itself many times in the sedimentary record and that is, or is inferred to be, causally linked to an oscillating system and, as a consequence, is (nearly) periodic and has time significance (Strasser et al., 2004).

If a sequence of lithofacies associations and their early diagenetic features are analysed at cm-scale along discrete (3-4 metres) intervals, a grouping of few elementary cycles (bundles) emerges (Fig. 7). Each bundle can be viewed as a small facies sequence with a deepening-shallowing trend delineating a larger environmental oscillation. The limits of bundles correspond to elementary cycle boundaries marked by deeper meteoric diagenesis (Em1- or Em2-type discontinuity surface). Moreover, taking into account very marked bundle limits, larger groups of cycles (superbundles) can be recognised. Each superbundle shows a deepening-shallowing facies sequence, formed by 2-4 bundles. Elementary cycles and their groups imply hierarchically ordered environmental oscillations of different frequencies.

The systematic development of emersion-related features, which characterise the top of the cycles (very often entirely developed in the subtidal domain before their emersion), claims for a control due to sea level oscillations and precludes an interpretation based on autocyclic processes of tidal flat retrogradation-progradation. Other genetic mechanisms, like subsidence pulsation of tectonic origin, can be also excluded because the ApCP was in its late stage of thermal subsidence during Valanginian-Hauterivian time and was characterised by very constant subsidence rates.

The mechanism that can best explain both the hierarchical organisation of these cyclic sequences and the diffusion of emersion overprinted subtidal cycles is an orbitally driven (Milankovitch-type), high-frequency sea-level fluctuation (D'Argenio et al., 1997, 1999; D'Argenio et al., 2004; Ferreri et al., 2004; D'Argenio et al., 2008, 2011). The 86 elementary cycles are organised in 25 bundles and in 7 superbundles (SL1 to SL7), with an average thickness of 324 cm and 1138 cm, respectively (Fig. 7). Elementary cycles have been related to the



precession and/or the obliquity signals, while bundles and superbundles are considered to record the short- and long-eccentricity periodicities, respectively (Brescia et al., 1996; D’Argenio et al., 1997; Tagliaferri et al., 2001; Ferreri et al., 2004). The orbital cycles appear superimposed on longer ( $\geq 800$  Kyr) Transgressive/Regressive Facies Trends (T/RFTs) that can be considered as 3<sup>rd</sup> order cycles (*sensu* Vail et al., 1991). Stacking pattern of the superbundles suggests 3 complete T/RFTs (SL1+SL2=T1/R1, SL3+SL4=T2/R2 and SL5 to SL7=T3/R3) (Fig. 7).

### Sequence stratigraphy

Even if this inner sector of the platform shows prevailing aggradational geometry, the superbundles and T/RFTs can be interpreted

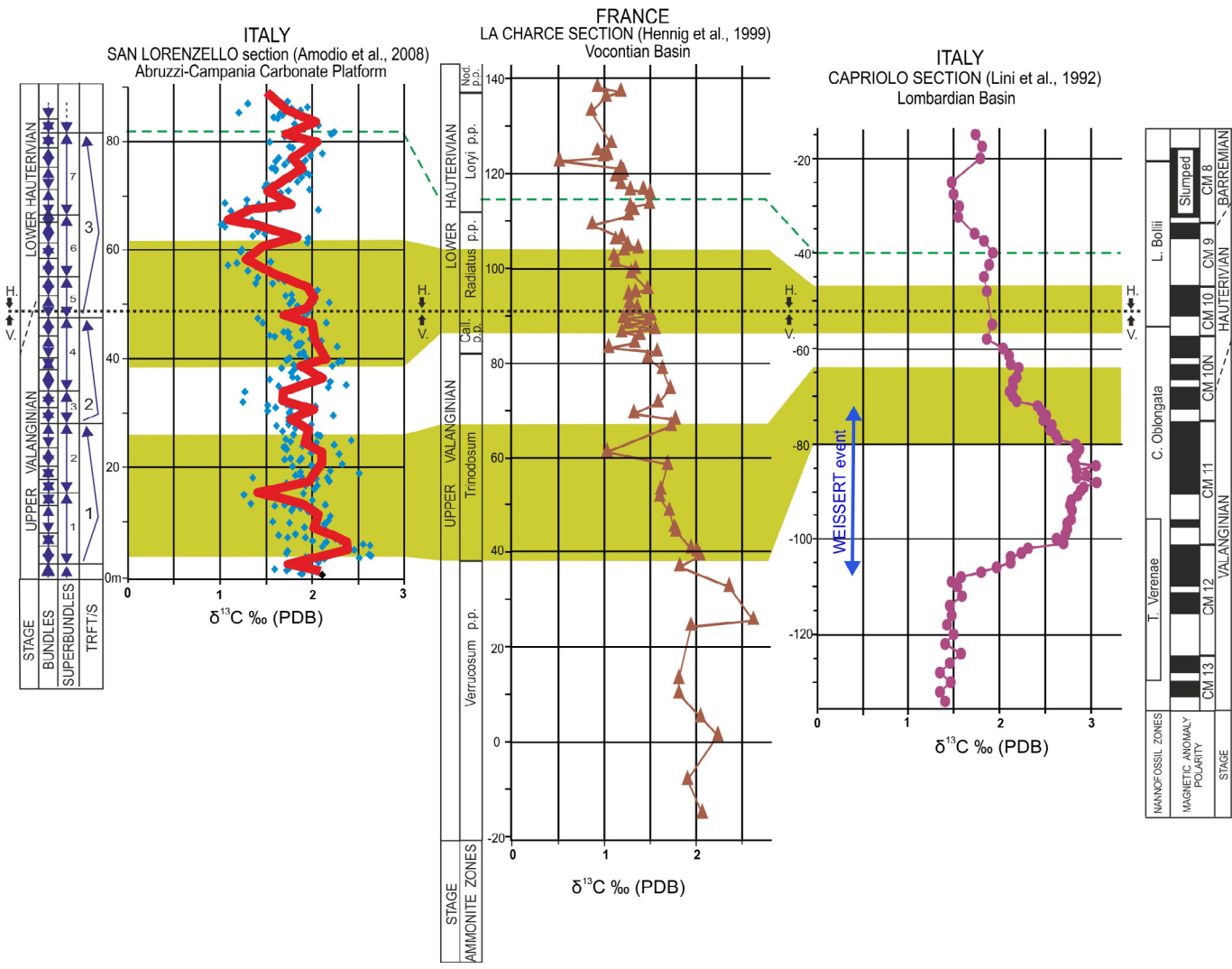
Fig. 7 - San Lorenzello lithostratigraphy. From the left to the right: age, thickness, lithostratigraphic column based on the lithofacies associations, lithofacies histogram created by cyclic organisation of the sediments and their early diagenetic features (elementary cycles); C-isotope stratigraphy, cyclostratigraphy and sequence stratigraphy. T/RFTs = Transgressive/Regressive Facies Trends; TR=Transgressive systems tract; HS=Highstand systems tract; MFS=maximum flooding surface; SB=sequence boundary. Key for lithofacies associations and lithofacies see Table 1 (from Amodio et al., 2008, modified).



in terms of depositional sequences and systems tracts, irrespective of the eustatic control on the cyclicity (D'Argenio et al., 1997, 1999, 2008, 2011). In particular, the facies trends and stacking patterns within the superbundles allow to delineate, also at outcrop scale, the position of sequence boundaries and maximum flooding surfaces (Goldhammer et al., 1990; Schlager et al., 1994; D'Argenio et al., 1997, 1999). The sequence boundaries correspond to superbundle limits, while the maximum flooding surfaces are indicated by the most open marine lithofacies associations (Amodio, 2006, 2010). Within each superbundle the transgressive systems tract is characterised by lithofacies associations, and their related early diagenetic features, denoting more open lagoonal settings and a prevailing early marine cementation. In contrast, the highstand systems tract, above a maximum flooding surface, is characterised by a stacking pattern of elementary cycles and bundles that match aggradational and/or regressive trends (D'Argenio et al., 2004; Wissler et al., 2004; Amodio et al., 2011, 2013a, b; Amodio and Weissert, 2017). Using these criteria, also the T/RFTs can be interpreted in terms of sequence stratigraphy (Fig. 7). In the San Lorenzello section, 7 depositional sequences (SL1-SL7) and 3 T/RFTs have been defined.

### Carbon-isotope stratigraphy

Amodio et al. (2008) added a high-resolution carbon-isotope stratigraphy (Fig. 7) to this section, demonstrating that the influence of the depositional environment and diagenesis on the  $\delta^{13}\text{C}$  signal is negligible and that the carbon-isotope ratio of bulk carbonate in this carbonate platform setting recorded a signal comparable to that of the global open ocean. The long-term  $\delta^{13}\text{C}$  oscillations were correlated with the coeval reference curves from the hemipelagic La Charce (Vocontian Basin, France, Hennig et al., 1999) and from the pelagic Capriolo (southern Alps, northern Italy, Lini et al., 1992) sections, although the shallow-marine  $\delta^{13}\text{C}$  profile was more "noisy" than the pelagic ones (Fig. 8). This correlation suggested that only the upper part of the "Weissert event" (*sensu* Erba et al., 2004) is recorded in the San Lorenzello section. The available data allowed calibrating the platform section using the ammonite biozonation of La Charce section (Bulot et al., 1992) and the magnetostratigraphy of Capriolo section (Channell et al., 1993). A good correspondence has been recently demonstrated between the position of the Valanginian-Hauterivian boundary in the San Lorenzello section, as constrained by the shallow-water biostratigraphy (Martino et al., 2019; Amodio et al., 2020, 2023) and the position indicated by C-isotope stratigraphy (Amodio et al., 2008) (Fig. 9). A new biostratigraphic event has been well calibrated by C-isotope stratigraphy: *Selliporella johnsonii* (Praturlon, 1964) nov. comb. appears at the end of the Weissert event and disappears at the Valanginian-Hauterivian boundary (Barattolo et al., 2021). This taxon exhibits a short



stratigraphic distribution in a time interval characterised by recovery of carbonate production soon after the Valanginian global crisis.

**Orbital chronostratigraphy**  
 Cyclostratigraphy can be used not only to undertake high-resolution correlations of carbonate platform successions cropping out at a great distance (D'Argenio et al., 2004; Ferreri et al., 2004; Wissler et al., 2004; Amodio et al., 2011, 2013a, b; Amodio and Weissert, 2017), but also to create chronostratigraphic charts based on orbital duration of bundles and superbundles. Such charts are based on the assumptions that: a) the superbundles are depositional sequences induced to long-eccentricity cycles (400 Kyr, in D'Argenio et al., 1997); b) the maximum flooding surfaces of superbundles are isochronous; c) the highest probability of omission in the stratigraphic record is at the boundaries of the T/RFTs. The estimated orbital chronostratigraphy indicates that the whole interval (SL1-SL8 base) lasted not less than 3.0

Fig. 8 - Correlation of the San Lorenzello  $\delta^{13}\text{C}$  curve with the pelagic sections of La Charce (Hennig et al., 1999) and Capriolo (Lini et al., 1992). The thick red line represents a smoothed curve resulting from 15-point running average filter. The green bands highlight time-equivalent intervals characterised by analogous  $\delta^{13}\text{C}$  patterns; the horizontal squared-line indicates the La Charce Valanginian-Hauterivian boundary and its time equivalent at San Lorenzello and Capriolo as suggested by the C-isotope correlation; the green dashed-line connects the uppermost isochronous C-isotope correlation points (from Amodio et al., 2008, modified).

<https://doi.org/10.3301/GFT.2022.06>

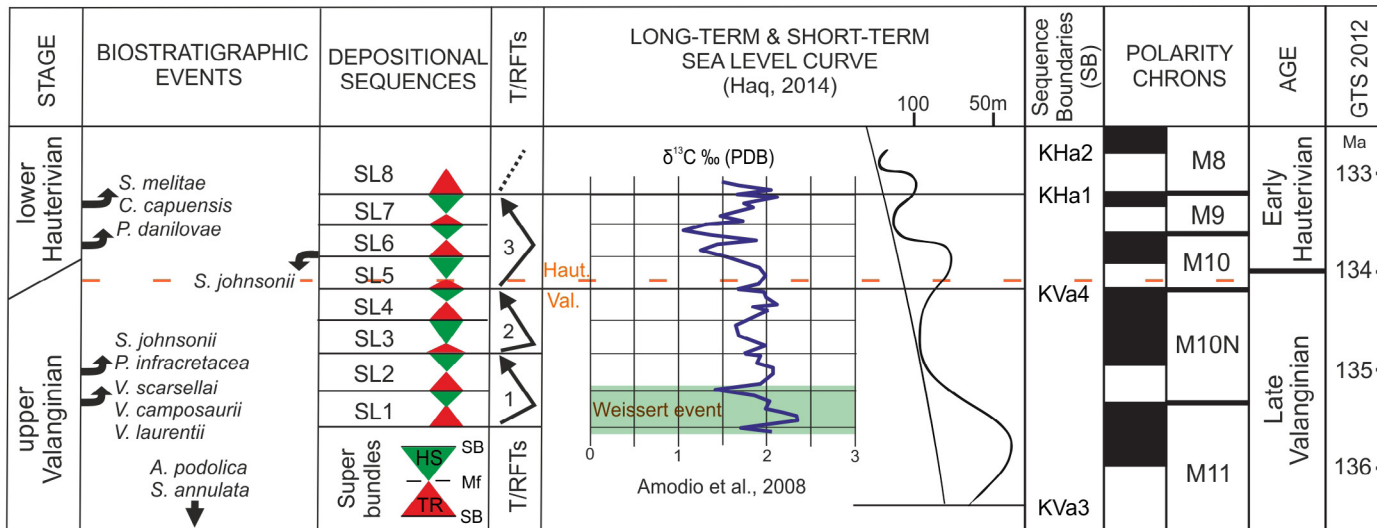


Fig. 9 - Biostratigraphic and sequence-stratigraphic (superbundles and T/RFTs) framework of the San Lorenzello section plotted against the "global" Sequence Boundaries revisited by Haq (2014) and anchored to the Valanginian-Hauterivian eustatic curve and the geochronology. The smoothed  $\delta^{13}\text{C}$  curve (Amodio et al., 2008) is showed on the left of the eustatic curve. The San Lorenzello section records the upper part of Weissert event as well as the precise location of the Valanginia-Hauterivian boundary, immediately below the last occurrence of *Selliporella johnsonii* (Martino et al., 2019; Barattolo et al., 2021).

Myr. This duration is comparable with that provided by the recent astrochronology of Martinez et al. (2015), which attributed to the equivalent interval of La Charce  $\delta^{13}\text{C}$  record an absolute age from 133.5 to 130.5 Ma (see Fig. 8, p. 169 in Martinez et al., 2015).

**Global correlation**

In order to better define the origin of the T/RFTs, their depositional architecture has been combined with their chronological ages obtained by the detailed biostratigraphy (Fig. 9). The results of previous C-isotope correlation (from SL1 to SL7) from Amodio et al. (2008), which includes the Valanginian-

Hauterivian boundary, have been also considered, to correlate the T/RFTs disconformities individuated at San Lorenzello with the SBs recently revisited and anchored to the Cretaceous global sea-level curve by Haq (2014). Consequently, the RFT peaks n. 2 and 3 of the San Lorenzello section have been correlated with the KVa4 and KHa1 sequence boundaries of Haq (2014), respectively (Fig. 9).

**Stop 1.2: The Early Miocene transgression at Pietraroja (41°20'59"N - 14°33'09"E)**

The village of Pietraroja is famous for its Lower Cretaceous "fossiliferous plattenkalk" ("*calcari selciferi e ittiolitiferi di Pietraroja*"; Catenacci and Manfredini, 1963) hosted in lower Albian lithographic limestones. The depositional environment of the plattenkalk has been debated for more than 50 years and variously interpreted

<https://doi.org/10.3301/GFT.2022.06>



either as a shallow lagoon or as an intra-platform basin. In the most recent and accurate reconstruction, the sequence hosting the *plattenkalk* is interpreted as an abandoned channel-fill sequence, documenting a major transgressive event (Carannante et al., 2006). Local tectonics created a very complex palaeotopography, with wide emerged areas contiguous to shallow-water carbonate banks and relatively deep-water channelised areas. The Pietraroja *plattenkalk* contains a very rich fauna of fossil vertebrates (fishes, reptilians, amphibians), molluscs, crustaceans, and fossil plants, which have been collected and described since more than 150 years (see Bravi and Garassino, 1998, and references therein; see also Bartiromo, 2013, for a recent description of the fossil plant remains). The most famous fossil of the Pietraroja *plattenkalk* is an exquisitely preserved juvenile individual of a theropod dinosaur, described as *Scipionix samniticus* (Dal Sasso and Signore, 1998; Dal Sasso and Maganuco, 2011), which became a local celebrity with the name of “Ciro”.

The Lower Cretaceous limestones are disconformably overlain by the Lower Miocene (Burdigalian-Langhian) “Cusano formation”. The deposits of the “Cusano formation” consist of several lithofacies, including bryozoan and melobesian grainstone-rudstone and floatstone, rhodolitic rudstone, melobesian bindstone, bryozoan and melobesian rudstone-floatstone with *Orbulina* wackestone matrix (Carannante et al., 1994). They have been referred to a foramol/rhodalgial carbonate factory (Carannante et al., 1988; Carannante and Simone, 1996). Modern and fossil examples of foramol/rhodalgial deposits have been mainly described in temperate-type open shelves and are characterised mainly by heterozoan assemblages (James, 1997). However similar facies occur also outside of temperate zone (Brandano et al., 2022). The absence of the reef-builders (typical of photozoan tropical platforms) along with the absence of significant early diagenetic processes (due to the prevailing low-Mg calcite composition of the foramol/rhodalgial assemblages) produces mainly loose carbonate deposits consisting of unlithified skeletal debris which are prone to re-mobilisation. In the foramol/rhodalgial systems, a significant part of the fossil sedimentary bodies represents re-mobilised to re-worked skeletal debris and only a minor part of the produced skeletal grains is normally preserved as *in situ* deposits. Off-shelf sediment transport is often routed through complex submarine channel networks. Examples of these channelised foramol-rhodalgial deposits have been described by Bassi et al. (2010) in the Pietraroja and Regia Piana areas.

In this stop, you will have a close look at the disconformity between the Lower Cretaceous “requienid and gastropod limestones” and the Lower Miocene “Cusano formation”, in a small, abandoned quarry just out of the Pietraroja village (Fig. 10). The lower part of the quarry wall exposes dark grey limestones with a mud-supported texture (mudstones-wackestones) (Fig. 11a). They can be dated as lower Aptian for the presence of *Sabaudia capitata*, *S. minuta*, *Cuneolina laurentii*, *Nezzazata isabellae*, and *Dictyoconus* cfr. *algerianus* (Fig. 11b).



Fig. 10 - Google Earth view of the area of Pietraroja. The white star marks the position of the small quarry of stop 1.2.

Above the disconformity, the basal interval of the “Cusano formation” is represented by about 4-5 metres of bryozoan and rhodolith floatstone, with a fine-grained matrix containing serpulids, fragments of thin-shelled bivalves, echinoid plates and spines, benthic foraminifera (including small rotaliids, *Heterostegina* sp., *Amphistegina* sp., *Operculina* sp., *Sphaerogypsina* sp.), and rare planktonic foraminifera (Fig. 11c). This lithofacies, corresponding to facies BLL-1 of Bassi et al. (2010), is also found in sedimentary dykes cutting the Lower Cretaceous substrate. A few metres upward, the first interval of the “Cusano formation” is truncated by an intensely burrowed and bioeroded submarine hardground (Fig. 11e). Above the hardground, sedimentation resumed with deposition of rhodolith rudstone to floatstone with a coarser-

grained matrix, containing ostreids, pectinids, echinoid fragments and spines, benthic foraminifera (including *Amphistegina* sp., *Sphaerogypsina* sp., small rotaliids) and rare planktonic foraminifera (Fig. 11d). These sediments, corresponding to facies BLL-2 of Bassi et al. (2010), have been deposited in a shallower environment and later re-mobilised and redeposited in a deeper-water channelised system.

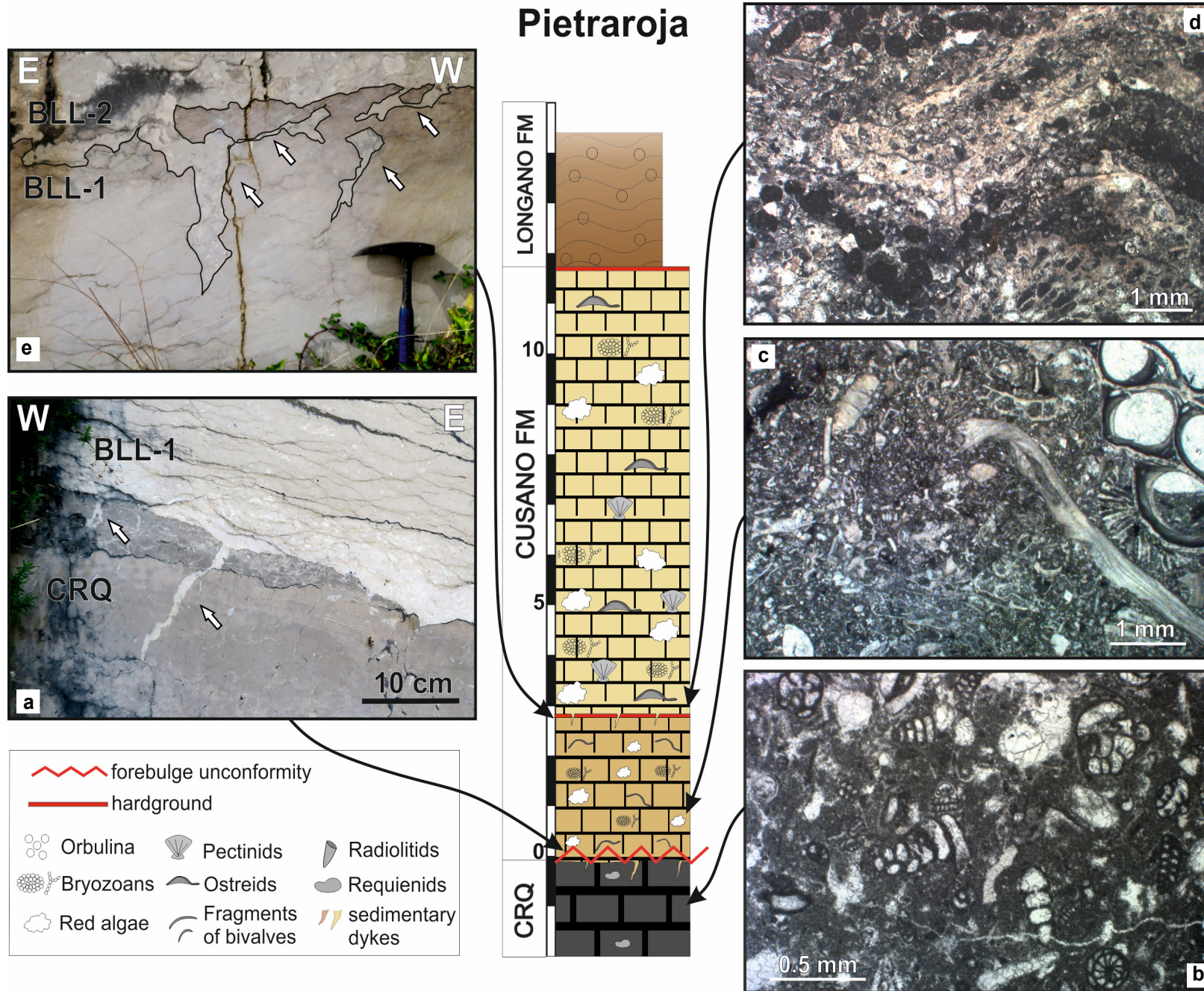


Fig. 11 - Schematic stratigraphy of the succession exposed in the area of Pietraraja. a) outcrop of the unconformity separating the Lower Cretaceous limestones (CRQ) from the Lower Miocene "Cusano formation" (BLL1). b) microfacies of the Lower Cretaceous limestones with *Saubadia* sp. and nezzatids. c) and d) microfacies of the Lower Miocene "Cusano formation". e) outcrop photograph of the hardground separating the two intervals of the Cusano (BLL-1/BLL-2). See text for further explanations.



### Stop 1.3: The mid-Cretaceous bauxites at Regia Piana (41°21'50"N - 14°31'46"E)

In this stop, you will look at the mid-Cretaceous bauxites interposed between the Lower Cretaceous "requienid and gastropod limestones" and the Upper Cretaceous "radiolitid limestones" in the Regia Piana locality. The outcrop can be easily reached by walking downslope from a bend in the road to Bocca della Selva (Fig. 12).

The outcrop can be easily reached by walking downslope from a bend in the road to Bocca della Selva (Fig. 12).

The bauxite horizon of Regia Piana is 0.5–2.0 m thick (Fig. 13). It extends laterally for more than 500 m, with several interruptions and pinch-out closures. Traces of previous exploitation are visible through a series of small galleries. Mining was active in discontinuous phases from 1920 to 1965 (Mondillo et al., 2011). The Lower Cretaceous limestones underlying the bauxite horizon are affected by pervasive meteoric dissolution penetrating as deep as ten metres. Larger palaeokarstic cavities, cm to dm in size, normally occluded by reddish to yellowish/greenish geopetal mechanical filling, are found in the beds immediately underlying the unconformity.

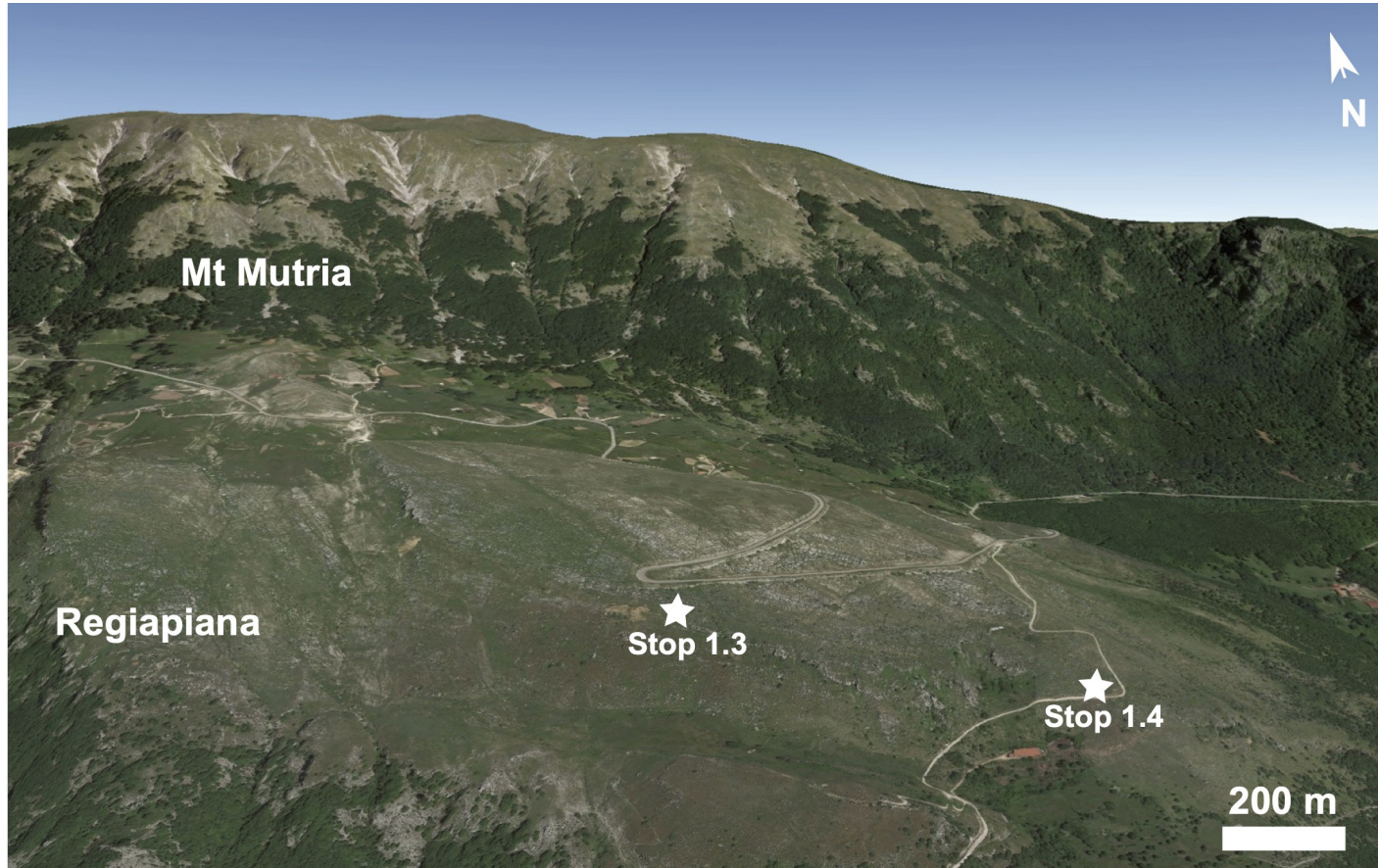


Fig. 12 - Google Earth view of the area of the Regia Piana, with Mt Mutria in the background. In stop 1.3 you will look at the bauxite horizon interposed between the Lower Cretaceous "*calcarei con requienie e gasteropodi*" formation and the Upper Cretaceous "*calcarei a radiolitidi*" formation. In stop 1.4 you will look at the "Cusano formation", overlying the forebulge unconformity, and at the phosphatic hardground, marking the Middle Miocene drowning of the shelf.



Fig. 13 - a) and b) field view of the mid-Cretaceous bauxite horizon at the Regia Piana.

The uppermost metre of the bedrock is cut by elongated cavities with sharp margins, which are occluded by a yellow to reddish bauxitic filling with oolitic texture.

The bauxitic horizon consists of two distinct intervals separated by a sharp contact. The lower interval may be described as an ooidal bauxitic packstone. Bauxitic ooids are normally whitish, with diameters of  $>1$  mm. The colour of the matrix ranges from white to yellow to pink. The upper interval is made of bauxitic floatstone with red to black iron-rich pisoids and subangular clasts of bauxite in a matrix similar to that of the lower interval. Greyish pyritiferous bauxitic deposits can be also observed, suggesting post-depositional reducing conditions. Boehmite and hematite are the most abundant minerals especially in the ooids, whereas kaolinite is found at higher levels in the groundmass (Boni et al., 2013). The general grain size of the intergrown minerals (hydroxides and clays) is less than  $10\ \mu\text{m}$ . Using SEM-EDS, a large number of tiny detrital minerals (size ranges  $5\text{--}100\ \mu\text{m}$ ) has been detected, both in the ooids and in the bauxite matrix (Mondillo et al., 2011). Hafnium-rich

and Sc- and Ca-bearing zircon, rutile, monazite, and ilmenite have commonly been detected, together with xenotime and titanomagnetite (Boni et al., 2013).

Above the bauxite horizon, nodular clayey and marly deposits (30-40 cm) are followed by ostracod/miliolid mudstones to wackestones, locally enriched in characean oogons, small rotaliids and *Thaumatoporella* sp. This facies was deposited in a restricted lagoon with freshwater input. Moving upward, normal marine conditions are testified by rudist limestones, even if intercalations of ostracod/rotaliid wackestones, pointing to more restricted and possibly brackish conditions, are frequent. Greenish clayey horizons, associated with nodular limestones and pseudobreccia,

witnesses short periods of subaerial exposure.

Mid-Cretaceous bauxite deposits occur in several localities of the southern and central Apennines (Abruzzi and Campania Regions) and in Puglia (Gargano and Murge area) (Fig. 14). They can be classified as karst bauxites and are associated to one or two regional stratigraphic gaps (with a total duration of some million years) that originated during subaerial exposure of the carbonate platform in a humid tropical climate. Two gaps with m-thick bauxite deposits are present in Mt Orsello,

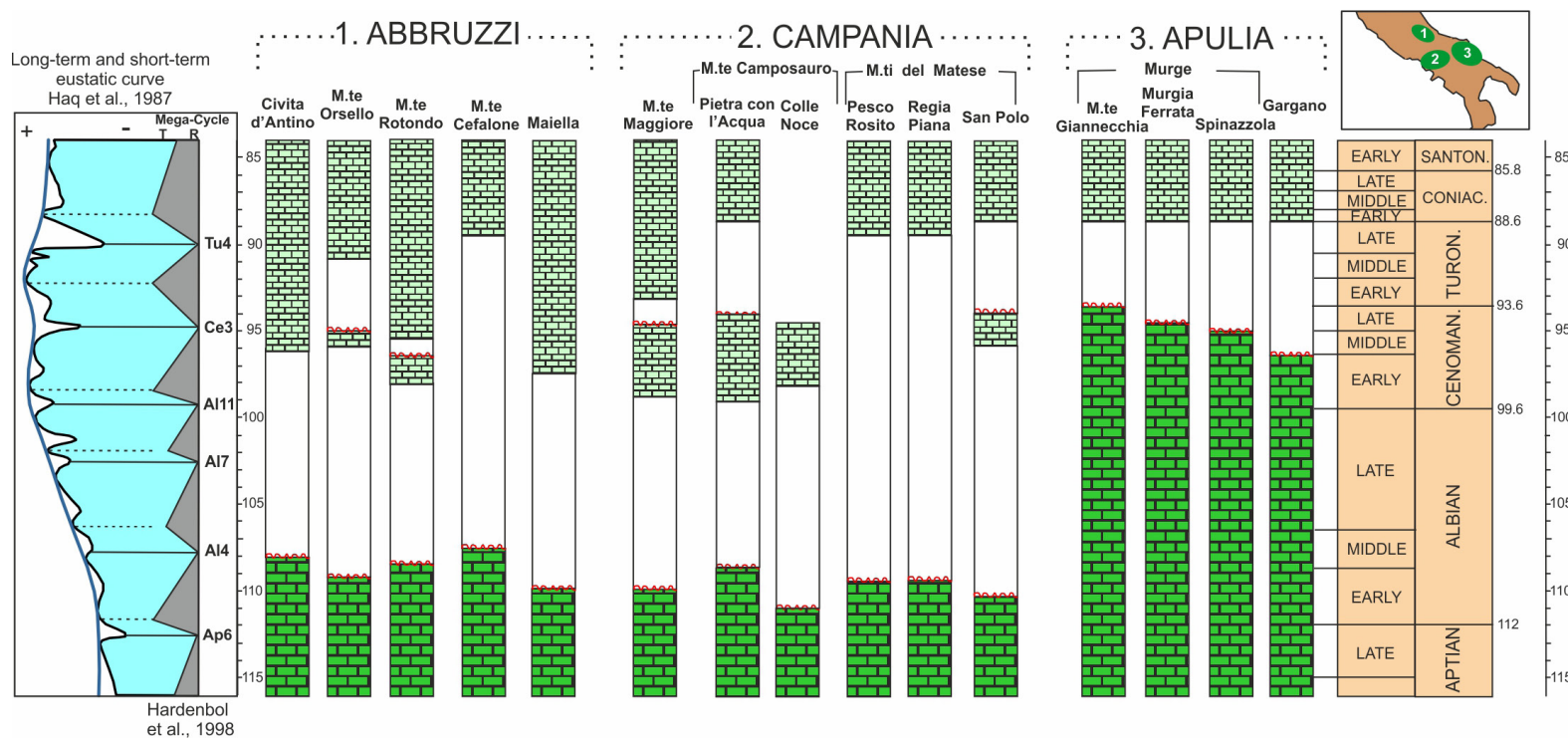


Fig. 14 - The mid-Cretaceous gaps associated with karst bauxites (white areas in the lithostratigraphic columns) are of different ages in different localities of the central and southern Apennines. These gaps are due to erosion plus non carbonate sedimentation and occur around the Albian-Cenomanian maximum of the sea-level. These pieces of evidence indicate that the bauxite-palaeokarst occurrences are clearly diachronous and do not fit with the eustatic oscillations reported by Haq et al. (1987). This sketch was modified from Mindszenty et al. (1995) and updated from D'Argenio et al. (2011).



while a single gap is reported for other Abruzzi bauxite occurrences. In Campania, the bauxite bedrock is Albian and its cover is latest Turonian in age. Also, here a single or two bauxite levels are known. The marine sediments intercalated between the two bauxite deposits are not ubiquitous. The Apulia bauxites are thicker (up to > 40m), rest on deeply karstified bedrock (northern Murge, Gargano) and are younger (middle-late Cenomanian and Turonian). A wind-borne volcanic source has long been suggested for the Southern Apennine bauxites, but it has been proven by mineralogical and geochemical evidence only recently. Zircon age populations are broadly consistent with a Dinaric and Carpatho–Balkan wind-borne volcanic source (Boni et al., 2012). The pattern of age distribution of the gaps and the different palaeotopographic relief of the bauxites and palaeokarstic deposits, clearly indicate that subaerial exposure of the carbonate platform was controlled by the interplay of regional tectonics and eustatism (Fig. 14) (Carannante et al., 1994; D’Argenio and Mindszenty, 1995; Mindszenty et al., 1995; Carannante et al., 2009; D’Argenio et al., 2011).

### **Stop 1.4: The Early Miocene transgression and the Middle Miocene drowning of the carbonate platform at Regia Piana (41°21’36”N - 14°32’09”E)**

The Regia Piana locality, in the Matese massif offers a beautiful window on the Early to Middle Miocene evolution of the southern Apennines. The southern Apennine fold-and-thrust belt is a classic example of retreating collisional belt. The main stratigraphic constraints used so far to reconstruct the timing of its deformation and the shortening rate are the ages of the first siliciclastic deposits of the foredeep and wedge-top basins (e.g., Vitale and Ciarcia, 2013). Obtaining reliable high-resolution ages for these turbiditic deposits has unfortunately proved difficult and has produced controversial results, because they are poorly fossiliferous, and their microfossil assemblages are usually dominated by reworked specimens. On the other hand, another key point in the evolution of the thrust belt are the shallow-water deposits of the so-called “Miocene transgression”. These deposits, lying unconformably on the Cretaceous (or Palaeogene) carbonate platform substrate, constitute the base of the syn-orogenic foreland basin megasequence (Fig. 15). They record the first phase of flexural subsidence of the foreland during the Apennine belt emplacement and their diachronous age tracks the progressive northeastward migration of the Apennines thrust front and of its foreland basin system. Obtaining high-resolution ages for the base of the Miocene transgressive deposits sitting on top of the forebulge unconformity would put a precise constraint on the foreland flexuration and on the shortening rate. However, this task cannot be successfully accomplished by biostratigraphy: even the most refined biozonations of Lower Miocene shallow-water carbonates, based

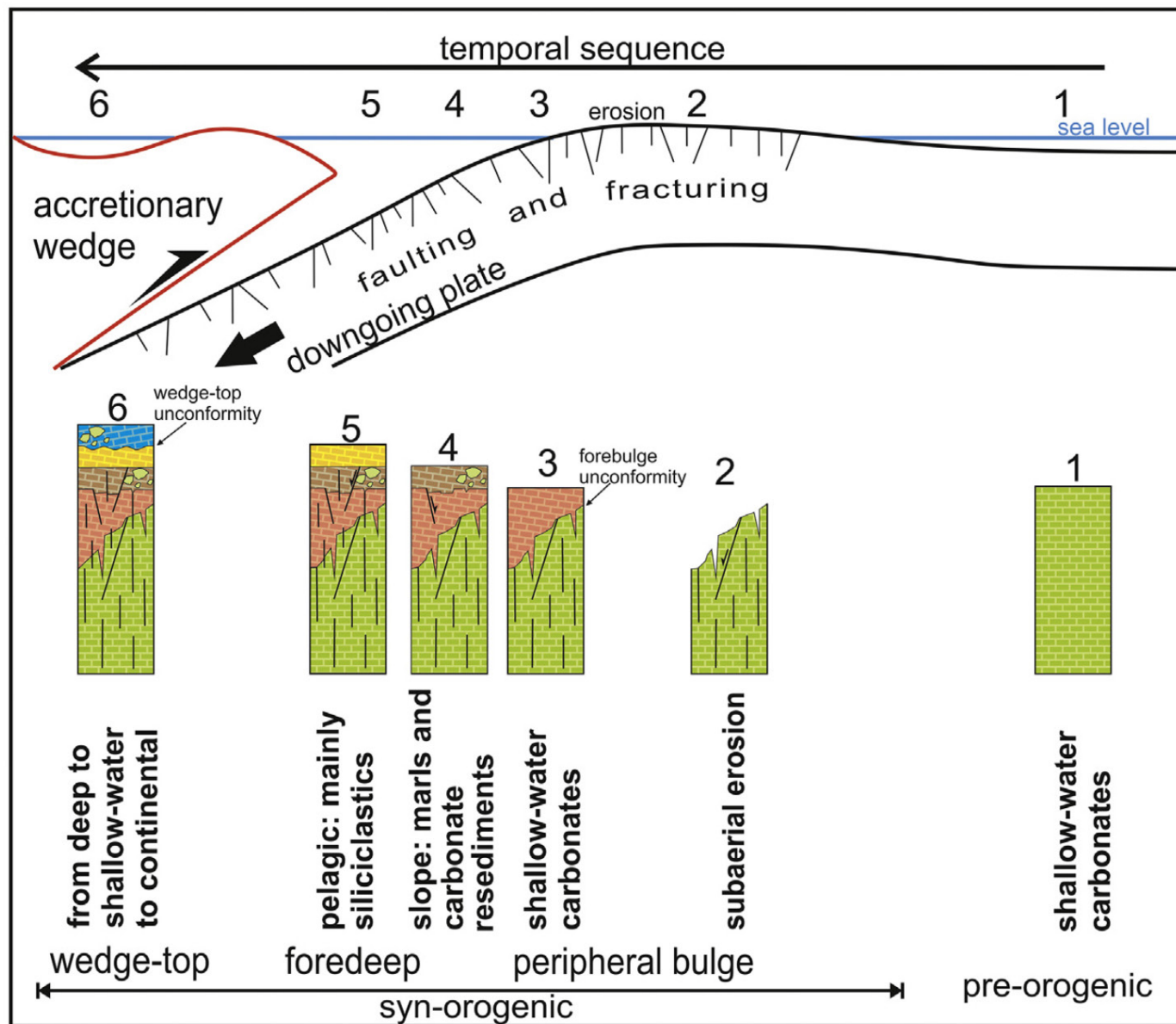


Fig. 15 - Cartoon showing the synorogenic evolution of the southern Apennine foreland plate, from subaerial exposure in the peripheral forebulge, to initial flexural subsidence (marked by the Early Miocene transgression), to drowning in the foredeep stage. From Sabbatino et al. (2020).

on larger benthic foraminifera (i.e., miogypsinids and lepidocyclinids), are plagued by low-resolution (biozones have durations in the order of a few Myr) and poor chronostratigraphic calibration. A convenient alternative is using strontium isotope stratigraphy, which can achieve a resolution of 0.1-0.5 Myr for Miocene marine carbonates and is tied to the Geological Time Scale. In this stop, along a trail that joins the main road, you will look at the unconformity separating the “radiolitid limestones” from the “Cusano formation” (Fig. 16). The contact is marked by a stylolitic surface (Figs. 16a, c) separating the grey-coloured mud-supported Upper Cretaceous limestones with rudist shells and benthic foraminifers from the grain-supported Lower Miocene whitish limestones, dominated by coralline red algae and bryozoans (Fig. 16a, c). The Upper Cretaceous substrate is densely bored by lithophagous organisms. A gap of nearly 70 Myr is present between the top of the

<https://doi.org/10.3301/GFT.2022.06>



“radiolitid limestones”, dated by biostratigraphy as upper Coniacian (for the presence of *Accordiella conica*, *Rotalispira scarsellai*, *Dicyclina schlumbergeri*, and *Montcharmontia apenninica*) (Fig. 16b), and the base of the “Cusano formation”, dated as middle Burdigalian ( $18.8 \pm 0.2$  Myr) by strontium isotope stratigraphy (Sabbatino et al., 2020, 2021).

Moving upslope along the same trail, the “Cusano formation” is overlain by the thinly bedded marly limestones with *Orbulina* of the “Longano formation”. The passage is marked by a m-thick level of phosphatic calcarenites, which witnesses the progressive drowning of the “Cusano formation” open shelf (Fig. 16d). The base of the “Longano formation” has been dated as lower Serravallian by planktic foraminifers and calcareous nannoplankton (Lirer et al., 2005). The phosphatic level consists of rudstones-floatstones with the typical bioclasts of the “Cusano formation” (coralline red algae, bryozoans, balanids, rotaliid benthic foraminifers) in a matrix with glauconitic and phosphatic grains and abundant planktic foraminifers (including *Orbulina* sp.). Shark teeth are also common in this interval. The phosphatic level has been interpreted as a hardground generated during progressive drowning of palimpsest sediments of the “Cusano formation” in an area of upwelling (Carannante, 1982). Similar Miocene phosphatic intervals have been described in many localities of the Mediterranean area (see Föllmi et al., 2008, 2015, and references therein).

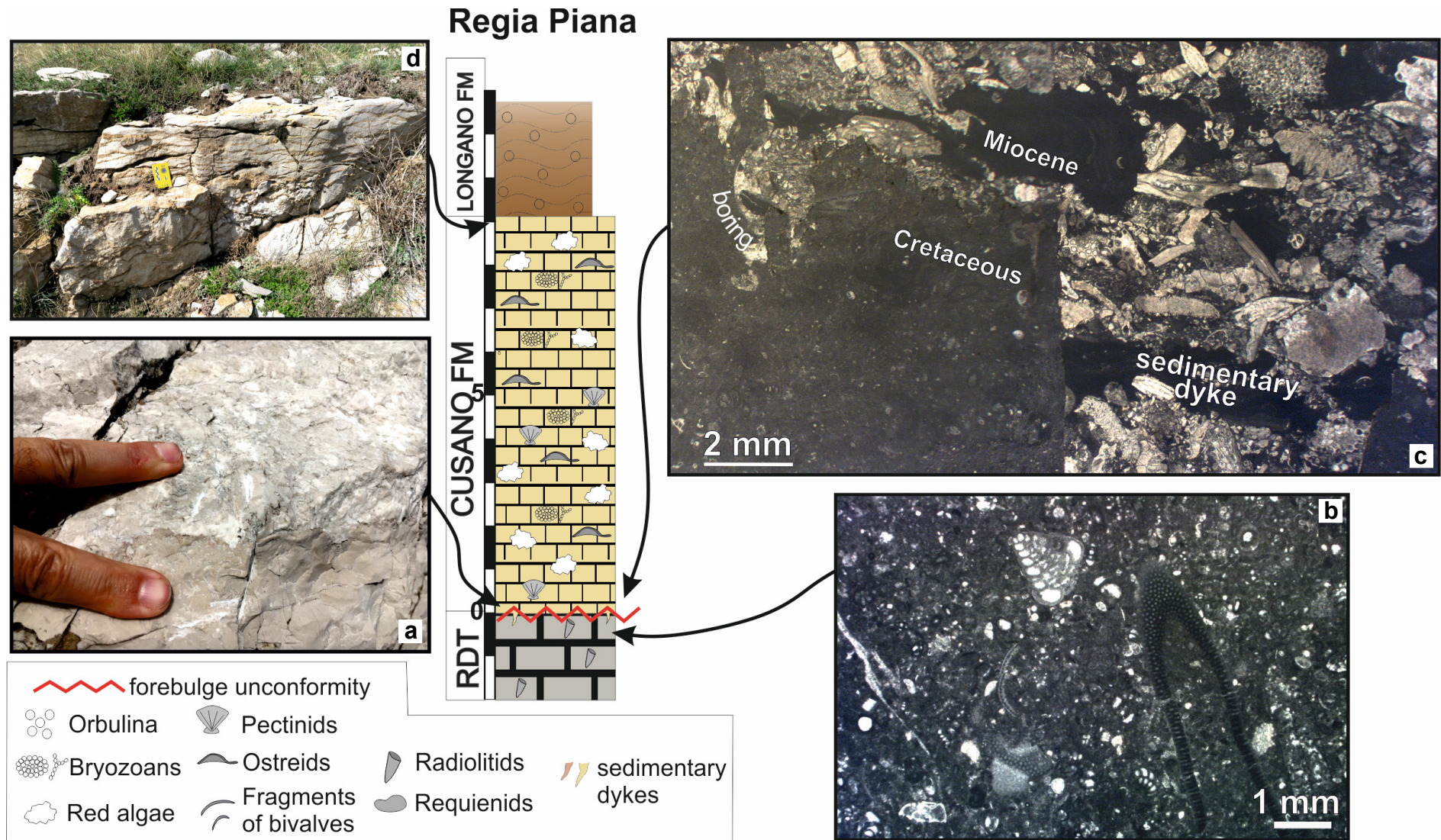


Fig. 16 - Schematic stratigraphy and facies of the succession exposed along the trail of stop 1.4, in the area of the Regia Piana. a) outcrop photograph of the unconformity separating the Upper Cretaceous "radiolitic limestones" (RDT) from the Lower Miocene "Cusano formation". b) microfacies of the Upper Cretaceous "radiolitic limestones", with *Accordiella conica* and *Thaumatoporella parvovesiculifera*. c) microfacies photographs of the unconformity separating the Upper Cretaceous "radiolitic limestones" (RDT) from the Lower Miocene "Cusano formation". d) outcrop photograph of the phosphatic hardground separating the "Cusano formation" from the "Orbulina marls" of the "Longano formation". See text for further explanations.



## DAY 2

You leave Naples heading east on the A16 highway and then south-southeast on the A30 highway toward Salerno. The A30 highway goes through a plain filled by alluvial sediments and pyroclastic deposits of the Somma-Vesuvius. The plain is bordered to the northeast by a calcareous ridge, made by the Mesozoic limestones of Apennine Carbonate Platform. The carbonates are blanketed by a thick pyroclastic cover that has been involved during the past decades in some disastrous landslides (see [Fiorillo and Wilson, 2004](#) and references therein). To the southwest of the plain there is the volcanic edifice of the Somma-Vesuvius. After the first stop in a quarry near to the village of Mercato San Severino, you will head south toward Salerno, along a narrow valley bordered by Upper Triassic dolomitised shallow-water carbonates. From Salerno you will drive south along the A3 highway, which you will leave at San Mango Piemonte for the second stop at the base of Mt Tobenna. From there, you will continue southward along the A3 highway, until Battipaglia, and then south toward the Cilento promontory, making a short stop at the archeological site of Paestum for a light lunch. From Paestum you will drive through the village of Capaccio, climbing on the Mt Soprano-Mt Chianello ridge, which is made of Cretaceous shallow-water limestones with a thin cover of Cenozoic limestones. The third stop is close to the village of Monteforte Cilento, along the road to Roccadaspide.

### Stop 2.1: The *Lithiotis* limestones and the carbonate platform record of the early Toarcian OAE in the Maiellaro quarry of Mercato San Severino (40°46'43"N - 14°43'37"E)

The "*Lithiotis* member" of the *Palaeodasyclus* Limestones and the overlying "oolitic and oncolitic limestones" are beautifully exposed in the Maiellaro quarry, in the locality "Costa", 2 km west of the Mercato San Severino village (Figs. 17 and 18). The quarry is mainly devoted to the extraction of crushed and broken limestone, but in the past from the same site the limestones of the "*Lithiotis* member" were quarried as an ornamental stone, which has been used in many important historical buildings in Naples, including the Royal Palace (Piazza Plebiscito), the Orsini di Gravina Palace (known as Palazzo Gravina) and the National Archaeological Museum (MANN).

The Lower Jurassic succession exposed in the Maiellaro quarry has been studied by [Trecalli et al. \(2012\)](#), who used carbon isotope stratigraphy to establish precise correlations with reference sections and to interpret the record of facies and biotic change in the framework of the palaeoenvironmental perturbations associated

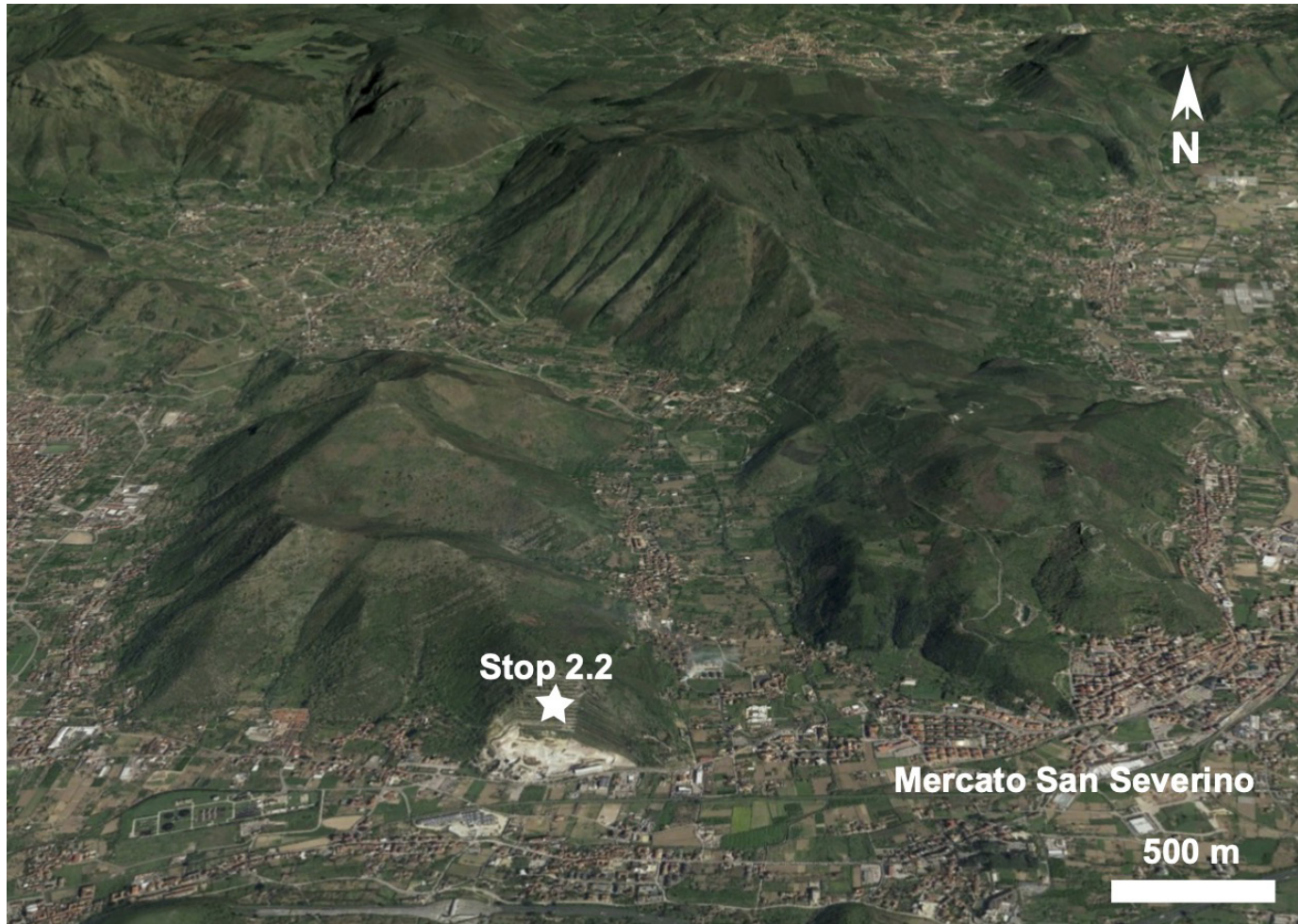


Fig. 17 - Google Earth view of the area of Mercato San Severino, showing the Maiellaro quarry (stop 2.1) where we will look at the record of the Toarcian oceanic anoxic event in the ApCP.

with the early Toarcian OAE. More recently, Posenato et al. (2018) added new data on the taxonomic composition and on the taphonomy of the bivalve shell accumulations.

### Lithostratigraphy

The “*Lithiotis* member” consists mainly of metre-thick bivalve biostromes, alternating with coarse-grained peloidal-intraclastic grainstones and rudstones with abundant remains of the dasycladalean alga *Palaeodasycladus mediterraneus*. Many beds are capped by mm- to cm-thick discontinuous levels of green marls, which penetrate downward, filling a complex network of irregular cavities. The thickest marly levels occur as distinct clusters, alternating with dm-thick beds of mudstones-wackestones with ostracods, thin-shelled gastropods and rare charophyte oogons. Irregularly

branching, spar-filled cavities and large dissolution cavities, partially filled by crystal silt are common in these mudstones-wackestones. The latter facies is also found as nodules within the thickest marly levels. The lowest cluster of thicker marly levels occurs at 79-88 m from the base of the section. A second cluster occurs between 116 and 120 m. In this uppermost part of the “*Lithiotis* member”, the bivalve biostromes become thinner,

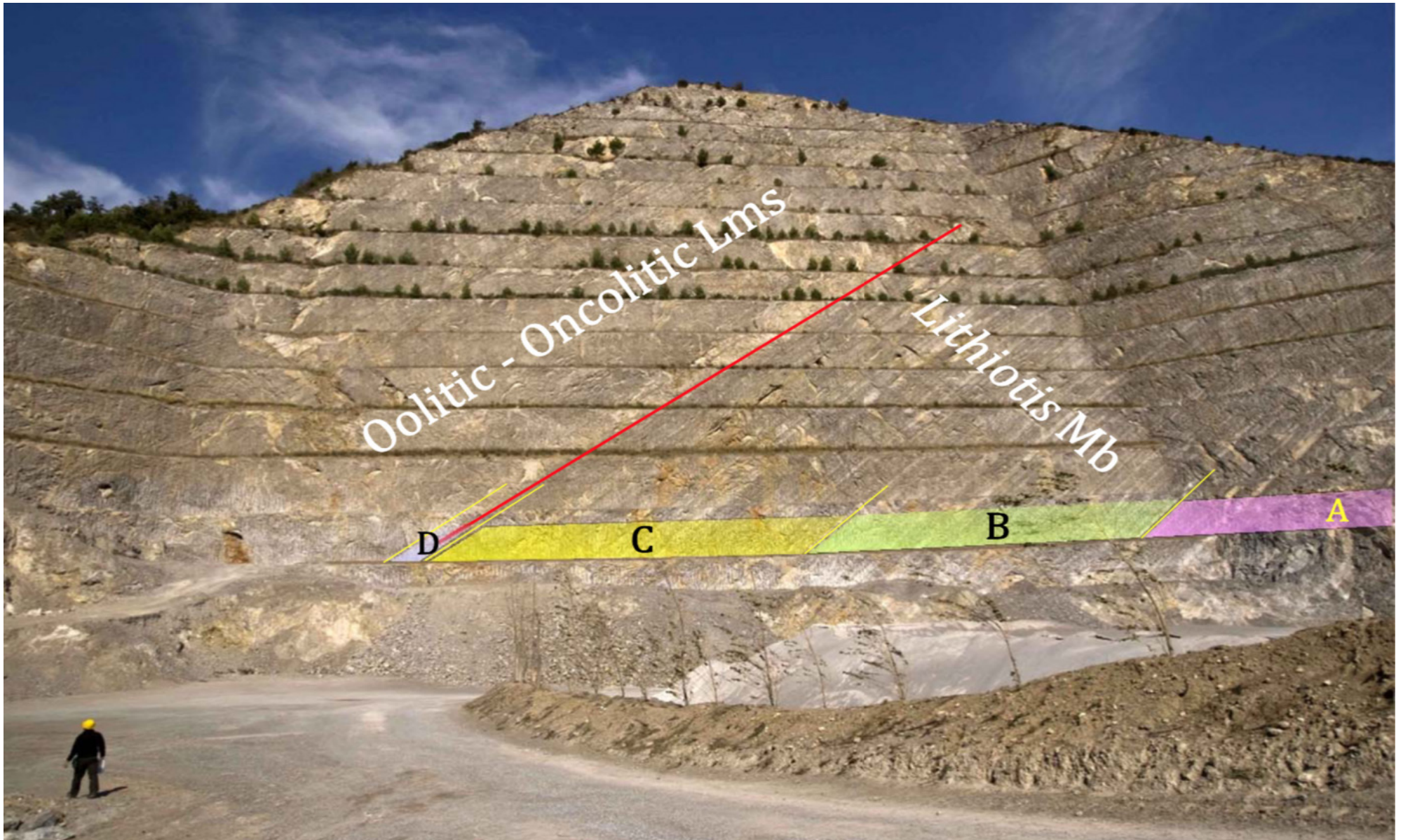


Fig. 18 - The Maiellaro quarry, near Mercato San Severino (Salerno). The quarry face exposes the passage between the "Lithiotis member" (*Lithiotis Mb*) of the "Palaeodasycladus Limestones" and the overlying "oolitic and oncolitic limestones" (Oolitic-Oncolitic Lmst). The intervals A-D refer to the taphofacies described by Posenato et al. (2018). See text for further explanations. From Posenato et al. (2018), reproduced by permission of Elsevier.

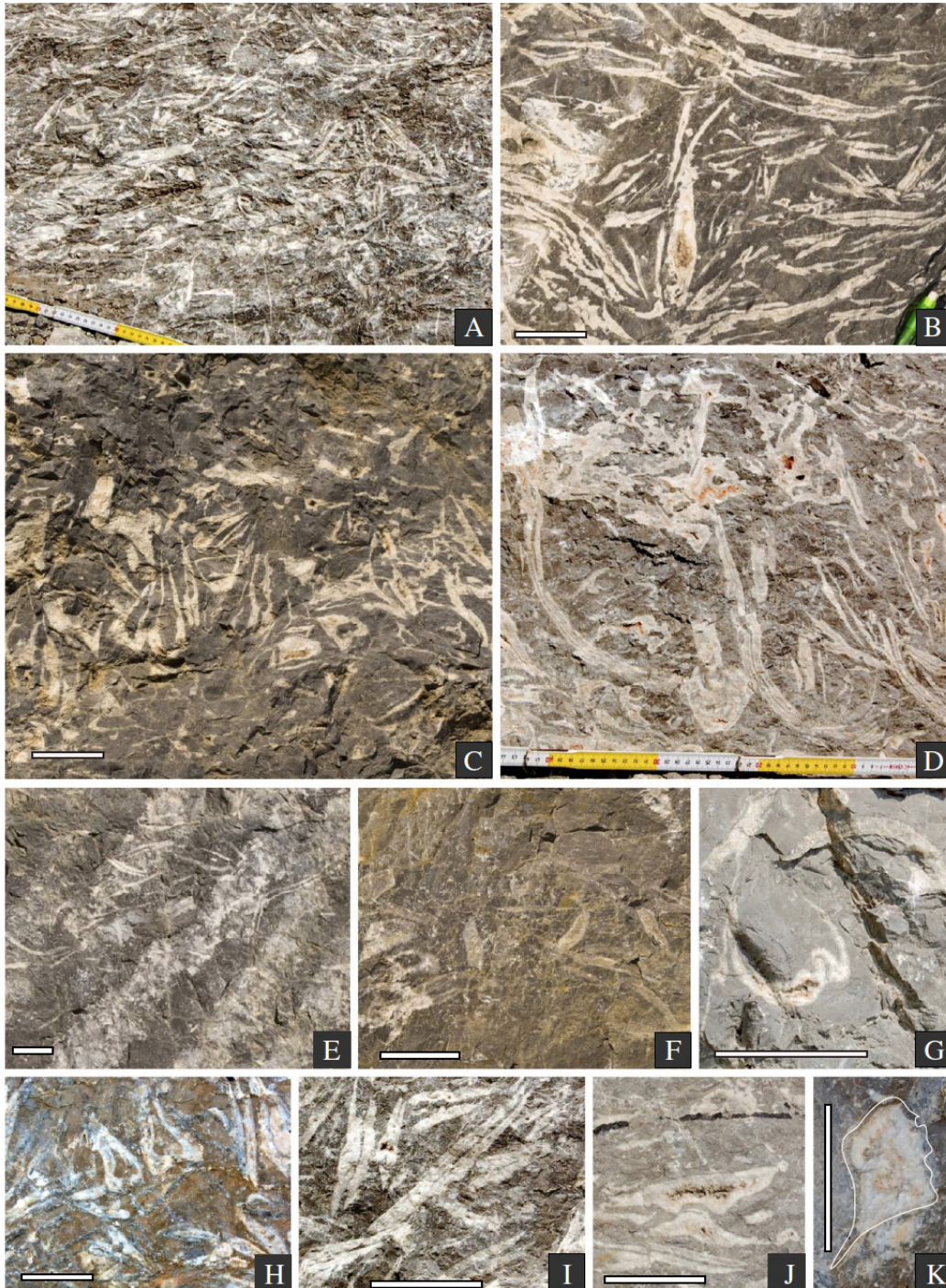


more discontinuous, and less frequent. Moreover, grain-supported lithofacies are replaced by mud-rich facies, consisting of mudstones with ostracods and thin-shelled gastropods and mudstones-wackestones with benthic foraminifers and *P. mediterraneus*. The lowest bed of oolitic grainstone is at 126.1 m from the base of the section. It is overlain by a 15 cm-thick bivalve floatstone with dull whitish to pink subangular stout fragments of bivalve shells. At the top of this bed the bivalve shells are truncated by a sharp surface overlain by a massive 130 cm-thick bed of oolitic grainstone. The next bed is made of oolitic limestone with a few pinkish-abraded fragments of bivalve shells with a thin oolitic coating. From there to the top, the section is made exclusively of massive unfossiliferous oolitic grainstones. The ooids show mainly a concentric tangential microfabric but radial and radial-concentric ooids are also frequent.

### Taxonomic composition and taphonomy of the bivalve biostromes

In Tethyan and Panthalassan marine shallow-water and lagoonal settings, the Early Jurassic time is characterised by the appearance and diffusion of large (up to 50-70 cm high), aberrant and constrictal-growth bivalves known as lithiotids (e.g., Broglio Loriga and Neri, 1976; Fraser et al., 2004; Posenato and Masetti, 2012). This informal group includes several, not systematically related, gregarious taxa such as *Lithiotis*, *Cochlearites*, *Lithioperna*, *Mytiloperna*, *Opisoma*, and *Gervilleioperna*.

*Lithiotis* is characterised by strongly asymmetric valves. Transverse sections of the umbonal region of the thicker valve are easily distinguishable by their sub-trapezoidal outline and the presence of umbonal cavities in the dorsal region of the body cavity (see Figure 2 in Chinzei, 1982). Specimens doubtfully attributed to this genus occur in the upper part of the “*Lithiotis* member” and in the lowermost part of “oolitic and oncolitic limestones”. *Cochlearites* is characterised by transverse sections of the umbonal region with a median internal furrow on the thicker (left) valve and a median internal ridge on the thinner (right) valve (Fig. 19j; see also Figure 3 in Chinzei, 1982). It is very abundant in the Maiellaro quarry, especially in the middle and upper part of the “*Lithiotis* member”. This bivalve occurs commonly in life position, locally in form of bouquet-like aggregates (Fig. 19d). *Lithioperna* has large and flattened shells that resemble, in transverse section, a couple of nearly equidimensional lenses, occasionally with an asymmetric small and rounded inner cavity corresponding to the anterior, cone-like extension of body cavity (Fig. 19a, b). This genus has a wide stratigraphic distribution in the studied succession. *Mytiloperna* has a mytiliform shell with a very thick dorsal region, where it shows a massive triangular transverse section with an anterior inner small cavity, corresponding to the cone-like extension of the body cavity. *Mytiloperna*, mostly represented by articulated shells about 10 cm in size (Figs. 19c, h), is very



common and has a wide stratigraphic distribution in the Maiellaro quarry. The edgewise recliner *Opisoma*, with the typical moustache-like outline of the hinge region in the transverse section (see figure 4 in Posenato et al., 2013), occurs scattered in the Maiellaro quarry (Figs. 19k). *Gervilleioperna* has not been found in the “*Lithiotis* member” of the Maiellaro quarry. Megalodontids, characterised by a thick shell with the typical subtriangular to heart-shaped outline in cross-sections (Fig. 19g), are common in the whole succession, although they do not form significant shell concentrations.

Four taphofacies were distinguished in the “*Lithiotis* member” of the Maiellaro quarry, based on variations in the taphonomic characters of the shell beds (i.e.,

Fig. 19 - Bivalves in the Lower Jurassic limestones of the Maiellaro quarry. (A) Densely packed bivalve accumulation dominated by *Lithioperna* in life position (lower part of taphofacies B). (B) Detail of the former accumulation. (C) Articulated shells of *Mytiloperna* in life position (taphofacies C). (D) A bouquet-like aggregation of large *Cochlearites* shells in life position (taphofacies B). (E) Sparse accumulation of *Lithioperna* (taphofacies C). (F) Fragmented and possibly reworked *Lithiotis* shells (taphofacies D, lowermost part of the “oolitic and oncolitic limestones”). (G) Articulated shell of a megalodontid (taphofacies B). (H) Articulated shells of *Mytiloperna* and *Lithioperna* (taphofacies A). (I) Articulated shells of *Lithioperna* (taphofacies B). (J) Articulated shells of *Cochlearites* (taphofacies B). (K) *Opisoma* (taphofacies A). Scale bars = 5 cm. From Posenato et al. (2018), reproduced by permission of Elsevier.



packing/articulation/fragmentation average indices, mean value of maximum shell size; Fig. 20a).

The lower taphofacies A is about 47 m thick; its base is marked by the appearance of the lithiotid accumulations. Bivalve biostromes of the taphofacies A are dominated by *Mytiloperna*. *Lithioperna* appears at about 8 m above the base of this interval. *Cochlearites* is rare and was recognised only in three accumulations, at about 25 m above the base and in the upper part of the unit. The taphofacies B, about 35 m thick, corresponds to the interval with the greatest abundance of lithiotid accumulations (Fig. 20b), the highest averaged packing index, and the maximum

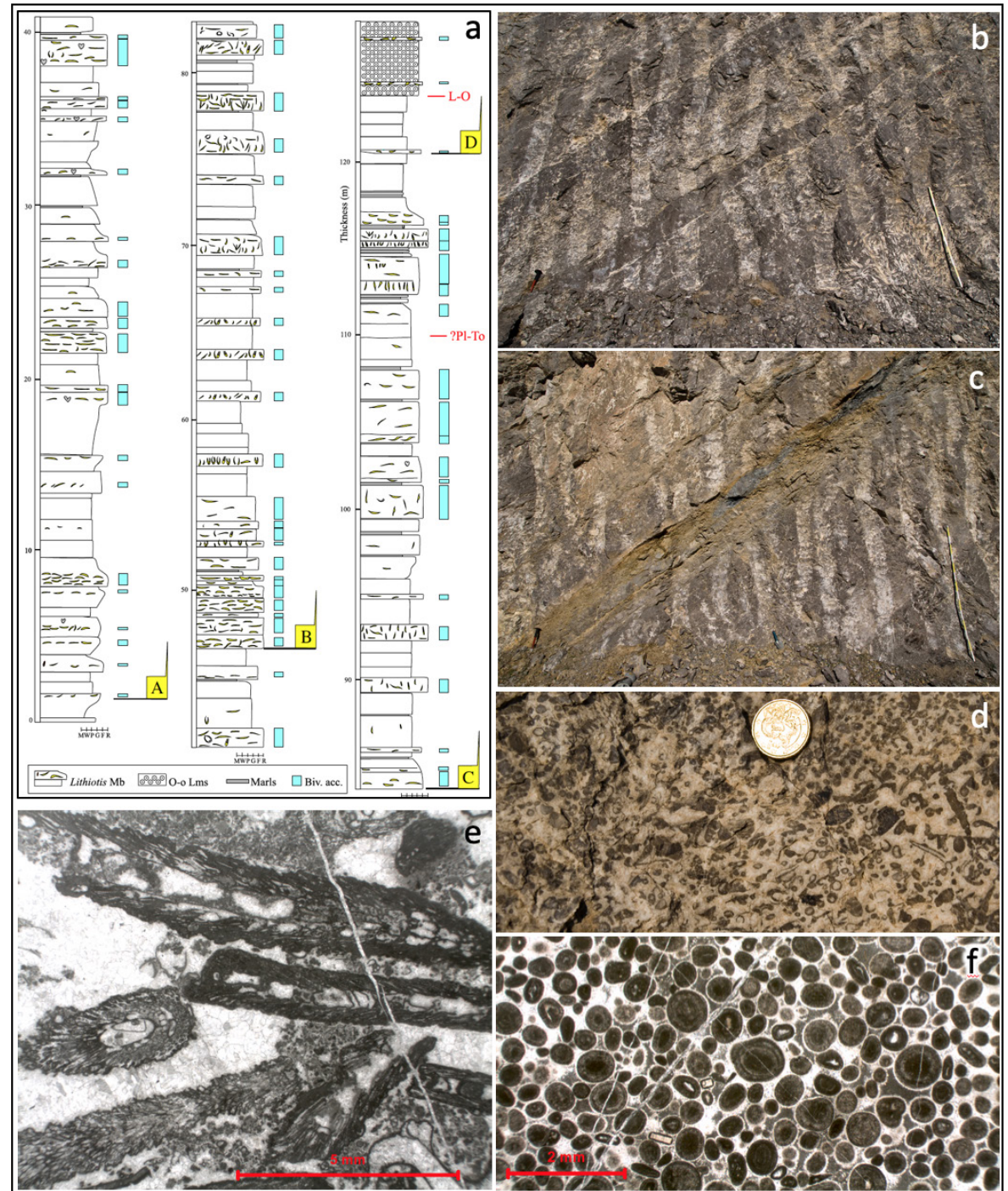


Fig. 20 - Lower Jurassic limestones of the Maiellaro quarry. a) Lithologic log with taphofacies. b) thick and dense accumulations of lithiotid bivalves in taphofacies B. c) a thick argillaceous interlayer, with nodules of micritic limestone, in the uppermost part of the *Lithiotis* (close to the inferred position of the Pliensbachian-Toarcian boundary). d) outcrop view of a limestone bed crowded with thalli of the dasycladalean alga *Palaeodasycladus mediterraneus*. e) thin section microphotograph of a grainstone with *P. mediterraneus*. f) thin section microphotograph of an oolitic grainstone at the base of the "oolitic and oncolitic limestones". From Posenato et al. (2018), reproduced by permission of Elsevier.



shell size. The shell accumulations of this interval consist mostly of *Cochlearites*, predominantly represented by articulated shells, often in life position. *Mytiloperna* and *Lithioperna* are abundant. The taphofacies C, about 38 m thick, records a marked decrease in shell size and frequency. Also, the packing index and articulation index show a marked decrease. The taphofacies D, about 7 m thick, consists of three shell beds characterised by fragmented and probably reworked shells. There are no articulated shells, and the packing index is very low.

### Carbon isotope stratigraphy

Trecalli et al. (2012) developed a carbon isotope stratigraphy for the Lower Jurassic of the Maiellaro quarry, based on paired curves of carbonate carbon ( $\delta^{13}\text{C}_{\text{carb}}$ ) and organic carbon ( $\delta^{13}\text{C}_{\text{org}}$ ). The most prominent features shown by the carbon isotope profiles (see Fig. 21) are two sharp negative carbon isotope excursions (CIE) with an intervening positive excursion. The first negative CIE occurs in the upper part of the “*Lithiotis* member” and is recorded only by the  $\delta^{13}\text{C}_{\text{org}}$  curve, with a shift of about 3–4‰. Its absence in the carbon isotope record of the carbonate component could be due to diagenetic overprint. The second negative CIE starts in the uppermost beds of the “*Lithiotis* member” and reaches the lowest values in the first beds of the “oolitic and oncolitic limestones”. This excursion is recorded by both components but is distinctly larger in the  $\delta^{13}\text{C}_{\text{org}}$  (4–5‰) than in the  $\delta^{13}\text{C}_{\text{carb}}$  curve (2–2.5‰). In Figure 21, the carbon isotope curves of the Maiellaro quarry (labelled “Mercato San Severino”) and Mt Sorgenza (the other section studied by Trecalli et al., 2012, and previously published by Woodfine et al., 2008) are correlated with the high-resolution curves of two key sections for the T-OAE: Peniche (Portugal, Hesselbo et al., 2007; Suan et al., 2008) and the Yorkshire composite (UK, Kemp et al., 2011). The first negative CIE of the  $\delta^{13}\text{C}_{\text{org}}$  curves of the ApPC is correlated with the Pliensbachian–Toarcian boundary excursion and the second negative CIE with the T-OAE excursion. This correlation is compatible with the available biostratigraphic constraints, which support an age close to the Pliensbachian–Toarcian boundary for the extinction of *P. mediterraneus* (Bassoulet, 1997; Barattolo and Romano, 2005) and for the demise of lithiotid bivalves (Fraser et al., 2004). The correlation is also broadly supported by the strontium isotope stratigraphy of Woodfine et al. (2008), showing that, in the Mt Sorgenza section, the lowest Sr isotope values, corresponding to the Pliensbachian–Toarcian boundary (McArthur et al., 2000), occur at the level of the first CIE (Fig. 21).

### Palaeoenvironmental evolution of the Apennine Carbonate Platform across the early Toarcian OAE

Using the chemostratigraphic correlation of Figure 21, the Early Jurassic evolution recorded by the successions exposed in the Maiellaro quarry can be discussed in the framework of late Pliensbachian–early Toarcian

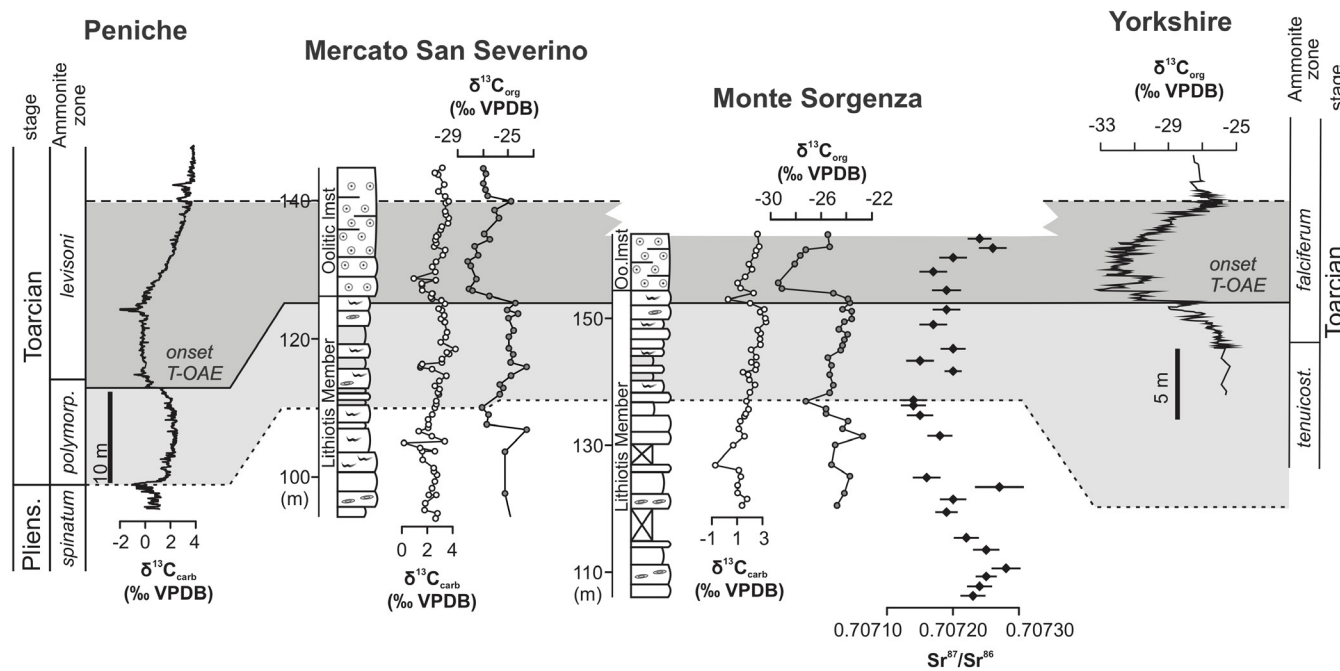


Fig. 21 - Chemostratigraphic correlation of the platform carbonate sections of the southern Apennines with the reference sections of Peniche (Lusitanian basin, Hesselbo et al., 2007) and of the Yorkshire composite (UK, Kemp et al., 2011). The prominent negative CIE recorded in the ApCP sections at the boundary between the *Lithiotis/Palaeodasyclus* Limestones and the "oolitic and oncolitic limestones", is correlated with the T-OAE CIE. This correlation is broadly consistent with biostratigraphy and with the strontium isotope stratigraphy of Mt Sorgenza (taken from Woodfine et al., 2008). From Trecalli et al. (2012), reproduced by permission of Elsevier.

palaeoenvironmental perturbations. During the Pliensbachian, the ApCP was a very healthy carbonate platform in the supersaturated shallow waters of the tropical Tethys Ocean. Like many Lower Jurassic carbonate platforms of that latitudinal belt, it was dominated by hyper-productive aragonitic biocalcifiers: the massive bivalves of the lithiotid group (Fraser et al., 2004) and the calcareous alga *P. mediterraneus*. The lithiotid beds of the ApCP can be interpreted as biostromes in a subtidal lagoonal setting. Dense meadows of *P. mediterraneus* developed in the same lagoonal setting. Dense meadows of *P. mediterraneus* developed in the same lagoonal setting. The green marly levels capping the limestone beds, and infiltrating downwards, originated during high-frequency events of subaerial exposure of the platform top. They show many analogies with similar greenish

marls of the Purbeckian (lowermost Cretaceous) of the Jura Mountains (Strasser, 1988). Clusters of thicker nodular marls, associated with restricted marine to paralic ostracodal mudstones-wackestones, indicate longer and closely recurrent phases of subaerial exposure, marking sequence-boundary zones (*sensu* Strasser et al., 2000).

Based on carbon isotope stratigraphy (Fig. 21), the most prominent sequence-boundary zone occurs in the earliest Toarcian (i.e., above the lowest negative CIE). This interval is characterised by thinner and less recurrent



lithiotid biostromes (uppermost part of lithofacies C in [Posenato et al., 2018](#); see Fig. 19) and by an overall shift to mud-dominated facies. However, lithiotid bivalves and dasycladalean algae (*P. mediterraneus*) were still abundant when fully marine facies developed. This pattern suggests that in the resilient ApCP there was no significant biotic change across the Pliensbachian–Toarcian boundary.

A pronounced change occurred in the early Toarcian and is closely associated with the T-OAE CIE (Fig. 21): lithiotid bivalves and *P. mediterraneus* disappeared and the carbonate factory switched from a biogenic to a chemical mode, with the massive occurrence of unfossiliferous oolitic limestones. The late Pliensbachian–early Toarcian evolution described above for the ApCP is not a local pattern. The lithiotid bivalves were the most prolific carbonate producers of many Tethyan carbonate platforms during the Pliensbachian ([Fraser et al., 2004](#)). The green alga *P. mediterraneus* is also a very typical component, often in rock-forming abundance, in Lower Jurassic shallow-water limestones ([Sokač, 2001](#)). In many Tethyan carbonate platforms the demise of the lithiotid bivalves/*Palaeodasycladus* carbonate factory coincides with platform drowning in the Pliensbachian, in some cases heralded by the backstepping of platform margin facies onto inner lagoonal facies. In the resilient platforms that survived even this drowning event close to the Pliensbachian–Toarcian boundary, the shift from a biotic carbonate factory, dominated by lithiotid bivalves and *P. mediterraneus*, to a chemical carbonate factory, dominated by oolites, is a common pattern. In the Pelagonian Carbonate Platform (NE Evvoia, Greece) lithiotid limestones are abruptly overlain by oolitic limestones ([Scherreiks et al., 2009](#)) at a level that, within the uncertainty of poor biostratigraphic dating, could be coeval with the shift observed in the ApCP. In the Adriatic Carbonate Platform, lithiotid limestones are overlain by dark and heavily bioturbated limestones (“spotty limestones”) in the NW part of the platform (Slovenia, central and W Croatia and W Bosnia), while the rest of the platform was characterised by oolitic limestones ([Vlahović et al., 2005](#)). Carbon isotope stratigraphy suggests that the boundary between the lithiotid limestones and the “spotty limestones” is diachronous, but the final demise can be definitely linked to the onset of the T-OAE ([Sabatino et al., 2013](#)).

### **What caused the demise of the lithiotids bivalves/*Palaeodasycladus* carbonate factory?**

Acidification of surface waters has been invoked to explain the dramatic decrease in pelagic carbonate production by nannoplankton and the reduction in size of some species across the T-OAE ([Erba, 2004](#); [Mattioli et al., 2004](#); [Tremolada et al., 2005](#)). Ocean acidification as the major cause of the early Toarcian reef crisis is also supported by the recent analysis of the PaleoReefs database ([Kiessling and Simpson, 2011](#)). More recently, ocean acidification at the onset of the T-OAE and during the OAE has been supported also by boron isotopes



data on brachiopods (Müller et al., 2020). The decrease in surface water carbonate saturation could have been caused by the massive injection of isotopically depleted CO<sub>2</sub>, which is generally invoked to explain the early Toarcian negative CIE (Cohen et al., 2007, and references therein).

Trecalli et al. (2012), using a palaeo-physiology approach (Knoll et al., 2007), proposed that the demise of lithiotid bivalves and of the dasycladalean algae was caused by ocean acidification across the T-OAE.

### What is the meaning of the massive oolitic limestones?

The widespread occurrence of oolitic limestones following the demise of the lithiotids bivalves/*Palaeodasycladus* carbonate factory is a common feature in many resilient platforms of the Tethyan Ocean. Ooids are a common component of tropical shallow-water carbonate sediments. Conditions necessary for their formation are: (1) water supersaturated with respect to aragonite or high Mg-calcite; (2) a source of nuclei; and (3) a means of agitation. The abundance of oolitic sands in the Bahamas and their rarity in the Pacific atolls indicates that elevated carbonate supersaturation is the essential factor limiting the global distribution of oolitic sands today (Rankey and Reeder, 2009). The same factor seemingly controlled the uneven distribution of ooids in the Phanerozoic record (Sandberg, 1985; Opdyke and Wilkinson, 1990).

Trecalli et al. (2012) used a biogeochemical model, developed by Kump et al. (2009) for the marine geological signature of an ocean acidification event, to explain the abrupt shift from biotic hypercalcifiers to oolites in the Lower Jurassic of the ApCP (Fig. 22). The Pliensbachian “healthy” carbonate factory, dominated by hypercalcifiers (i.e., lithiotid bivalves and dasycladalean algae) corresponds to the pre-event steady-state of the model. The demise of hypercalcifiers across the onset of the T-OAE would correspond to the short interval of ocean acidification recorded by the “dissolution interval” of the Kump et al. (2009) model. The widespread occurrence of massive oolitic limestones after the demise of the hypercalcifiers would represent the “overshoot” in the CaCO<sub>3</sub> preservation of the Kump et al. (2009) model. In the absence of massive biocalcifiers, chemical precipitation could have been the only effective way to buffer the increasing alkalinity of the shallow-water ocean, forced by enhanced continental weathering and possibly also by dissolution of deep-water carbonates. A similar scenario has been proposed for the Permian–Triassic biocalcification crisis, which records the abrupt transition from skeletal to microbial and oolitic facies in carbonate platforms across the tropics, coeval with a biotic crisis and a large carbon cycle perturbation (Li et al., 2019, and references therein).

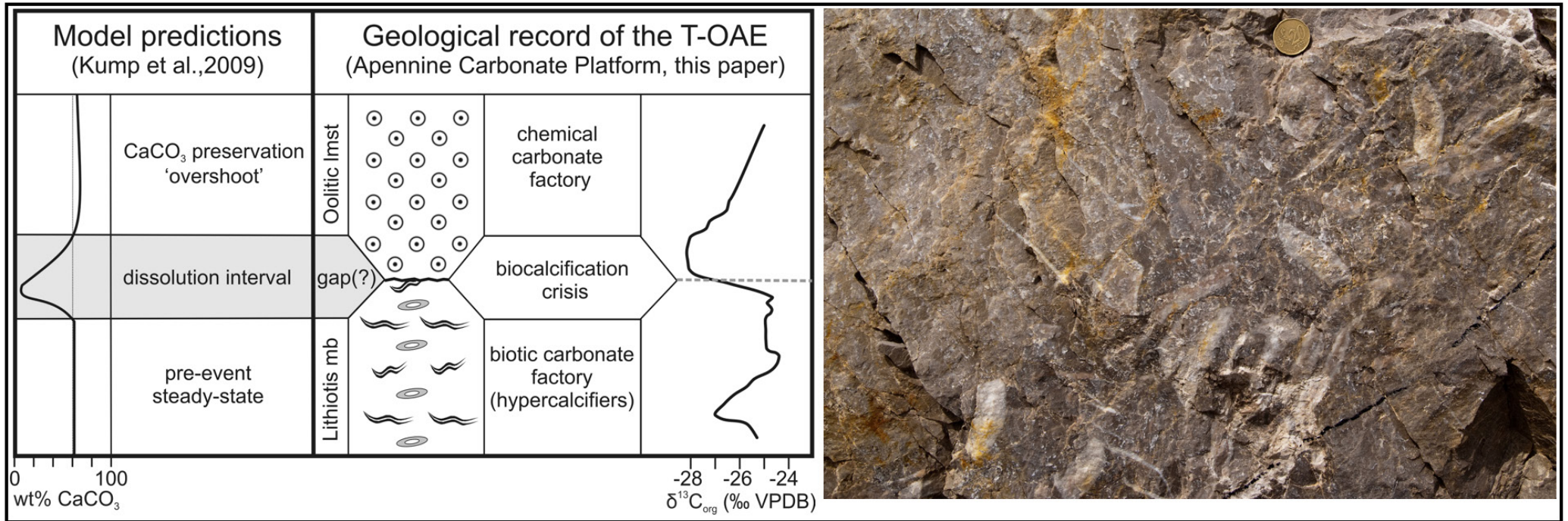


Fig. 22 - Left: A comparison between the late Pliensbachian-early Toarcian evolution of the ApCP and the expectations of a biogeochemical model of ocean acidification (Kump et al., 2009). The demise of the hypercalcifiers of the lithiotids/*Palaeodasycladus* carbonate factory is interpreted as a biocalcification crisis, triggered by an episode of ocean acidification. The massive occurrence of ooids is interpreted to represent the post-crisis carbonate saturation overshoot. Right: the last bed with lithiotids, truncated by oolitic limestones.

**Stop 2.2: The Orbitolina level at Mt Tobenna and its relations with the Aptian OAE1 (40°41'56"N - 14°51'49"E)**

In this stop you will look at the "Orbitolina level", a m-thick lithostratigraphic marker of Gargasian age (late Aptian), in a classical locality at the base of Mt Tobenna (De Castro, 1963; Cherchi et al., 1978) (Fig. 23). A nearly 800 m thick succession of Cretaceous limestones (lower Aptian-Coniacian) is exposed on the southern slope of Mt Tobenna, covering the middle and upper part of the "requienid and gastropod limestones" and the lower part of the "radiolitid limestones". The Aptian of Mt Tobenna has been the object of detailed studies, dealing mainly with cyclostratigraphy and C-isotope stratigraphy (Raspini, 1998, 2001, 2012; D'Argenio et al., 1999, 2004).

<https://doi.org/10.3301/GFT.2022.06>

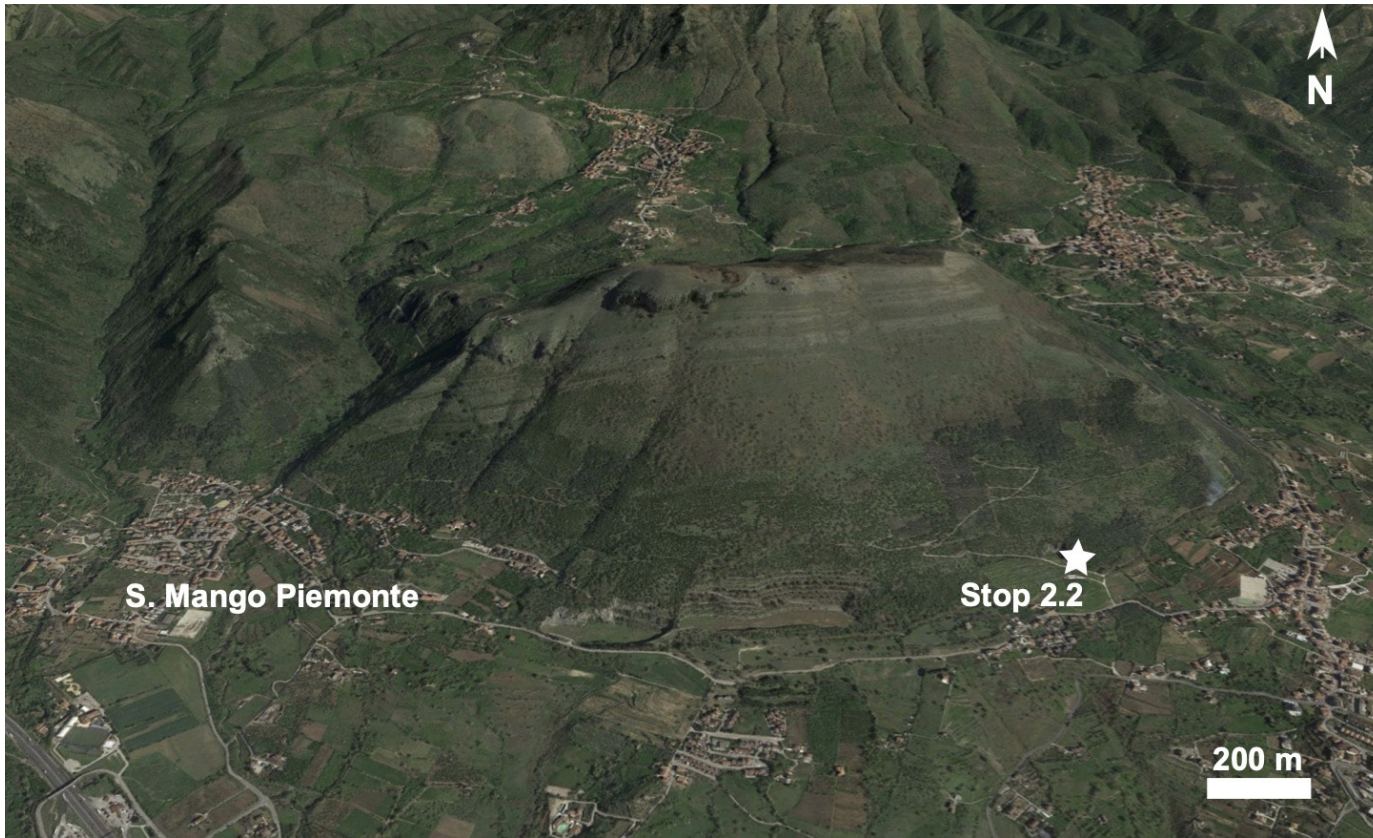


Fig. 23 - Google Earth view of the southern slope of Mt Tobenna. The white star marks the location of the small abandoned quarry of stop 2.2. The "Orbitolina level" is exposed in the quarry and along the path west of the quarry.

A section about 50 m thick, encompassing in its lower part the "Orbitolina level", has been described by Di Lucia et al. (2012), starting in a small abandoned quarry at the base of Mt Tobenna and continuing along the lower part of the mountain slope (Fig. 23). The section can be divided into two intervals (A and B) based on lithofacies trends (Fig. 24). The first part of interval A (0–7 m) consists mainly of an alternation of chara-ostracodal mudstones-wackestones, bio-peloidal packstones-grainstones with nubecularids, and mili-ostracodal wackestones. Between 7 and 15 m from the base of the section, the most frequent lithofacies consists of algal wackestones-packstones with *Salpingoporella dinarica*, alternating with bio-peloidal

packstones-grainstones. A prominent bed of requienid floatstone is present at 11 m from the base of the section. The "Orbitolina level" occurs at 15 m from the base of the section (Fig. 24). It contains specimens of *Mesorbitolina parva* and *Mesorbitolina texana* (Fig. 25). Below the wavy base of the "Orbitolina level", the underlying bed is penetrated down to about 1m by a dense network of dissolution cavities filled by orbitolinid packstones. The "Orbitolina level" is overlain by 70 cm of bio-peloidal packstones-grainstones. The remaining part of interval A is dominated by chara-ostracodal mudstones-wackestones alternating with cm- to dm- thick levels of greenish marls. The thickest marly levels contain nodules of chara-ostracodal mudstones. Interval

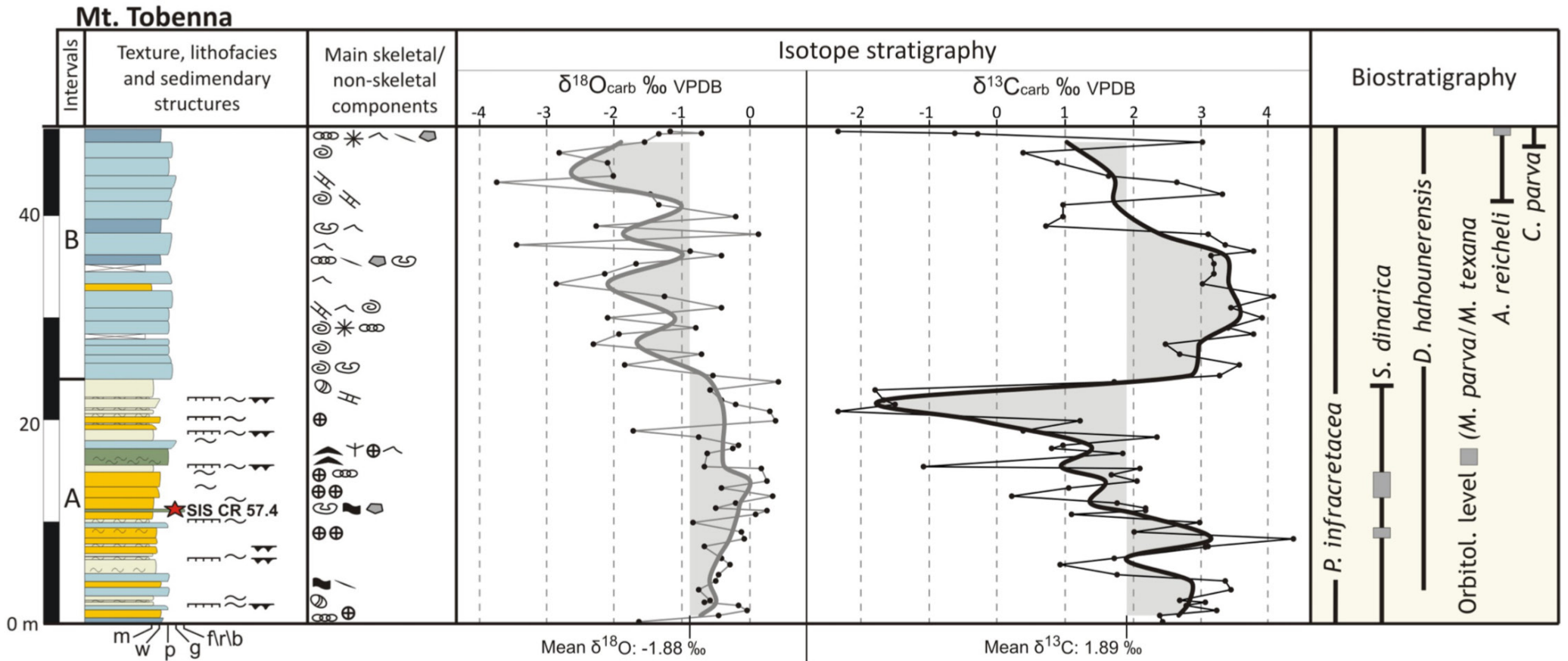


Fig. 24 - Mt Tobenna section: lithological-sedimentological log, isotope stratigraphy and biostratigraphy. The thick curves represent the 3-point moving averages of O- (grey) and C-isotope ratios (black). From Di Lucia et al. (2012).

B (24–48.5 m) was logged on the mountain slope immediately west of quarry edge. It is dominated by bio-peloidal packstones-grainstones with abundant benthic foraminifers, with a few beds of mili-ostacodal mudstones-wackestones. *Lithocodium/Bacinella* nodules are a frequent component in the interval between 26 and 36 m from the base of the section. The section ends with a bed of foraminiferal packstone crowded with *Archaeoalveolina reicheli*.



## The age of the “*Orbitolina level*” and its relationship with the Aptian OAE1a

Di Lucia et al. (2012) integrated carbon isotope stratigraphy and biostratigraphy to establish a correlation between the Mt Tobenna section (and four other sections of the ApPC), with pelagic reference sections of the Tethyan realm (Fig. 26). Based on this correlation, the “*Orbitolina level*” was correlated with the C7 segment of the standard reference curve. However, precise correlation based on the carbon isotope profile is problematic, because of the many gaps of unknown duration present in the Mt Tobenna and in other sections. The problem of gaps has been recently tackled by Graziano and Raspini (2018), who placed the “*Orbitolina level*” of Mt Faito (some 34 km west of Mt Tobenna) within the C8 segment of the carbon isotope curve (middle part of the Gargasian). With the latter correlation, the “*Orbitolina level*” could be coeval with the orbitolinid-rich levels at the base of the Artxueta Formation of the Basque-Cantabrian Basin, which have been interpreted as the facies expression of the late Aptian cold snap (McAnena et al., 2013; Millan et al., 2014).

Based on its late Aptian (Gargasian) age, supported by biostratigraphy (the first appearance of *M. parva* is at the base of the Gargasian, according to Schroeder et al., 2010) and carbon isotope stratigraphy, the “*Orbitolina level*” of the southern Apennines is definitely younger than the Selli level (OAE1a) and could be equivalent of the late Aptian Fallot level of the Vocontian basin (Friedrich et al., 2003). In the ApPC there is another interval rich of flat conical orbitolinids, referable to *Palorbitolina lenticularis*, which is older than the marly “*Orbitolina level*” (containing *Mesorbitolina parva* and *M. texana*). According to the carbon isotope stratigraphy correlation of Di Lucia et al. (2012) and Amodio and Weissert (2017), this *Palorbitolina* interval straddles the Barremian-Aptian boundary, corresponds to the C2 segment of the reference curves for carbon isotope stratigraphy and can be correlated with the lower *Orbitolina* beds of the northern Tethyan Helvetic platform (Arnaud et al., 1998; Clavel et al., 2002; Föllmi et al., 2007; Föllmi and Gainon, 2008).

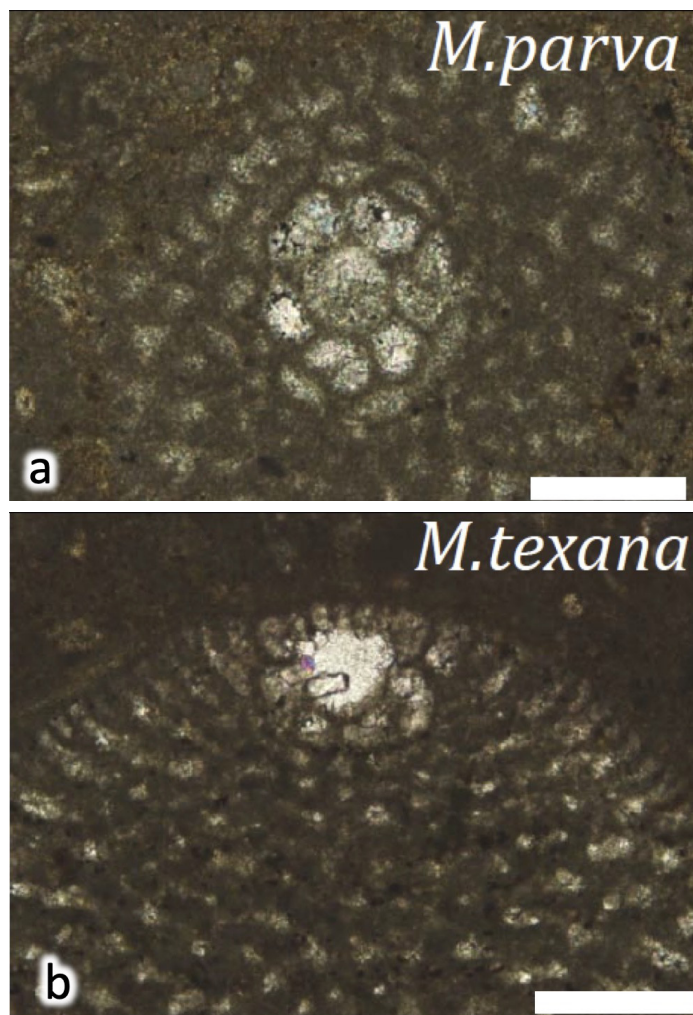


Fig. 25 - *Mesorbitolina parva* (transversal section) and *Mesorbitolina texana* (axial section) from the “*Orbitolina level*” of Mt Tobenna. Scale bar is 200  $\mu\text{m}$  in both photographs.

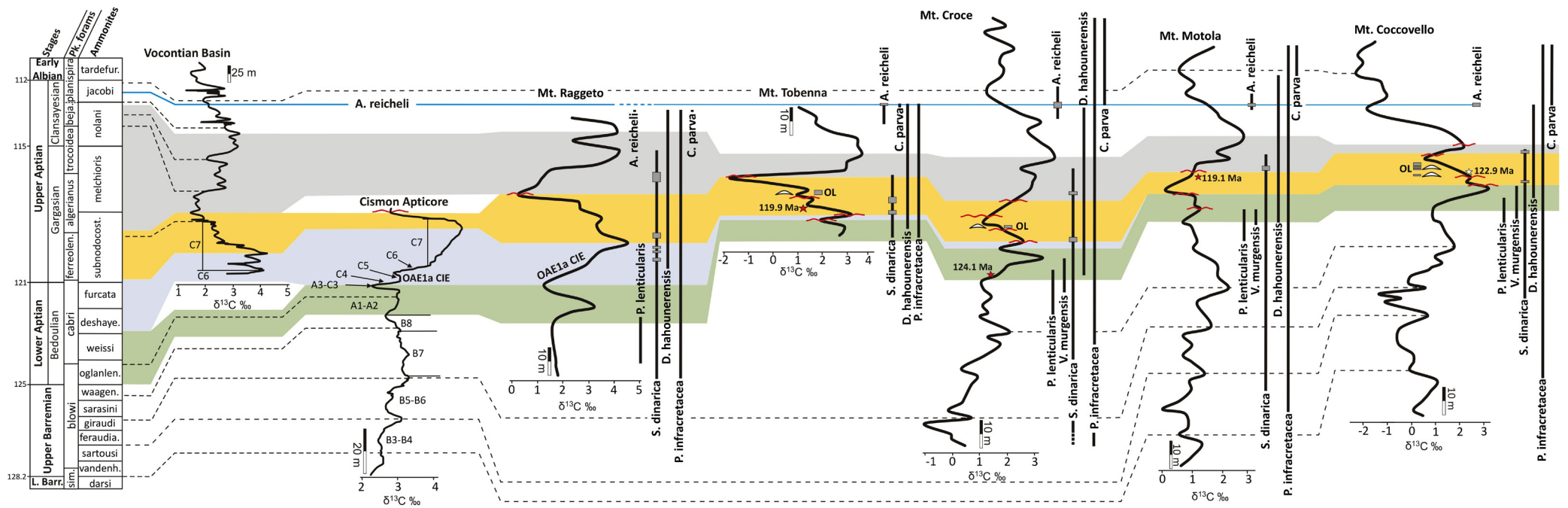
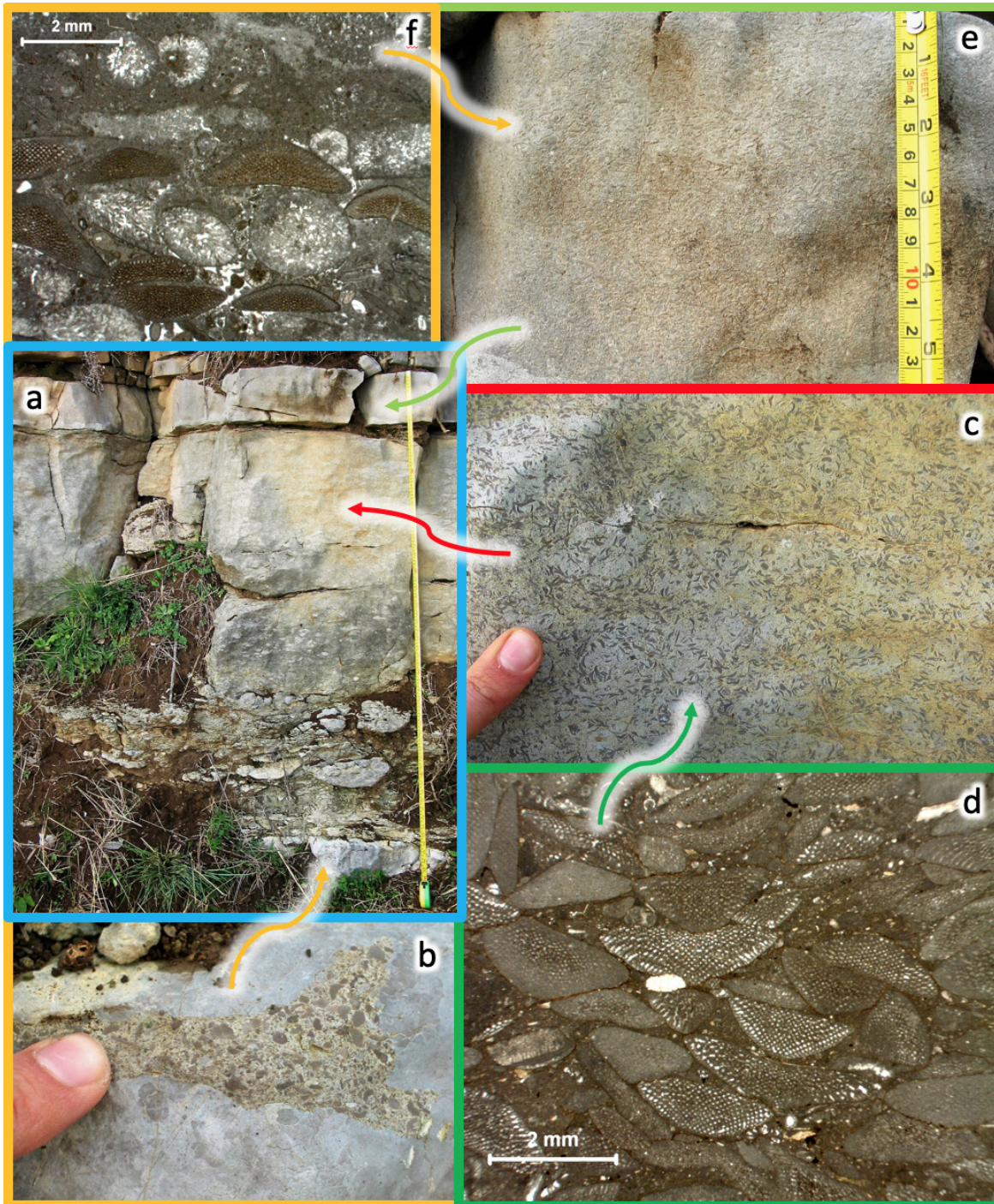


Fig. 26 - Chemostratigraphic correlation of the five sections of the ApCP with the reference section of the Cismon Apticore (Belluno Basin, northern Italy, Erba et al., 1999) and with the composite hemipelagic curve of south-eastern France (Herrle et al., 2004; Föllmi et al., 2006). From Di Lucia et al. (2012).

### Taphonomy and palaeoenvironmental meaning of the “*Orbitolina* level”.

The “*Orbitolina* level” is a complex shell concentration made generally of two distinct beds, separated by an erosional surface (Fig. 27a). The first bed consists of green marls to marly limestones overlying a subaerial exposure surface and filling a network of cavities penetrating for 10-15 cm down into the substrate (Fig. 27b). Carbonate content increases upward, but a more complex pattern of carbonate-rich and clay-rich levels could have been partly concealed by differential compaction and bioturbation. Skeletal remains are almost exclusively represented by flat conical orbitolinids (Fig. 27c, d), with only rare pelecypod shells and calcareous algae (*Salpingoporella dinarica* and *Boueina hochstetteri moncharmontiae*). The second bed is a bioclastic packstone very rich in flat conical orbitolinids and codiaceans (*Boueina hochstetteri moncharmontiae*) (Fig. 27e, f). Two fundamental questions need to be addressed for the “*Orbitolina* level”: what is the origin of this complex shell concentration and what is its palaeoenvironmental meaning in terms of water depth? *In situ* (i.e., not reworked)



shell concentrations can be formed by the interplay of different characters, including increased shell production, sedimentary condensation and increased shell preservation (Kidwell, 1986; Tomašových, 2006). The latter is only relevant for shells that can be easily destroyed physically or by dissolution (not the case of the “*Orbitolina* level”). Micritisation of the orbitolinid tests could be used as a proxy of condensation, assuming that the longer a test is exposed on the sea floor, the more it will be affected by micritisation. The high alteration level of the orbitolinids suggests that the extremely high shelliness of the “*Orbitolina* level” is related to reduced rate of sedimentation more than to increased rate of shell production (Fig. 28c). The second question (does the “*Orbitolina* level” mark an increase of water depth?) is

Fig. 27 - The “*Orbitolina* level” at the base of Mt Tobenna. a) outcrop photograph showing the lower marly interval and the upper, calcareous interval of the “*Orbitolina* level”. b) detail of the underlying bed, penetrated by cavities filled by orbitolinid-rich marly limestone. c) detail of the calcareous interval of the “*Orbitolina* level”, crowded with orbitolinid tests (the dark, lenticular spots). d) microfacies of interval shown in c. e) detail of the uppermost part of the “*Orbitolina* level”. f) microfacies of the interval shown in d, with orbitolinids and codiacean algae (*Boueina hochstetteri moncharmontiae*).

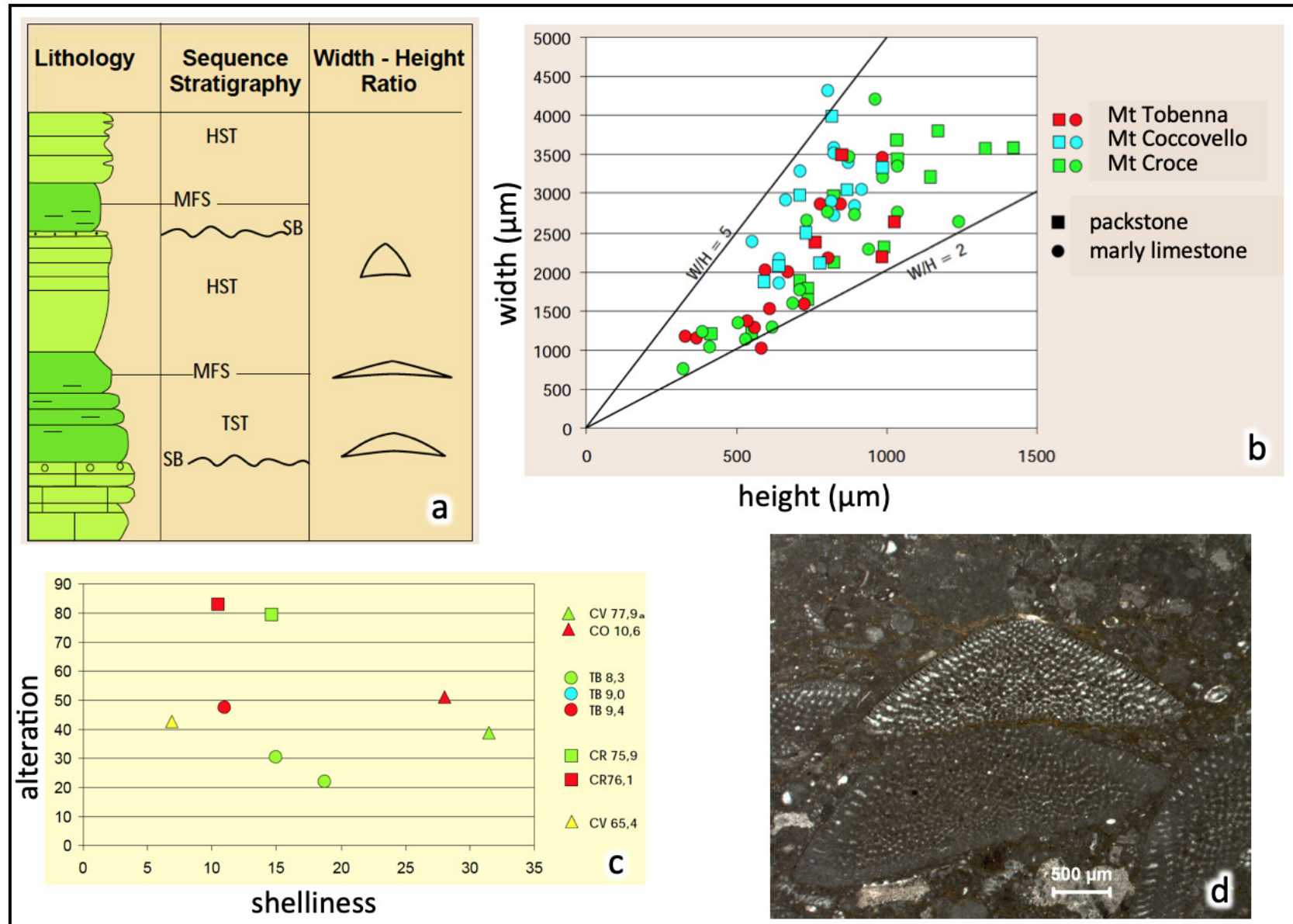


Fig. 28 - Taphonomy of the "Orbitolina level". a) sequence stratigraphic distribution of orbitolinid morphotypes (from Jones et al., 2004). b) width to height ratio of orbitolinid tests from the "Orbitolina level" of the Apennines. c) alteration vs. shelliness graph for the "Orbitolina level". d) orbitolinid tests of the "Orbitolina level" showing variable degree of micritisation (see text for further explanations).



much more complicated and needs to be addressed in terms of palaeoecology and functional morphology. Morphology of orbitolinid tests, namely their width-height ratio, has been traditionally related to water depth, with low-conical (flat) assemblages referred to deeper environments. It has also been suggested that flat conical orbitolinids are typically found in marls and argillaceous limestones, because they were adapted to higher nutrient supply. Since orbitolinids were most probably symbiont-bearing, light penetration exerted a more direct control than water-depth on their morphology: i.e., flat conical tests in marls could be responding more to water turbidity than to water depth. The abundance of codiaceans in the packstone at the top of the “*Orbitolina* level” suggests that light penetration had increased enough to support prolific green-algal growth. This was related either to a decrease of water depth and/or to more transparent water, as terrigenous input slowed down. Nutrient availability was however still sufficient to favor the flourishing of flat orbitolinids and codiacean algae, both supposed to prefer mesotrophic conditions. On this ground, we should expect “flatter” morphotypes in the more argillaceous lower and middle part of the “*Orbitolina* level”, compared with relatively “higher” morphotypes in the packstone. However, we did not find two distinctly separate clusters in a graph of width vs. height of the test (Fig. 28b). This finding would suggest that orbitolinid shell morphology is not responding so strictly to light penetration. Marls and argillaceous limestones with flat orbitolinids have been interpreted as maximum flooding facies (see for example Vilas et al., 1995; Jones et al., 2004). The *Orbitolina*-bearing marls of central-southern Italy are consistently found on top of a sequence boundary. At Mt Tobenna they fill microkarstic cavities into the substrate. Their position and facies (high clay content) are consistent with a maximum flooding interpretation. High nutrient input, low carbonate/high clay content, stratigraphic condensation, shell concentration, and the low-conical morphology of the orbitolinids in the “*Orbitolina* level” could therefore be all different facets of a maximum flooding phase.

### Stop 2.3: The *Thalassinoides* beds and the carbonate platform record of the Cenomanian-Turonian boundary OAE2 at Monteforte Cilento (40°22'10"N - 15°11'27"E)

A thick succession of Cretaceous shallow-water carbonates of the ApPC, overlain by the Eocene limestones and marls of the “Trentinara formation” and by the Lower Miocene glauconitic calcarenites of the “Roccadaspide formation”, is exposed in the mountain ridge made by Mt Sottano-Mt Vesole-Mt Chianello in the northern sector of the Cilento promontory (Fig. 29). In this stop you will look in detail at the upper Cenomanian-lower Turonian interval near the village of Monteforte Cilento, along the road to Roccadaspide. This is one of the sections that

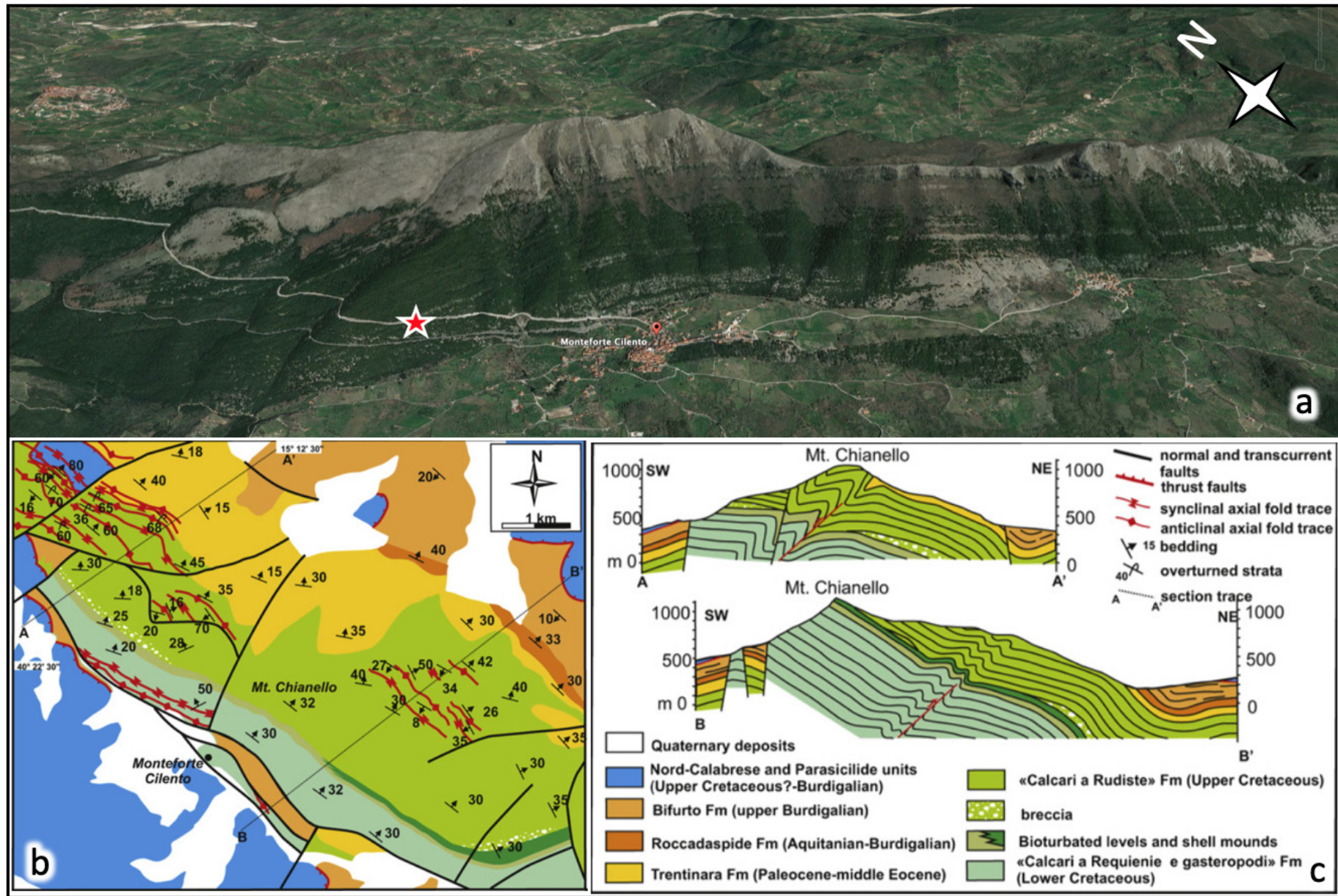


Fig. 29 - The Mt Chianello ridge in Northern Cilento. a) Google earth view; the red star marks the locality of stop 2.3. b) geological map. c) geological cross sections (figures b and c, from Vitale et al., 2012, reproduced by permission of Elsevier).



has been used to describe the record of the OAE2 (Bonarelli level equivalent) in the ApCP (Parente et al., 2007; Frija and Parente, 2008; Parente et al., 2008). Along the same roadcut, the underlying Albian-Cenomanian interval, witnesses alternating phases of arid to wet climate in a restricted platform environment (Simone et al., 2012; Iannace et al., 2014).

### Facies evolution, biostratigraphy, and carbon isotope stratigraphy

Parente et al. (2007) subdivided the upper Cenomanian-lower Turonian of Monteforte Cilento into four intervals (Fig. 30). Interval A (0–50 m) is mainly made of laminated and massive dolostones alternating with more or less dolomitised mudstones with ostracods and small miliolids. Foraminiferal wackestones and packstones become common in the last few metres of this interval. The occurrence of *Pseudorhapydionina dubia* indicates a middle Cenomanian age. Sedimentological evidence of subaerial exposure is represented by brecciated and/or laminated dolomitic caps. These facies points to deposition in very shallow water in a restricted platform environment. Interval B (50–62 m) starts with two distinct levels of radiolitid floatstone, separated by ostreid–foraminiferal wackestones, and continues with bioturbated foraminiferal wackestones–packstones with dolomite-filled *Thalassinoides* burrows. This interval contains a rich benthic foraminiferal assemblage (*Cisalveolina fraasi*, *Chrysalidina gradata*, *Coxites zubairensis*, *Pseudorhipidionina casertana*, *Pseudorhapydionina dubia*, *Pseudodolituonella reicheli*, *Daxia cenomana*, *Biplanata peneropliformis*) pointing to a late Cenomanian age. The facies and the rich and diverse fossil assemblages of this interval indicates deposition in more open marine conditions. Interval C (62–102 m) is made of thick-bedded bioturbated dolomitic limestones alternating with burrow-mottled dolostones and with intercalations of structureless sucrosic dolostones. Where not dolomitised, the bedrock consists of bioclastic mudstone–wackestone with fine-grained echinoid debris (plates and spines), fragments of thin-shelled bivalves, heterohelicids (mostly *Heterohelix moremani*), calcispheres, rare specimens of *Hedbergella* sp. and *Whiteinella* sp. Some beds are rich in fragments of pycnodontid ostreids. This marked change in the fossil association, and particularly the abundance of planktonic foraminifera, indicates a deepening trend, leading to a temporary drowning of this sector of the carbonate platform. Interval D (102–106 m) consists of peloidal–bioclastic limestones. The most frequent microfacies are mudstones–wackestones with miliolids, nezzazatids, calcareous algae (*Thaumatoporella* sp. and *Decastronema* sp.) and rare gastropods. These sediments indicate the resumption of the shallow-water carbonate factory. Carbon isotope stratigraphy has been used by Parente et al. (2007, 2008) to establish a high-resolution correlation between the Monteforte Cilento section (and other sections of the ApPC) and the reference section of Eastbourne, in the English Chalk Basin. The  $\delta^{13}\text{C}$  curves of all the studied sections show a pronounced positive

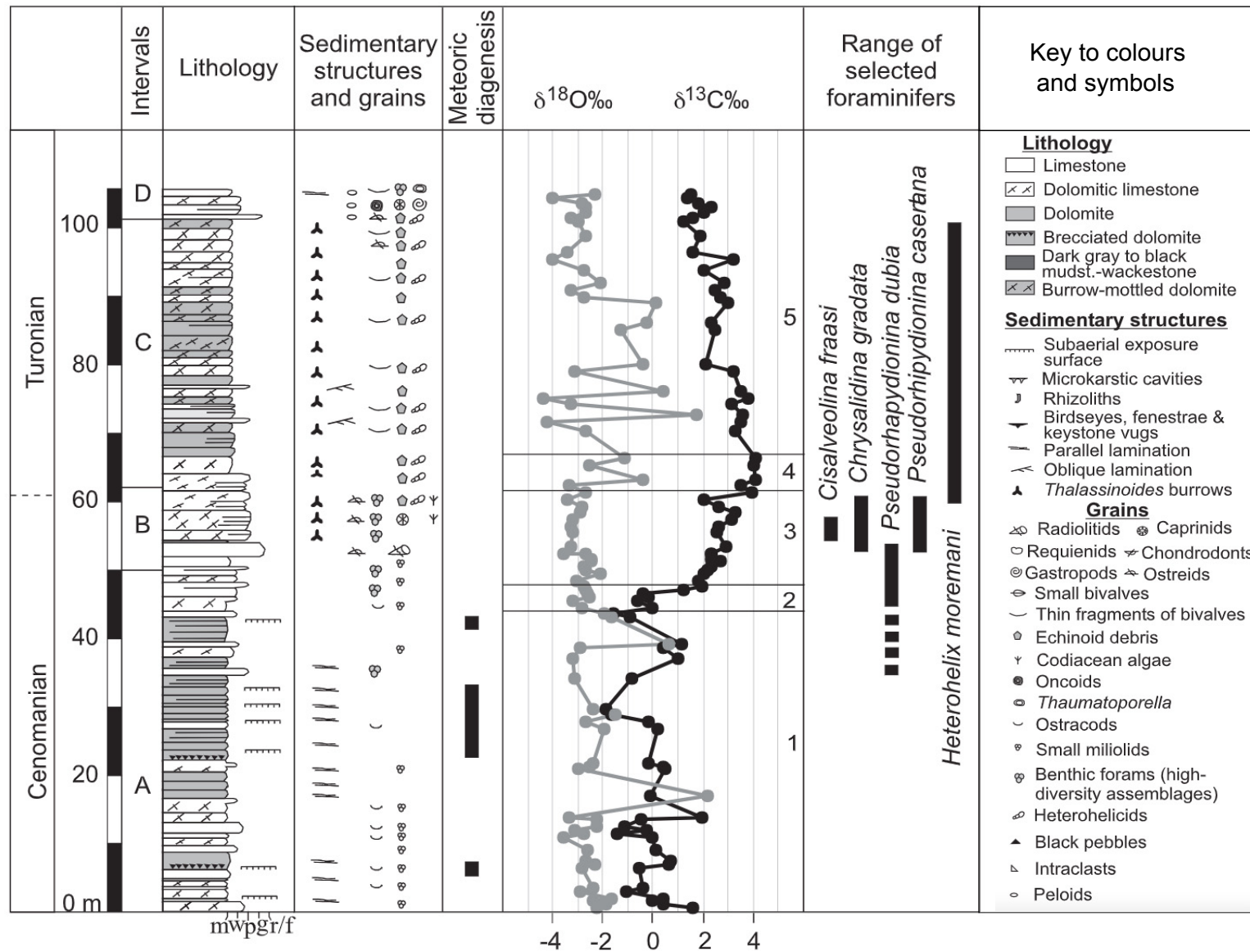


Fig. 30 - Monteforte Cilento section: lithological-sedimentological log, oxygen and carbon-isotope stratigraphy, and range of the most significant benthic foraminifers. The section has been subdivided into four intervals (A-D) on the basis of lithofacies and biostratigraphy. The  $\delta^{13}C$  curve has been subdivided into five segments (1-5). The Cenomanian-Turonian boundary is placed according to the most used biostratigraphic schemes. From Parente et al. (2007).

<https://doi.org/10.3301/GFT.2022.06>



excursion of  $\sim 3\text{‰} - 4\text{‰}$  (Fig. 31). Using the upper-Cenomanian larger foraminifer *Cisalveolina fraasi* as a biostratigraphic tie point, this excursion can be correlated with the well-known Cenomanian-Turonian carbon isotope excursion associated with the OAE2. More in detail, the carbon isotope curves show an initial rise to a first peak, followed by a return to lower values (so-called trough phase), followed by a rise into another peak (second peak), succeeded by slightly lower, relatively constant but more persistent values (plateau phase) that continue until the beginning of a decay toward background levels. This pattern conforms exactly to the fine structure of the  $\delta^{13}\text{C}$  excursion at the Cenomanian-Turonian boundary in the European reference section of Eastbourne, England (Paul et al., 1999; Tsikos et al., 2004) (Fig. 32).

### Larger benthic foraminifera and the OAE2

The high-resolution chemostratigraphic correlation with reference deep-water sections was used by Parente et al. (2008) to discuss the response of the shallow-water carbonate platforms to the global palaeoenvironmental perturbations associated with the OAE2. In particular, it was demonstrated that the diversity of larger benthic foraminifera shows a pattern of stepped extinction (Figs. 32 and 33). During the first phase of OAE2, the diversity of larger foraminifera was at a maximum and the assemblages were dominated by K-strategists with relatively long-life cycles (including the alveolinids), adapted to the extremely nutrient-poor conditions typical of subtropical gyres in a stratified ocean (Fig. 34). An episode of intermittent cooling, known as the Plenus Cold Event, roughly corresponding to the trough phase of the Cenomanian-Turonian carbon isotope excursion, stimulated enhanced ocean mixing. Delivery of nutrient-rich waters to the shallow ocean triggered the contemporaneous extinction of the most extreme oligotrophs: rotaliporids in the open ocean and alveolinids on shallow carbonate platforms. This interval was also the time of drowning of certain carbonate platforms. Peri-Adriatic platforms (southern Apennines, Croatia, Greece) survived drowning, but their foraminiferal assemblages were heavily affected by the perturbation of the trophic resource continuum. Only those few species that could tolerate mesotrophic conditions survived extinction. High productivity persisted during the second peak and plateau phase of the carbon isotope excursion, sustained by efficient recycling of nutrients (Fig. 34). Under these conditions, R-selected opportunistic taxa dominated planktonic foraminifer assemblages while the overcoming of the mesotrophic threshold triggered the second step of extinction of the larger foraminifera. Post-extinction foraminiferal assemblages were dominated by small miliolids, textularids, and discorbids. This pattern is analogous to the community shift, from symbiont-bearing larger foraminifera to small heterotrophs, observed in recent tropical shallow-water environments in response to nutrient pollution (Hallock, 2000).

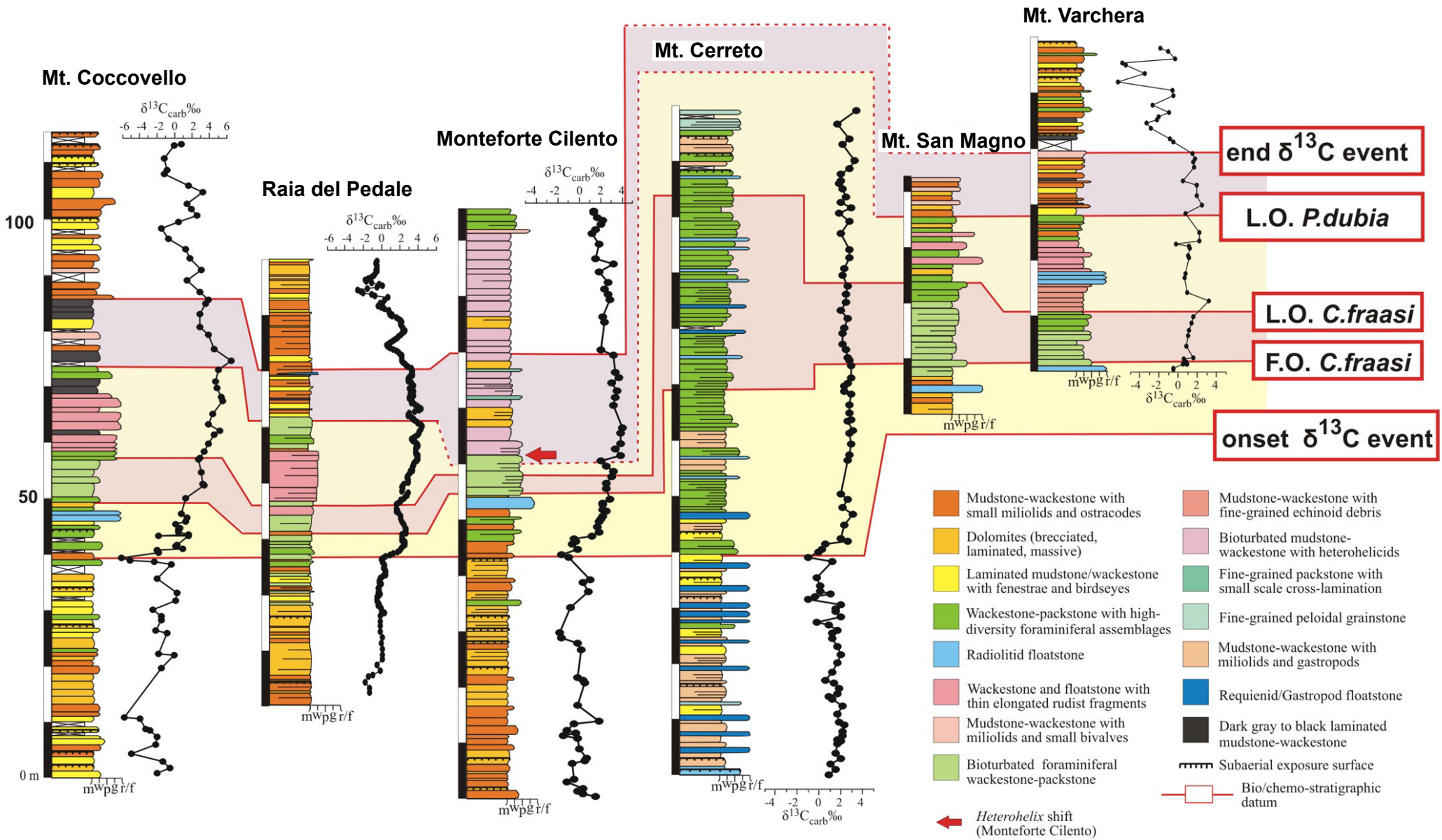


Fig. 31 - Lithofacies, carbon isotope stratigraphy and larger foraminifera events in the upper Cenomanian-lower Turonian of the ApCP. Bio-chemostratigraphic correlation of six sections distributed from Caserta (Mt Cerreto) to the Calabria-Basilicata border (Mt Coccovello).

<https://doi.org/10.3301/GFT.2022.06>

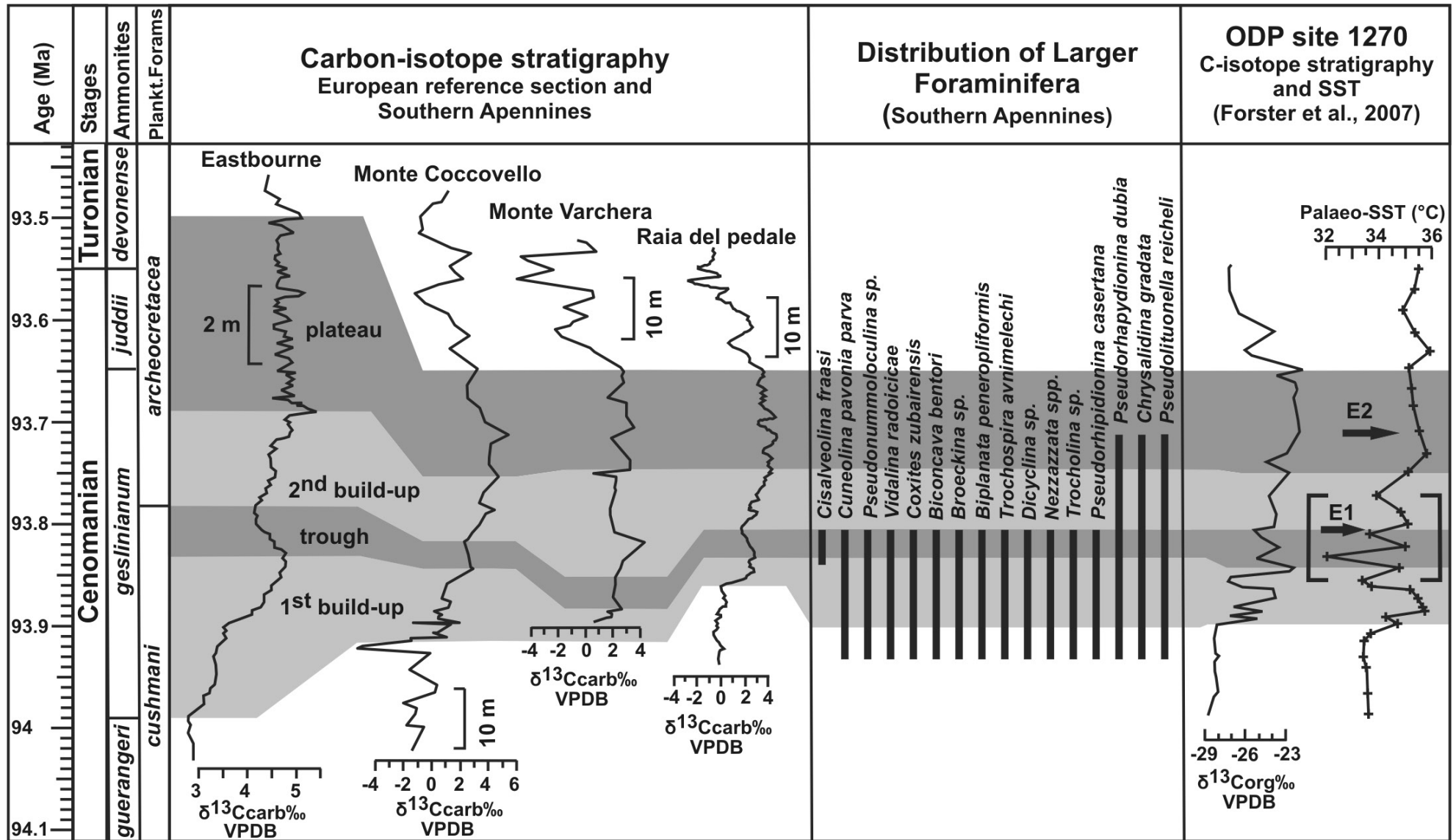
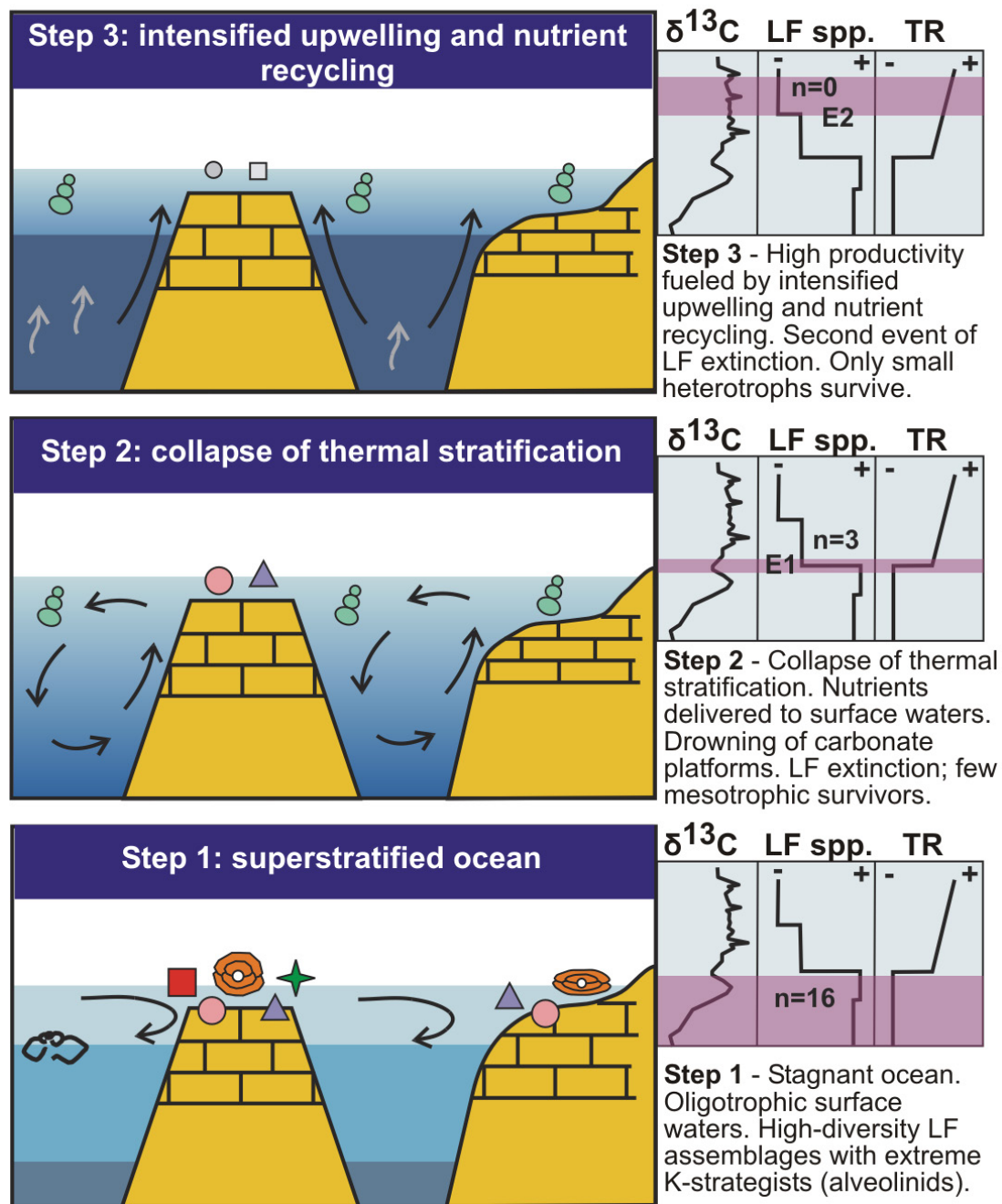


Fig. 32 - The extinction of larger foraminifera in the ApCP can be put in the framework of the OAE2 by a detailed carbon isotope correlation with the reference section of Eastbourne (Sussex, England; Paul et al., 1999) and with the ODP site 1270 in the tropical Atlantic, for which a high resolution record of sea-surface temperature (SST), based on the TEX86 proxy, has been established by (Forster et al., 2007). The first extinction event of larger foraminifera (E1) corresponds to the episode of thermal instability known as Plenus Cold Event. From Parente et al. (2008).





**The uppermost Cenomanian-lower Turonian *Thalassinoides* interval: a record of firmground bioturbation under incipient drowning.**

One of the most peculiar characters of the Cenomanian-Turonian interval in the ApCP is the presence of a regional correlatable interval characterised by selectively dolomitised *Thalassinoides* burrows, which make a very dense 3D boxwork of vertical burrows with both T- and Y-shaped bifurcations (Fig. 35). The diameter of the burrows ranges mainly from 0.7 to 1.5 cm. In the lower part of the bioturbated interval, the bedrock is a micritic limestone while the burrow infilling is selectively dolomitised. On weathered surfaces, the burrows stand out in relief (Fig. 35a), while on fresh surfaces they show as dark brown dolomite on the whitish micritic bedrock (Fig. 35b). Higher-up in the section, more intense burrowing and dolomitisation results in a mottled dolomite appearance. The stacking pattern consists of 1-2 m thick packages of bioturbated beds separated by sets of not-bioturbated thin beds.

Fig. 34 - Schematic model linking extinction of larger foraminifers to changes in nutrient availability and ocean circulation during OAE2. LF spp.: number of species of larger foraminifers in the southern Apennines Platform; TR: trophic resources in surface waters; E1: first extinction event; E2: second extinction event. From Parente et al. (2008).

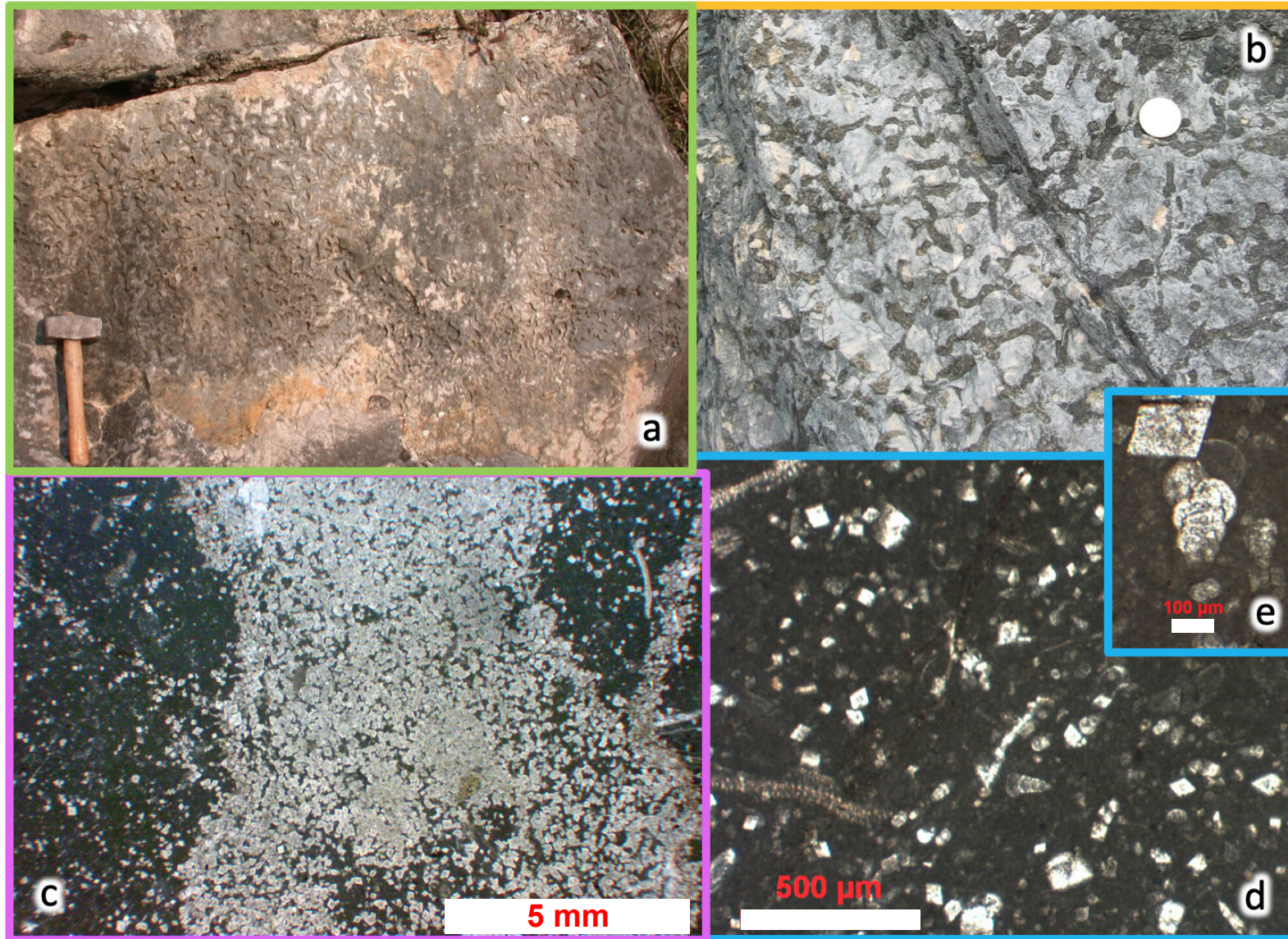


Fig. 35 - Selectively dolomitised *Thalassinoides* burrows in the upper Cenomanian-lower Turonian of Monteforte Cilento. a) the burrows stand out in relief on weathered surfaces. b) dark dolomitised burrows on a background of whitish micritic limestone. c) selectively dolomitised burrow infilling in thin section. d) mudstone with fine-grained echinoid debris and heterohelicids. e) *Heterohelix moremani*.



*Thalassinoides* burrows are typical constituent of the *Glossifungites* ichnofacies, representing an omission suite associated to firmgrounds (Pemberton et al., 2004). Firmgrounds develop during maximum flooding intervals under conditions of reduced sedimentation rates, which favour the exhumation at the seafloor of incipiently lithified surfaces. The stiff- to firm-ground character of the sediment and the reduced sedimentation rate ("omission") are demonstrated by the well-defined outline of the burrows ("elite trace fossils", with little or no post-burial deformation), by their high density and by their "open-burrow" character (i.e., the burrows stay open in the firm substrate and are passively infilled by post-omission sediment). A conceptual model for the selective dolomitisation of the upper Cenomanian *Thalassinoides* burrows of the ApCP can be borrowed from the very similar bioturbated facies of the Red River Formation, in the Ordovician of the Williston Basin (Canada and Northern US; see Gingras et al., 2004 and Jin et al. 2012). Bioturbation is responsible for altering the texture of the sediment in the periphery of the burrows and for establishing a textural heterogeneity between the bedrock and the post-omission burrow infilling (coarser? better sorted? more permeable). Bioturbation would also alter the geochemistry of the sediment, favouring preferential dolomitisation (microbially mediated?) (Fig. 35c) in the anoxic zone established by organic matter degradation. The wide synchronous occurrence of the *Thalassinoides* bioturbated facies on a regional scale can be put in relation to the fast sea-level rise during the late Cenomanian. Conditions favourable to the development of firmground substrates were further enhanced by reduced carbonate production on the carbonate platform under increased nutrient input.

### **Acknowledgements**

M. Parente and S. Amodio acknowledge funding by the Italian MUR under grant PRIN 2017RX9XXXY "Biota resilience to global change: biomineralization of planktic and benthic calcifiers in the past, present and future". The Authors are grateful to the Chairs and to the members of the field trip committee of the meeting Strati2019 for stimulating the organisation of a field trip on the stratigraphy and facies of the Apennine Carbonate Platform. Sincere thanks are due to Andrea Zanchi and Piero Gianolla, Editor in chief and AE of GFT&M, respectively, to the Editorial Managers: Fabio Massimo Petti, Angelo Cipriani and Diego Pieruccioni. We are also very grateful to Marco Brandano and Michele Morsilli for their suggestions and comments.

## REFERENCES

- Aigner T. (1985) - Storm depositional systems. Lect. Notes Earth Syst. Sci., 3, Springer-Verlag, Berlin, 17pp.
- Amodio S. (2006) - Foraminifera diversity changes and paleoenvironmental analysis: the Lower Cretaceous shallow-water carbonates of San Lorenzello, Campanian Apennines, southern Italy. *Facies*, 52, 53-67.
- Amodio S. (2010) - Barremian-Aptian shallow-water carbonates of Monte Faito (Sorrento Peninsula, southern Italy). Microstratigraphy, cyclostratigraphy and sequence stratigraphy. *Rend. Online Soc. Geol. It.*, 11, 482-483.
- Amodio S., Barattolo F., Martino M. (2020) - Carbonate ecosystem and environmental evolution during the Valanginian–Barremian: discussion on possible controlling factors in the Apennine Carbonate Platform record (Italy). *Cretac. Res.*, 108, 104351. <https://doi.org/10.1016/j.cretres.2019.104351>
- Amodio S., Barattolo F., Parente M. (2023) - The Early Cretaceous C-isotope record of shallow-marine carbonates: a transect across southern Alps, Apennines and Dinarides. *Rend. OnLine, Soc. Geol. It.*, 59, Special section - XIV Congresso GeoSed - Bari 2022. <https://doi.org/10.3301/ROL.2023.05>
- Amodio S., Barattolo F., Riding R. (2018) - Early Cretaceous dendritic shrub-like fabric in karstified peritidal carbonates from southern Italy. *Sediment. Geol.*, 373, 134-146. <https://doi.org/10.1016/j.sedgeo.2018.06.001>
- Amodio S., Ferreri V., D'Argenio B. (2011) - The Barremian-Aptian shallow-marine carbonates of Monte Faito and of Santa Maria bore cores (central-southern Apennines, Italy). Regional correlation based on cyclostratigraphy. *Rend. OnLine Soc. Geol. It.*, 17, 9-17.
- Amodio S., Ferreri V., D'Argenio B. (2013a) - Cyclostratigraphic and chronostratigraphic correlations in the Barremian-Aptian shallow-marine carbonates of the central-southern Apennines (Italy). *Cretac. Res.*, 44, 132-156. <http://dx.doi.org/10.1016/j.cretres.2013.04.003>
- Amodio S., Ferreri V., D'Argenio B. (2013b) - Lower Cretaceous carbon-isotope records of M. Faito and S. Maria sections (central-southern Italy). Platform to basin correlation and orbital calibration. *J. Mediterr. Earth Sci.*, 5, 3-6.
- Amodio S., Ferreri V., D'Argenio B., Weissert H., Sprovieri M. (2008) - Carbon-isotope stratigraphy and cyclostratigraphy of shallow-marine carbonates. The case of San Lorenzello, Early Cretaceous of southern Italy. *Cretac. Res.*, 29, 803-813.
- Amodio S. and Weissert H. (2017) - Palaeoenvironment and palaeoecology before and at the onset of Oceanic Anoxic Event (OAE)1a: Reconstructions from Central Tethyan archives. *Palaeogeogr., Palaeoclimatol., Palaeoecol.*, 479, 71-89.
- Arnaud H., Arnaud-Vanneau A., Blanc-Alétru M.C., Adatte T., Argot M., Delanoy G., Thieuloy J.P., Vermeulen J., Virgone A., Virlouvét B., Wermeille S. (1998) - Répartition stratigraphique des orbitolinidés de la plate-forme urgonienne subalpine et jurassienne (SE de la France). *Géol. Alp.*, 74, 3-89.
- Ascione A., Ciarcia S., Di Donato V., Mazzoli S., Vitale S. (2012) - The Pliocene-Quaternary wedge-top basins of southern Italy: an expression of propagating lateral slab tear beneath the Apennines. *Basin Res.*, 24, 456-474.
- Barattolo F., Amodio S., Bucur I.I., Martino M. (2021) - *Selliporella johnsonii* (Praturlon) nov. comb. and *Selliporella neocomiensis* (Radoičić) (green algae, Dasycladales), taxonomic reconsideration and chronostratigraphic calibration. *Cretac. Res.*, 125, 104848. <https://doi.org/10.1016/j.cretres.2021.104848>

- Barattolo F. and Pugliese A. (1987) - Il Mesozoico dell'Isola di Capri. Quad. Accad. Pontaniana, 8, 1-37, Napoli
- Barattolo F. and Romano R. (2005) - Shallow carbonate platform bioevents during the Upper Triassic-Lower Jurassic: an evolutive interpretation. Boll. Soc. Geol. Ital., 124, 123-142.
- Bartirromo A. (2013) - Plant remains from the Lower Cretaceous Fossil-Lagerstätte of Pietraroja, Benevento, southern Italy. Cretac. Res., 46, 65-79. <http://dx.doi.org/10.1016/j.cretres.2013.08.013>
- Bassi D., Carannante G., Checconi A., Simone L., Vigorito M. (2010) - Sedimentological and palaeoecological integrated analysis of a Miocene channelized carbonate margin, Matese Mountains, Southern Apennines, Italy. Sediment. Geol. 230, 105-122.
- Bassoulet J.P. (1997) - Algues dasycladales. Distribution des principales especes. In: Cariou E., Hantzpergue P. (Eds.), Biostratigraphie du Jurassique ouest-Européen et Méditerranéen Mém. Centres Rech. Explo. Prod. Elf Aquitaine, 17, 339-341.
- Berra F., Jadoul F., Anelli A. (2010) - Environmental control on the end of the Dolomia Principale/ Hauptdolomit depositional system in the central Alps: Coupling sea-level and climate changes. Palaeogeogr., Palaeoclimatol., Palaeoecol., 290 (1-4), 138-150.
- Berra F., Delfrati L., Ponton M. (2007) - Dolomia Principale. Quaderni del Servizio Geologico d'Italia, III, 7, 63-72.
- Bonardi G., Cinque A., De Capoa P., Di Staso A., Esposito P., Guida D., Mazzoli S., Parente M., Radoicic R., Sgrosso A., Siervo V., Zamparelli V. (2016) - Note illustrative della Carta Geologica d'Italia alla scala 1:50.000, F. 521 Lauria, 143 pp., S.EL.CA, Firenze.
- Boni M., Reddy S.M., Mondillo N., Balassone G., Taylor, R. (2012) - A distant magmatic source for Cretaceous karst bauxites of southern Apennines (Italy), revealed through SHRIMP zircon age dating. Terra Nova, 24, 326-332.
- Boni M., Rollinson G., Mondillo N., Balassone G., Santoro L. (2013) - Quantitative mineralogical characterization of karst bauxite deposits in the Southern Apennines, Italy. Econ. Geol., 108, 813-833.
- Bosellini A. (2002) - Dinosaurs "re-write" the geodynamics of the eastern Mediterranean and the paleogeography of the Apulia Platform. Earth-Sci. Rev., 59, 211-234.
- Brandano M., Westphal H., Mateu-Vicens G. (2010) - The Sensitivity of a Tropical Foramol-Rhodalgial Carbonate Ramp to Relative Sea-Level Change: Miocene of the Central Apennines, Italy. IAS Spec. Publ., 42, 89-106.
- Brandano M., Mateu-Vicens G., Baceta J.I. (2022) - Understanding carbonate factories through palaeoecological and sedimentological signals – Tribute to Luis Pomar. Sedimentology, 69, 5-23. <https://doi.org/10.1111/sed.12965>
- Bravi S. and Garassino A. (1998) - New biostratigraphic and palaeoecologic observations on the "Plattenkalk" of the lower Cretaceous (Albian) of Pietraroja (Benevento, S Italy), and its decapod crustacean assemblage. Atti Soc. It. Sci. Nat., Museo Civ. Stor. Nat. Milano, 138/1997 (I-II), 119-171.
- Brescia M., D'Argenio B., Ferreri V., Pelosi N., Rampone S., Tagliaferri, R. (1996) - Neural net aided detection of astronomical periodicities in geologic records. Earth Planet. Sci. Lett., 139, 33-45.
- Broglio Loriga C. and Neri C. (1976) - Aspetti paleobiologici e paleogeografici della facies a "Lithiotis" (Giurese inf.). Riv. Ital. Paleontol. Stratigr., 82, 651-706.
- Bulot L.G., Thieuloy J.P., Blanc E., Klein J. (1992) - Le cadre stratigraphique du Valanginien supérieur et de l'Hauterivien du Sud-Est de la France: Définition des biochronozones et caractérisation de nouveaux biohorizons. Géol. Alp., 68, 13-56.

- Butler R.W.H., Mazzoli S., Corrado S., De Donatis M., Di Bucci D., Gambini R., Naso G., Nicolai C., Scrocca D., Shiner P., Zucconi V. (2004) - Applying thick-skinned tectonic models to the Apennine thrust belt of Italy: limitations and implications. In: McClay K.R. (Ed.), *Thrust Tectonics and Petroleum Systems*. AAPG Memoir, 82, 647-667.
- Caggiati M., Gianolla P., Breda A., Celarc B., Preto N. (2018) - The start-up of the Dolomia Principale/Hauptdolomit carbonate platform (Upper Triassic) in the eastern Southern Alps. *Sedimentology*, 65(4), 1097-1131. <https://doi.org/10.1111/sed.12416>
- Carannante G. (1982) - Modello deposizionale e diagenetico di un livello fosfatico del Miocene carbonatico dell'Appennino Campano. *Rend. Soc. Geol. It.*, 5, 15-20.
- Carannante G., Cherchi A., Simone L. (1995) - Chlorozoan versus foramol lithofacies in Late Cretaceous rudist limestones. *Palaeogeogr. Palaeoclimatol. Palaeoecol.*, 119, 137-154.
- Carannante G., D'Argenio B., Mindszenty A., Ruberti D., Simone L. (1994) - Cretaceous-Miocene shallow water carbonate sequences. Regional unconformities and stacking patterns. Guidebook, Excursion A2, 15th IAS Regional Meeting, Ischia, Italy, 29-59.
- Carannante G., Esteban M., Milliman J.D., Simone L. (1988) - Carbonate lithofacies as paleolatitude indicators: problems and limitations. In: Nelson, C.S. (Ed.), *Non-tropical Shelf Carbonates - Modern and Ancient*. *Sediment. Geol.*, 60, 333-346.
- Carannante G., Graziano R., Ruberti D., Simone L. (1997) - Upper Cretaceous temperate-type open shelves from north-ern (Sardinia) and southern (Apennines-Apulia) Mesozoic Tethyan margins. In: James N.P. and Clarke J.A.D. (Eds.), *Cool-water carbonates*. *SEPM Spec. Publ.*, 56, 309-325.
- Carannante G., Matarazzo R., Pappone G., Severi, C. (1988) - Le Calcareniti Mioceniche della Formazione di Roccadaspide (Appennino Campano-Lucano). *Mem. Soc. Geol. It.*, 41, 775-789.
- Carannante G., Pugliese A., Ruberti D., Simone L., Vigliotti M., Vigorito M. (2009) - Evoluzione cretacea di un settore della piattaforma apula da dati di sottosuolo e di affioramento (Appennino campano-molisano). *Boll. Soc. Geol. It.*, 128, 3-31.
- Carannante G., Signore M., Vigorito M. (2006) - Vertebrate-rich Plattenkalk of Pietraroia (Lower Cretaceous, Southern Apennines, Italy): a new model. *Facies*, 52(4), 555-577. <https://doi.org/10.1007/s10347-006-0075-z>
- Carannante G. and Simone L. (1996) - Rhodolith facies in the central-southern Apennines Mountains, Italy. In: Franseen, E.K., Esteban, M., Rouchy, J.-M. (Eds.), *Models for Carbonate Stratigraphy from Miocene Reef Complexes of Mediterranean Regions*. *Concepts in Sedimentology and Paleontology SEPM*, 5, 261-275.
- Carras N., Conrad M.A., Radoičić R. (2006) - *Salpingoporella*, a common genus of Mesozoic Dasycladales (calcareous green algae). *Rev. de Paléobiologie*, 25(2), 457-517.
- Catenacci E., Manfredini M. (1963) - Osservazioni stratigrafiche sulla Civita di Pietraroia (Benevento). *Boll. Soc. Geol. It.* 82, 65-92.
- Cello G., Guerra I., Tortorici L., Turco E., Scarpa R. (1982) - Geometry of the neotectonic stress field in southern Italy: geological and seismological evidence. *J. Struct. Geol.*, 4, 385-393.
- Channell J.E.T., D'Argenio B., Horvath F. (1979) - Adria, the African Promontory, in Mesozoic Mediterranean palaeogeography. *Earth-Sci. Rev.*, 15, 213-292.

- Channell J.E.T., Erba E., Lini, A. (1993) - Magnetostratigraphic calibration of the Late Valanginian carbon isotope event in pelagic limestones from Northern Italy and Switzerland. *Earth Planet. Sci. Lett.*, 118, 145-166.
- Cherchi A., De Castro P., Schroeder R. (1978) - Sull'età dei livelli a Orbitolinidi della Campania e delle Murge Baresi (Italia meridionale). *Boll. Soc. Nat. Napoli*, 87, 363-385.
- Chinzei K. (1982) - Morphological and structural adaptations to soft substrates in the Early Jurassic monomyarians *Lithiotis* and *Cochlearites*. *Lethaia*, 15, 179-197.
- Chiocchini M., Chiocchini R.A., Didaskalou P., Potetti, M. (2008) - Microbiostratigrafia del Triassico superiore, Giurassico e Cretacico in facies di piattaforma carbonatica del Lazio centro-meridionale e Abruzzo: revisione finale. *Mem. Descr. Carta Geol. d'It.*, 5-170.
- Chiocchini M. and Mancinelli A. (1977) - Microbiostratigrafia del Mesozoico in facies di piattaforma carbonatica dei Monti Aurunci (Lazio meridionale). *Studi Geol. Camerti*, 3, 109-152.
- Cinque A., Patacca E., Scandone P., Tozzi M. (1993) - Quaternary kinematic evolution of the Southern Apennines. Relationships between surface geological features and deep lithospheric structures. *Annali di Geofisica*, 36, 249-260.
- Clavel B., Schroeder R., Charollais J., Busnardo R., Martin Closas C., Decrouez D., Sauvagnat J., Cherchi, A. (2002) - Les "Couches inférieures "orbitolines" (Chaines subalpines septentrionales): mythe ou réalité? *Rev. de Paléobiologie*, 21, 865-871.
- Cohen A.S., Coe A.L., Kemp D.B. (2007) - The Late Palaeocene- Early Eocene and Toarcian (Early Jurassic) carbon isotope excursions: a comparison of their time scales, associated environmental changes, causes and consequences. *J. Geol. Soc.*, 164, 1093-1108.
- Dal Sasso C. and Maganuco S. (2011) - *Scipionyx samniticus* (Theropoda: Compsognathidae) from the Lower Cretaceous of Italy. *Mem. Soc. It. Sci. Nat. e Museo Civico St. Nat. Milano*, XXXVII(I), Milano 281pp.
- Dal Sasso C. and Signore M. (1998) - Exceptional soft-tissue preservation in a theropod dinosaur from Italy. *Nature*, 392, 383-387.
- D'Argenio B., De Castro P., Emiliani C., Simone L. (1975) - Bahamian and Apenninic limestones of identical lithofacies and age. *AAPG Bull.*, 59, 524-530.
- D'Argenio B., Ferreri V., Amodio S. (2008) - Sequence stratigraphy of Cretaceous carbonate platforms: a cyclostratigraphic approach. In: Amorosi A., Haq B.U., Sabato L. (Eds.), *Advances in Application of Sequence Stratigraphy in Italy*. *Geol. Acta Spec. Publ.*, 1, 157-172.
- D'Argenio B., Ferreri V., Amodio S., (2011) - Eustatic cycles and tectonics in the Cretaceous shallow Tethys. Central-Southern Apennines. *Ital. J. Geosci.*, 130, 119-127. <https://doi.org/10.3301/IJG.2010.27>
- D'Argenio B., Ferreri V., Amodio S., Pelosi N. (1997) - Hierarchy of high-frequency orbital cycles in Cretaceous carbonate platform strata. *Sediment. Geol.*, 113, 169-193.
- D'Argenio B., Ferreri V., Raspini A., Amodio S., Buonocunto F.P. (1999) - Cyclostratigraphy of a carbonate platform as a tool for high-precision correlation. *Tectonophysics*, 315, 357-385.

- D'Argenio B., Ferreri V., Weissert H., Amodio S., Buonocunto F.P., Wissler L. (2004) - A multidisciplinary approach to global correlation and geochronology. The Cretaceous shallow-water carbonates of southern Apennines, Italy. In: D'Argenio B., Fischer A.G., Premoli Silva I., Weissert H., Ferreri V. (Eds.), *Cyclostratigraphy: Approaches and case histories*. SEPM Spec. Publ., 81, 103-122.
- D'Argenio B. and Mindszenty A. (1995) - Bauxites and related paleokarst: tectonic and climatic event markers at regional unconformities. *Ecl. Geol. Helv.*, 88, 453-499.
- De Castro P. (1963) - Nuove osservazioni sul livello ad Orbitoline in Campania. *Boll. Soc. Nat. Napoli*, 71, 103-135.
- De Castro P. (1991) - Mesozoic. In: Barattolo F., De Castro P., Parente M. (Eds.), *Field trip guide-book, 5th Int. Symposium on Fossil Algae*. 21-38.
- Dercourt J., Zonenshain L.P., Ricou L-E., Kazmin V.G., Le Pichon X., Knipper A.L., Grandjacquet C., Sbertshikov I.M., Geysant J., Lepvriers C., Pechersky D.H., Boulin J., Sibuet J-C., Savostin L.A., Sorokhtin O., Westphal M., Bazhenov M.L., Lauerh J.P., Biju-Duval B. (1986) - Geological evolution of the Tethys belt from the Atlantic to the Pamirs since the Lias. *Tectonophysics*, 123, 241-315.
- Dewey J.F., Helman M.L., Turco E., Hutton D.H.W., Knott, S.D. (1989) - Kinematics of the Western Mediterranean. In: Coward M.P., Dietrich D., Park R.G. (Eds.), *Alpine Tectonics*. Geol. Soc. Lond. Spec. Publ., 45, 265-283.
- Di Lucia M., Trecalli A., Mutti M., Parente M. (2012) - Bio-chemostratigraphy of the Barremian-Aptian shallow-water carbonates of the southern Apennines (Italy): pinpointing the OAE1a in a Tethyan carbonate platform. *Solid Earth*, 3(1), 1-28.
- Erba E. (2004) - Calcareous nannofossils and Mesozoic oceanic anoxic events. *Mar. Micropaleontol.*, 52, 85-106.
- Erba E., Bartolini A., Larson R.L. (2004) - Valanginian Weissert oceanic anoxic event. *Geology*, 32, 149-152.
- Erba E., Channell J.E.T., Claps M., Jones C., Larson R.L., Opdyke B.N., Silva I.P., Riva A., Salvini G., Torricelli S. (1999) - Integrated stratigraphy of the Cismon APTICORE (Southern Alps, Italy): a "reference section" for the Barremian-Aptian interval at low latitudes, *J. Foraminifer. Res.*, 29, 371-391.
- Ferreri V., Amodio S., Sandulli R., D'Argenio B. (2004) - Orbital chronostratigraphy of the Valanginian-Hauterivian boundary. A cyclostratigraphic approach, In: D'Argenio B., Fischer A.G., Premoli Silva I., Weissert H., Ferreri V. (Eds.), *Cyclostratigraphy. Approaches and Case Histories*. SEPM Spec. Publ., 81, 153-166.
- Fiorillo F. and Wilson R.C. (2004) - Rainfall induced debris flows in pyroclastic deposits, Campania (southern Italy). *Eng. Geol.*, 75, 263-289.
- Flügel E. (2010) *Microfacies of Carbonate Rocks*. Springer, Berlin, Heidelberg, 924pp.
- Föllmi K.B., Bodin S., Godet A., Linder P., van de Schootbrugge B. (2007) - Unlocking paleo-environmental information from early Cretaceous shelf sediments in the Helvetic Alps: stratigraphy is the key! *Swiss J. Geosci.*, 100, 349-369.
- Föllmi K.B. and Gainon F. (2008) - Demise of the northern Tethyan Urgonian carbonate platform and subsequent transition towards pelagic conditions: the sedimentary record of the Col de la Plaine Morte area, central Switzerland. *Sediment. Geol.*, 205, 142-159.

- Föllmi K.B., Gertsch B., Renevey J.P., de Kaenel E., Stille P. (2008) - Stratigraphy and sedimentology of phosphate-rich sediments in Malta and southeastern Sicily (latest Oligocene to early Late Miocene). *Sedimentology*, 55, 1029-1051.
- Föllmi K.B., Godet A., Bodin S., Linder P. (2006) - Interactions between environmental change and shallow water carbonate buildup along the northern Tethyan margin and their impact on the Early Cretaceous carbon isotope record. *Paleoceanography*, 21, 4211-4216. <https://doi.org/10.1029/2006PA001313>
- Föllmi K.B., Hofmann H., Chiaradia M., de Kaenel E., Frijia G., Parente, M. (2015) - Miocene phosphate-rich sediments in Salento (southern Italy). *Sediment. Geol.*, 327, 55-71.
- Forster A., Schouten S., Moriya K., Wilson P.A., Sinninghe Damste J.S. (2007) - Tropical warming and intermittent cooling during the Cenomanian/Turonian oceanic anoxic event 2: Sea surface temperature records from the equatorial Atlantic. *Paleoceanography*, 22, PA1219, doi:10.1029/2006PA001349.
- Fraser N., Bottjer D., Fischer A. (2004) - Dissecting "Lithiotis" bivalves: implications for the Early Jurassic reef eclipse. *Palaios* 19, 51-67.
- Friedrich O., Reichelt K., Herrle J.O., Lehmann J., Pross J., Hemleben C. (2003) - Formation of the Late Aptian Niveau Fallot black shales in the Vocontian Basin (SE France): evidence from foraminifera, palynomorphs, and stable isotopes. *Mar. Micropaleontol.*, 49(1-2), 65-85.
- Frijia G. and Parente M. (2008) - Strontium isotope stratigraphy in the upper Cenomanian shallow-water carbonates of the southern Apennines: short-term perturbations of marine  $^{87}\text{Sr}/^{86}\text{Sr}$  during the oceanic anoxic event 2. *Palaeogeogr., Palaeoclimatol., Palaeoecol.*, 261, 15-29. <https://doi.org/10.1016/j.palaeo.2008.01.003>
- Frijia G., Parente M., Di Lucia M., Mutti M. (2015) - Carbon and strontium isotope stratigraphy of the Upper Cretaceous (Cenomanian-Campanian) shallow-water carbonates of southern Italy: Chronostratigraphic calibration of larger foraminifera biostratigraphy. *Cretac. Res.*, 53, 110-139.
- Gingras M.K., Pemberton S.G., Muelenbachs K., Machel H. (2004) - Conceptual models for burrow-related, selective dolomitization with textural and isotopic evidence from the Tyndall Stone, Canada. *Geobiology*, 2(1), 21-30.
- Goldammer R.K., Dunn P.A., Hardie L.A. (1990) - Depositional cycles, composite sea-level changes, cycle stacking pattern and the hierarchy of stratigraphic forcing. Examples from Alpine Triassic platform carbonates. *Geol. Soc. Am. Bull.*, 102, 535-562.
- Graziano R. and Raspini A. (2018) - High-resolution chronostratigraphy of palaeoecologic and isotopic changes in shallow-marine carbonates: Deciphering the completeness of the Aptian record in the Apennine carbonate platform (southern Italy). *Cretac. Res.*, 86, 97-128. <https://doi.org/10.1016/j.cretres.2017.12.008>
- Hallock P. (2000) - Symbiont-bearing foraminifera: Harbingers of global change. In: Lee J.J. and Muller P.H. (Eds.), *Advances in the biology of Foraminifera*. *Micropaleontology*, 46,(1), 95-104.
- Haq B.U., Hardenbol J., Vail P.R. (1987) - Chronology of fluctuating sea levels since the Triassic. *Science*, 237, 1156-1167.
- Haq B.U. (2014) - Cretaceous eustasy revisited. *Glob. Planet. Change*, 113, 44-58.
- Hennig S., Weissert H., Bulot L. (1999) - C-isotope stratigraphy, a calibration tool between ammonite- and magnetostratigraphy: the Valanginian-Hauterivian transition. *Geol. Carpath.*, 50, 91-96.

- Herrle J.O., Köbber P., Friedrich O., Erlenkeuser H., Hemleben C. (2004) - High-resolution carbon isotope records of the Aptian to lower Albian from SE France and the Mazagan Plateau (DSDP Site 545). A stratigraphic tool for paleoceanographic and paleobiologic reconstruction. *Earth Planet. Sci. Lett.*, 218, 149-161.
- Hesselbo S.P., Jenkyns H.C., Duarte L.V., Oliveira L.C.V. (2007) - Carbon-isotope record of the Early Jurassic (Toarcian) Oceanic Anoxic Event from fossil wood and marine carbonate (Lusitanian Basin, Portugal). *Earth Planet. Sci. Lett.*, 253, 455-470.
- Hippolyte J.C., Angelier J., Roure F. (1994) - A major geodynamic change revealed by Quaternary stress patterns in the Southern Apennines (Italy). *Tectonophysics*, 230, 199-210.
- Husinec A. and Read J.F. (2006) - Transgressive oversized radial ooid facies in the Late Jurassic Adriatic Platform interior: Low-energy precipitates from highly supersaturated hypersaline waters. *Geol. Soc. Am. Bull.*, 118(5-6), 550-556.
- Iannace A., Frijia G., Galluccio L., Parente M. (2014) - Facies and early dolomitization in Upper Albian shallow-water carbonates of the southern Apennines (Italy): paleotectonic and paleoclimatic implications. *Facies*, 60(1), 169-194.
- Iannace A., Parente M., Zamparelli V. (2005) - The Upper Triassic platform margin facies of Southern Apennines and their Jurassic fate: state of the art. *Boll. Soc. Geol. It.*, 124(1), 203-214.
- Iannace A. and Zamparelli V. (1996) - The serpulid-microbialite bioconstructions of the «Scisti Ittiolitici» basin of Giffoni Vallepiana (Upper Triassic, Southern Apennines). *Paleopelagos*, 6, 45-62.
- Iannace A. and Zamparelli V. (2002) - Upper Triassic platform margin biofacies and the paleogeography of Southern Apennines. *Palaeogeogr., Palaeoclimatol., Palaeoecol.*, 179, 1-18.
- James N.P. (1997) - The cool water carbonate depositional realm. In: James N.P. and Clarke J.A.D. (Eds.), *Cool-water Carbonates*. SEPM Spec. Publ., 56, 1-20.
- Jin J., Harper D.A.T., Rasmussen J.A., Sheehan, P.M. (2012) - Late Ordovician massive-bedded *Thalassinoides* ichnofacies along the palaeoequator of Laurentia. *Palaeogeogr., Palaeoclimatol., Palaeoecol.*, 367-368, 73-88.
- Jones B., Simmons M., Whittaker J. (2004) - Chronostratigraphic and paleoenvironmental significance of agglutinated and associated larger benthonic foraminifera from the Lower to "Middle" Cretaceous of the Middle East. In: Bubik M. and Kaminski M.A. (Eds.), *Proceeding of the Sixth International Workshop on Agglutinated Foraminifera*, Grzybowski Found. Spec. Publ., 8, 229-235.
- Kemp D.B., Coe A.L., Cohen A.S., Weedon G.P. (2011) - Astronomical forcing and chronology of the early Toarcian (Early Jurassic) oceanic anoxic event in Yorkshire, UK. *Paleoceanography*, 26, PA4210.
- Kiani Harchegani F. and Morsilli M. (2019) - Internal waves as controlling factor in the development of stromatoporoid-rich facies of the Apulia Platform margin (Upper Jurassic-Lower Cretaceous, Gargano Promontory, Italy). *Sediment. Geol.*, 380, 1-20.
- Kidwell S.M. (1986) - Models for fossil concentrations: paleo-biologic implications. *Paleobiology* 12, 6-24.
- Kiessling W. and Simpson C. (2011) - On the potential for ocean acidification to be a general cause of ancient reef crises. *Glob. Change Biol.*, 17, 56-67.
- Knoll A.H., Bambach R.K., Payne J., Pruss S., Fischer W. (2007) - A paleophysiological perspective on the end-Permian mass extinction and its aftermath. *Earth Planet. Sci. Lett.*, 256, 295-313.

- Kump L.R., Bralower T.J., Ridgwell A. (2009) - Ocean acidification in deep time. *Oceanography*, 22, 94-107.
- Lees A. (1975) - Possible influence of salinity and temperature on modern shelf carbonate sedimentation. *Mar. Geol.*, 19, 159-198.
- Li F., Gong Q., Burne R. V., Tang H., Su C., Zeng K., Zhang Y., Tan X. (2019) - Ooid factories operating under hothouse conditions in the earliest Triassic of South China. *Glob. Planet. Change*, 172, 336-354.
- Lini A., Weissert H., Erba E. (1992) - The Valanginian carbon-isotope event: a first episode of greenhouse climate conditions during the Cretaceous. *Terra Nova*, 4, 374-384.
- Lirer F., Persico D., Vigorito M. (2005) - Calcareous plankton biostratigraphy and age of the middle Miocene deposits of Longano Formation (eastern Matese Mountains, southern Apennines). *Riv. Ital. Paleontol. Stratigr.*, 111, 91-108.
- Martelli L. and Nardi G. (2005) Note Illustrative della Carta Geologica d'Italia alla scala 1:50.000, F. 503 Vallo della Lucania, 86pp. S.EL.CA, Firenze.
- Martinez M., Deconinck J.F., Pellenard P., Riquier L., Company M., Reboulet S., Moiroud M. (2015) - Astrochronology of the Valanginian–Hauterivian stages (Early Cretaceous): Chronological relationships between the Paraná–Etendeka large igneous province and the Weissert and the Faraoni events. *Glob. Planet. Change*, 131, 158-173.
- Martino M., Barattolo F., Amodio S., Parente M. (2019) - Early Cretaceous neritic carbonate community and facies response to palaeoenvironmental and sea-level changes: new evidences from the Apennine Carbonate Platform of southern Italy. In: Granier B. (Ed.), JK2018 International meeting around the Jurassic-Cretaceous boundary. *Carnets de Géologie, Madrid Book*, 01, 55-58. <https://doi.org/10.4267/2042/69811>
- Mattioli E., Pittet B., Bucefalo Palliani R., Röhl H.J., Schmid-Röhl A., Morettini, E. (2004) - Phytoplankton evidence for the timing and correlation of palaeoceanographical changes during the early Toarcian oceanic anoxic event (Early Jurassic). *J. Geol. Soc.*, 161, 685-693.
- Mazzoli S., Corrado S., De Donatis M., Scrocca D., Butler R.W.H., Di Bucci D., Naso G., Nicolai C., Zucconi V. (2000) - Time and space variability of "thin-skinned" and "thick-skinned" thrust tectonics in the Apennines (Italy). *Rend. Lincei Sci. Fis. Nat., serie 9*, 11, 5-39.
- Mazzoli S., Barkham S., Cello G., Gambini R., Mattioni L., Shiner P., Tondi E. (2001) - Reconstruction of continental margin architecture deformed by the contraction of the Lagonegro Basin, southern Apennines, Italy. *J. Geol. Soc.*, 158, 309-319.
- Mazzoli S., D'Errico M., Aldega L., Corrado S., Invernizzi C., Shiner P., Zattin M. (2008) - Tectonic burial and 'young' (< 10 Ma) exhumation in the southern Apennines fold and thrust belt (Italy). *Geology*, 36, 243-246. <https://doi.org/10.1130/G24344A.1>
- McAnena A., Floegel S., Hofmann P., Herrle J.O., Griesand A., Pross J., Talbot H.M., Rethemeyer J., Wallmann K., Wagner T. (2013) - Atlantic cooling associated with a marine biotic crisis during the mid-Cretaceous period. *Nat. Geosci.*, 6, 558-561.
- McArthur J.M., Donovan D.T., Thirlwall M.F., Fouke B.W., Matthey D. (2000) - Strontium isotope profile of the early Toarcian (Jurassic) oceanic anoxic event, the duration of ammonite biozones, and belemnite palaeotemperatures. *Earth Planet. Sci. Lett.*, 179, 269-285.
- Millan M.I., Weissert H.J., Lopez-Horgue, M.A. (2014) - Expression of the late Aptian cold snaps and the OAE1b in a highly subsiding carbonate platform (Aralar, northern Spain). *Palaeogeogr., Palaeoclimatol., Palaeoecol.*, 411, 167-179.

- Mindszenty A., D'Argenio B., Aiello G. (1995) - Lithospheric bulges recorded by regional unconformities. The case of Mesozoic-Tertiary Apulia. *Tectonophysics*, 252, 137-161.
- Mondillo N., Balassone G., Boni M., Rollinson G. (2011) - Karst bauxites in the Campania Apennines (southern Italy): a new approach. *Period. di Mineral.*, 80/3, 407-432.
- Montone P., Amato A., Pondrelli S. (1999) - Active stress map of Italy. *J. Geophys. Res.*, 104, 25595-25610.
- Morsilli M. and Bosellini A. (1997) - Carbonate facies zonation of the Upper Jurassic-Lower Cretaceous Apulia platform margin (Gargano Promontory, southern Italy). *Riv. It. Paleontol. Stratigr.*, 103, 193-206.
- Mostardini F. and Merlini S. (1986) - Appennino centro-meridionale. Sezioni geologiche e proposta di modello strutturale. *Mem. Soc. Geol. It.*, 35, 177-202.
- Müller T., Jurikova H., Gutjahr M., Tomašových A., Schlögl J., Liebetrau V., Duarte L., Milovský R., Suan G., Mattioli E., Pittet B., Eisenhauer A. (2020) - Ocean acidification during the early Toarcian extinction event: Evidence from boron isotopes in brachiopods. *Geology*, 48, 1184-1188.
- Oldow J.S., Ferranti L., Lewis D.S., Campbell J.K., D'Argenio B., Catalano R., Pappone G., Carmignani L., Conti P., Aiken C.L.V. (2002) - Active fragmentation of Adria, the north African promontory, central Mediterranean orogeny. *Geology*, 30/9, 779-782.
- Opdyke B. and Wilkinson B. (1990) - Paleolatitude distribution of Phanerozoic marine ooids and cements. *Palaeogeogr. Palaeoclimatol. Palaeoecol.*, 78, 135-148.
- Parente M., Frijia G., Di Lucia M. (2007) - Carbon-isotope stratigraphy of Cenomanian-Turonian platform carbonates from the southern Apennines (Italy): a chemostratigraphic approach to the problem of correlation between shallow-water and deep-water successions. *J. Geol. Soc.*, 164, 609-620.
- Parente M., Frijia G., Di Lucia M., Jenkyns H.C., Woodfine R.G., Baroncini F. (2008) - Stepwise extinction of larger foraminifera at the Cenomanian-Turonian boundary: a shallow-water perspective on nutrient fluctuations during Oceanic Anoxic Event 2 (Bonarelli Event). *Geology*, 36, 715-718.
- Patacca E. and Scandone P. (2001) - Late thrust propagation and sedimentary response in the thrust-belt-foredeep system of the Southern Apennines (Pliocene-Pleistocene). In: Vai G.B. and Martini I.P. (Eds.), *Anatomy of an Orogen: The Apennines and Adjacent Mediterranean Basins*. Kluwer Academic Publishers, Dordrecht, 401-440.
- Patacca E. and Scandone P. (2007) - Geology of Southern Apennines. *Boll. Soc. Geol. It.*, 7, 75-119.
- Paul C.R.C., Lamolda M.A., Mitchell S.F., Vaziri M.R., Gorostidi A., Marshall J.D. (1999) - The Cenomanian/Turonian boundary at Eastbourne (Sussex, UK): A proposed European reference section. *Palaeogeogr. Palaeoclimatol. Palaeoecol.*, 150, 83-121.
- Pedley M. and Carannante G. (2006) - Cool-water carbonate ramps: a review. *Geol. Soc. Spec. Publ.*, 255(1), 1-9.
- Pemberton S.G., MacEachern J.A., Saunders T. (2004) - Stratigraphic applications of substrate-specific ichnofacies: delineating discontinuities in the rock record. *Geol. Soc. Spec. Publ.*, 228(1), 29-62.
- Posenato R., Bassi D., Nebelsick J.H. (2013) - *Opisoma excavatum* Boehm, a Lower Jurassic photosymbiotic alatoform-chambered bivalve. *Lethaia*, 46(4), 424-437.

- Posenato R., Bassi D., Trecalli A., Parente M. (2018) - Taphonomy and evolution of Lower Jurassic lithiotid bivalve accumulations in the Apennine Carbonate Platform (southern Italy). *Palaeogeogr., Palaeoclimatol., Palaeoecol.*, 1-39.
- Posenato R., Masetti D. (2012) - Environmental control and dynamics of Lower Jurassic bivalve build-ups in the Trento Platform (Southern Alps, Italy). *Palaeogeogr. Palaeoclimatol. Palaeoecol.*, 361-362, 1-13. <https://doi.org/10.1016/j.palaeo.2012.07.001>
- Rankey E.C. and Reeder S.L. (2009) - Holocene ooids of Aitutaki Atoll, Cook Islands, South Pacific. *Geology* 37, 971-974.
- Raspini A. (1998) - Microfacies analysis of shallow-water carbonates and evidence of hierarchically organized cycles. Aptian of Monte Tobenna, southern Apennines, Italy: *Cretac. Res.*, 19, 197-223.
- Raspini A. (2001) - Stacking pattern of cyclic carbonate platform strata: Lower Cretaceous of southern Apennines, Italy. *J. Geol. Soc.*, 158, 353-366.
- Raspini A. (2012) - Shallow water carbonate platforms (Late Aptian–Early Albian, Southern Apennines) in the context of supraregional to global changes: re-appraisal of palaeoecologic events as reflectors of carbonate factory response. *Solid Earth*, 3, 225-249.
- Rusciadelli G., Ricci C., Lathuilière B. (2011) - The Ellipsactinia Limestones of the Marsica Area (Central Apennines): a reference zonation model for Upper Jurassic Intra-Tethys reef complexes. *Sediment. Geol.*, 233, 69-87.
- Sabatino N., Vlahović I., Jenkyns H.C., Scopelliti G., Neri R., Prtoljan B., Velic, I. (2013) - Carbon-isotope record and palaeoenvironmental changes during the early Toarcian oceanic anoxic event in shallow-marine carbonates of the Adriatic Carbonate Platform in Croatia. *Geol. Mag.* 150, 1085-1102.
- Sabbatino M., Vitale S., Tavani S., Consorti L., Corradetti A., Cipriani A., Arienzo I., Parente M. (2020) - Constraining the onset of flexural subsidence and peripheral bulge extension in the Miocene foreland of the southern Apennines (Italy) by Sr-isotope stratigraphy. *Sediment. Geol.*, 401, 105634. <https://doi.org/10.1016/j.sedgeo.2020.105634>
- Sabbatino M., Tavani S., Vitale S., Ogata K., Corradetti A., Consorti L., Arienzo I., Cipriani A., Parente M. (2021) - Forebulge migration in the foreland basin system of the central-southern Apennine fold-thrust belt (Italy): New high-resolution Sr-isotope dating constraints. *Basin Res.*, 33, 2817-2836. <https://doi.org/10.1111/bre.12587>
- Sandberg P.A. (1985) - Nonskeletal aragonite and pCO<sub>2</sub> in the Phanerozoic and Proterozoic. *Geophys. Monogr. Ser.*, 32, 585-594.
- Sartoni S. and Crescenti U. (1962) - Ricerche biostratigrafiche nel Mesozoico dell'Appennino meridionale. *Giornale di Geologia*, 29, 161-293.
- Scherreiks R., Bosence D., BouDagher-Fadel M., Meléndez G., Baumgartner P.O. (2009) - Evolution of the Pelagonian carbonate platform complex and the adjacent oceanic realm in response to plate tectonic forcing (Late Triassic and Jurassic), Evvoia, Greece. *Int. J. Earth Sci. (Geol. Rundsch.)*, 99, 1317-1334.
- Schettino A. and Turco E. (2011) - Tectonic history of the western Tethys since the Late Triassic. *Geol. Soc. Am. Bull.*, 123, 89-105.
- Schlager W., Rejmer J.J.G., Droxler A. (1994) - Highstand shedding of carbonate platforms. *J. Sediment. Res.*, 64/3, 270-281.
- Schroeder R., van Buchem F.S.P., Cherchi A., Baghbani D., Vincent B., Immenhauser A., Granier, B. (2010) - Revised orbitolinid biostratigraphic zonation for the Barremian – Aptian of the eastern Arabian Plate and implications for regional stratigraphic correlations. *GeoArabia Spec. Publ.*, 4, 1, 49–96.
- Selli R. (1957) - Sulla trasgressione del Miocene nell'Italia meridionale. *Giornale di Geologia*, 2, 1-54.

- Selli R. (1962) - Il Paleogene nel quadro della Geologia dell'Italia Centro- Meridionale. Mem. Soc. Geol. It., 3, 737-789.
- Shiner P., Beccacini A., Mazzoli S. (2004) - Thin-skinned versus thick-skinned structural models for Apulian Carbonate Reservoirs: constraints from the Val D'Agri Fields. Mar. Pet. Geol., 21, 805-827.
- Simone L., Bravi S., Carannante G., Masucci I., Pomoni-Papaioannou F. (2012) - Arid versus wet climatic evidence in the "middle Cretaceous" calcareous successions of the southern Apennines (Italy). Cretac. Res., 36, 6-23.
- Simone L., Carannante G., Ruberti D., Sirna M., Sirna G., Laviano A., Tropeano M. (2003) - Development of rudist lithosomes in the Coniacian-Lower Campanian carbonate shelves of central- southern Italy: high energy vs low-energy settings. Palaeogeogr. Palaeoclimatol. Palaeoecol., 200, 5-29. [https://doi.org/10.1016/S0031-0182\(03\)00442-5](https://doi.org/10.1016/S0031-0182(03)00442-5)
- Sokač B. (2001) - Lower and Middle Liassic calcareous algae (Dasycladales) from the Mt. Velebit (Croatia) and Mt. Trnovski Gord (Slovenia) with particular reference to genus Palaeodasycladus (Pia, 1920) 1927 and its species. Geol. Croat., 54, 133-257.
- Stampfli G.M. and Mosar J. (1999) - The making and becoming of Apulia. Mem. Sci. Geol., 51, 141-154.
- Strasser A. (1988) - Shallowing-upward sequences in Purbeckian peritidal carbonates (lowermost Cretaceous, Swiss and French Jura Mountains). Sedimentology, 35, 369-383.
- Strasser A., Hillgärtner H., Hug W., Pittet B. (2000) - Third-order depositional sequences resulting from Milankovitch cycles. Terra Nova, 12, 303-311.
- Strasser A., Hillgärtner H., Pasquier J.-B. (2004) - Cyclostratigraphic timing of sedimentary processes: an example from the Berriasian of the Swiss and French Jura Mountains. In: D'Argenio B., Fischer A.G., Premoli Silva I., Weissert H., Ferreri V. (Eds.), Cyclostratigraphy: Approaches and case histories. SEPM Spec. Publ., 81, 135-151.
- Suan G., Mattioli E., Pittet B., Mailliot S. (2008) - Evidence for major environmental perturbation prior to and during the Toarcian (Early Jurassic) oceanic anoxic event from the Lusitanian Basin, Portugal. Paleoceanography, 23, PA1202.
- Tagliaferri R., Pelosi N., Ciaramella A., Longo N., Milano M., Barone F. (2001) - Soft computing methodologies for spectral analysis in cyclostratigraphy. Comput. Geosci., 27(5), 535-548.
- Tomašových A., Fürsich F.T., Wilmsen M. (2006) - Preservation of Autochthonous Shell Beds by Positive Feedback between Increased Hardpart-Input Rates and Increased Sedimentation Rates. J. Geol., 114(3), 287-312.
- Trecalli A., Spangenberg J., Adatte T., Föllmi K.B., Parente M. (2012) - Carbonate platform evidence of ocean acidification at the onset of the early Toarcian oceanic anoxic event. Earth Planet. Sci. Lett., 357-358, 214-225.
- Tremolada F., van de Schootbrugge B., Erba E. (2005) - Early Jurassic schizosphaerellid crisis in Cantabria, Spain: implications for calcification rates and phytoplankton evolution across the Toarcian oceanic anoxic event. Paleoceanography, 20, PA2011. <https://doi.org/10.1029/2004PA001120>
- Tsikos H., Jenkyns H.C., Walsworth-Bell B., Petrizzo M.R., Forster A., Kolonic S., Erba E., Premoli Silva I., Baas M., Wagner T., Sinninghe Damsté J.S. (2004) - Carbon-isotope stratigraphy recorded by the Cenomanian-Turonian oceanic anoxic event: correlation and implications based on three key localities. J. Geol. Soc., 161, 711-719.

- Vail P.R., Audemard F., Bowman S.A., Eisner P.N., Perez-Cruz C. (1991) - The stratigraphic signatures of tectonics, eustasy and sedimentology - an overview. In: Einsele G., Ricken W., Seilacher A., (Eds.), *Cycles and Events in Stratigraphy*. Springer-Verlag, Berlin, 617-659.
- van Hinsbergen D.J.J., Torsvik T.H., Schmid S.M., Matenco L.C., Maffione M., Vissers R.L.M., Gürer D., Spakman W. (2020) - Orogenic architecture of the Mediterranean region and kinematic reconstruction of its tectonic evolution since the Triassic. *Gondw. Res.*, 81, 79-229.
- Vecchio E., Barattolo F., Hottinger L. (2007) - Alveolina horizons in the Trentinara Formation (southern Apennines, Italy): stratigraphic and paleogeographic implications. *Riv. It. Paleontol. Stratigr.*, 113(1), 21-42. <https://doi.org/10.13130/2039-4942/6356>
- Vecchio E. and Hottinger L. (2007) - Agglutinated conical foraminifera from the lower-middle eocene of the trentinara formation (southern Italy). *Facies*, 53(4), 509-533.
- Vilas L., Masse J.P., Arias C. (1995) - Orbitolina episodes in carbonate platform evolution: the early Aptian model from SE Spain, *Palaeogeogr. Palaeoclimatol. Palaeoecol.*, 119, 35-45.
- Vitale S. and Ciarcia S. (2013) - Tectono-stratigraphic and kinematic evolution of the southern Apennines/ Calabria–Peloritani Terrane system (Italy). *Tectonophysics* 583:164-182. <https://doi.org/10.1016/j.tecto.2012.11.004>
- Vitale S., Dati F., Mazzoli S., Ciarcia S., Guerriero V., Iannace A. (2012) - Modes and timing of fracture network development in poly-deformed carbonate reservoir analogues, Mt. Chianello, southern Italy. *J. Struct. Geol.*, 37, 223-235.
- Vlahović I., Tisljar J., Velic I., Maticec D. (2005) - Evolution of the Adriatic Carbonate Platform: palaeogeography, main events and depositional dynamics. *Palaeogeogr. Palaeoclimatol. Palaeoecol.*, 220, 333-360.
- Wissler L., Weissert H., Buonocunto F.P., Ferreri V., D'Argenio B. (2004) - Calibration of the Early Cretaceous time scale: a combined chemostratigraphic and cyclostratigraphic approach to the Barremian-Aptian interval. In: D'Argenio B., Fischer A.G., Premoli Silva I., Weissert H., Ferreri V. (Eds.), *Cyclostratigraphy. Approaches and case histories*. SEPM Spec. Publ., 81, 123-134.
- Woodfine R.G., Jenkyns H.C., Sarti M., Baroncini F., Violante C. (2008) - The response of two Tethyan carbonate platforms to the early Toarcian (Jurassic) oceanic anoxic event: environmental change and differential subsidence. *Sedimentology* 55, 1011-1028.
- Zamparelli V., Cirilli S., Iannace A., Jadoul F. (1999) - Palaeo-tectonic and palaeoceanographic controls on microbial-serpulid communities in the Norian-Rhaetian carbonates of Italy: a synthesis. In: Colacicchi R., Parisi G., Zamparelli V. (Eds.), *Bioevents and integrate stratigraphy of the Triassic and the Jurassic in Italy*. *Paleopelagos, Spec. Publ.*, 3, 7-84.
- Zarcone G., Petti F.M., Cillari A., Di Stefano P., Guzzetta D., Nicosia U. (2010) - A possible bridge between Adria and Africa: New palaeobiogeographic and stratigraphic constraints on the Mesozoic palaeogeography of the central Mediterranean area. *Earth-Sci. Rev.*, 103, 154-162.